

*THE EFFECT OF CONCRETE STRENGTH
ON THE SHEAR STRENGTH OF
REINFORCED CONCRETE BEAMS
WITH BAR CUTOFF*

JULY 1968

NO. 16

*Joint
Highway
Research
Project*

by
J. G. BORCHELT

*PURDUE UNIVERSITY
LAFAYETTE INDIANA*



Final Report

THE EFFECT OF CONCRETE STRENGTH ON THE SHEAR STRENGTH OF REINFORCED CONCRETE BEAMS WITH BAR CUTOFF

To: J. F. McLaughlin, Director
Joint Highway Research Project

From: H. L. Michael, Associate Director
Joint Highway Research Project

July 12, 1968

Project No.: C-36-56M

File No.: 7-4-13

The attached Final Report "The Effect of Concrete Strength on the Shear Strength of Reinforced Concrete Beams with Bar Cutoff" by J. Gregg Borchelt is presented to the Board for the record as completion of a research project. The research was approved in a Plan of Study on May 11, 1967. Professors M. J. Gutzwiller and R. H. Lee directed the study and Mr. Borchelt also used the report as his thesis for the MSCE degree.

The research was an experimental study of the ultimate behavior of reinforced concrete beams which fail in shear. It was found that failure occurred in two modes, shear compression and diagonal tension. Important factors in the type of failure were the shear span to depth ratio and the concrete strength.

The report is presented to the Board for the record and for review and comment.

Respectfully submitted,



Harold L. Michael
Associate Director

HLM:mz

cc: F. L. Ashbaucher	R. H. Harrell	C. F. Scholer
W. L. Dolch	J. A. Havers	M. B. Scott
W. H. Goetz	V. E. Harvey	W. T. Spencer
W. L. Grecco	G. A. Leonards	H. R. J. Walsh
G. K. Hallock	F. B. Mendenhall	K. B. Woods
M. E. Harr	R. D. Miles	E. J. Yoder
	J. C. Oppenlander	

Final Report

THE EFFECT OF CONCRETE STRENGTH ON THE SHEAR STRENGTH
OF REINFORCED CONCRETE BEAMS WITH BAR CUTOFF

by

J. Gregg Borchelt

Joint Highway Research Project

Project: C-36-56 M

File: 7-4-13

Purdue University

Lafayette, Indiana

July 12, 1968

ACKNOWLEDGMENTS

Acknowledgment is first made to the board members of the Joint Highway Research Project and to Professor G. A. Leonards, Director, for providing funds for the project.

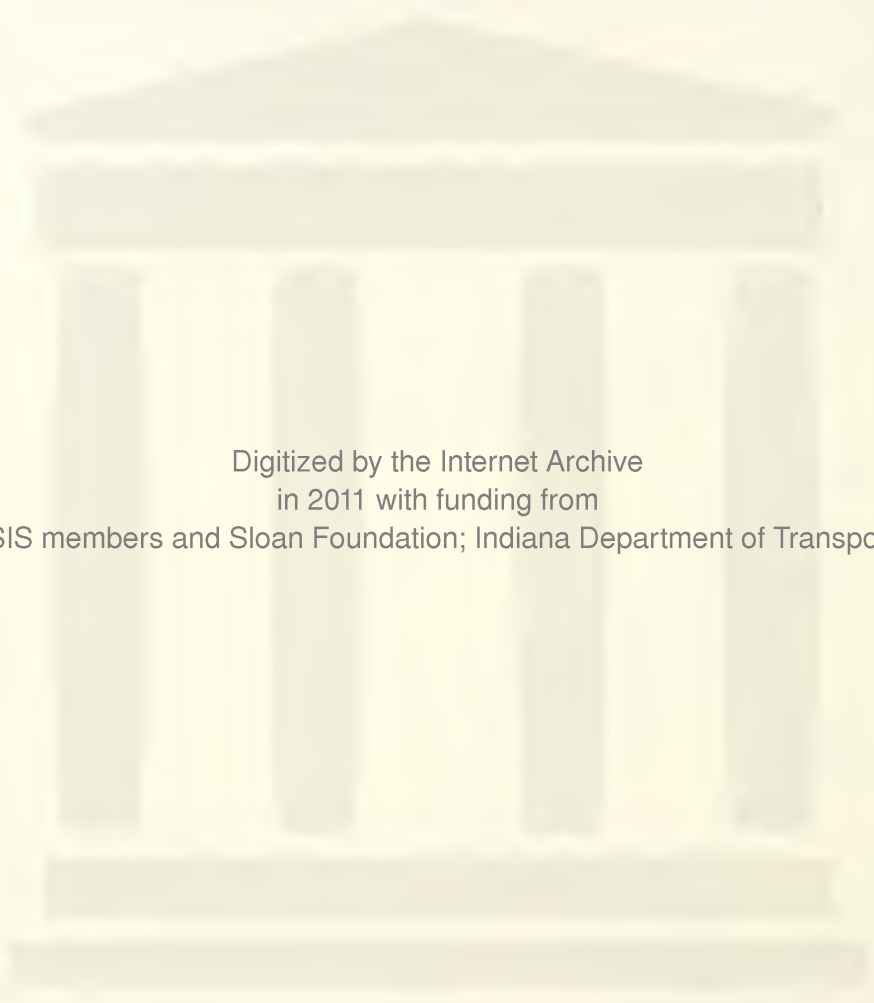
Special appreciation for their advice and guidance is given to Professors Martin J. Gutzwiller and Robert H. Lee, major professors.

The author also wishes to thank Mr. W. B. Telfer, laboratory technician, and the several graduate students for their generous assistance in the laboratory.

The encouragement and patience of the author's wife were especially welcome.

TABLE OF CONTENTS

	Page
LIST OF TABLES.....	vi
LIST OF FIGURES.....	viii
LIST OF SYMBOLS.....	xi
ABSTRACT.....	xiv
INTRODUCTION.....	1
Present Design Methods.....	6
Review of the Literature.....	8
Beams without Web Reinforcement.....	9
Beams with Web Reinforcement.....	12
PURPOSE AND SCOPE.....	15
TEST SPECIMENS AND PROCEDURE.....	16
Materials.....	20
Concrete Mix.....	20
Aggregates.....	21
Reinforcing Steel.....	22
Fabrication and Curing.....	23
Instrumentation and Testing Procedures.....	25
TEST RESULTS.....	29
Repeated Tests.....	36
Harvey.....	36
Beam IA-4 (No Stirrups - 2 Layers of Tension Steel).....	36
Beam IIB-5 (No Stirrups - AASHO Cutoff).....	37
Beam IIIB-5 (4" Stirrup Spacing - AASHO Cutoff).....	37
Beam IIIB-6 (No Stirrups - AASHO Cutoff).....	38
Wehr.....	47
Beam IIT-1 (No Stirrups - No Cutoff).....	47



Digitized by the Internet Archive
in 2011 with funding from
LYRASIS members and Sloan Foundation; Indiana Department of Transportation

TABLE OF CONTENTS (continued)

	Page
Spaman.....	51
Beam 1A (No Stirrups - Theoretical Cutoff)...	51
Beam IE (No Stirrups - No Cutoff).....	51
Beam IIA (3 1/2" Stirrup Spacing - Theoretical Cutoff).....	52
Beam IIB (3 1/2" Stirrup Spacing - No Cutoff).....	53
The Effect of Concrete Strength.....	65
Series I, 24" Shear Span.....	65
Beam I-1 ($f'_c = 2,740$ psi).....	65
Beam I-2 ($f'_c = 3,600$ psi).....	66
Beam I-3 ($f'_c = 3,820$ psi).....	66
Beam I-4 ($f'_c = 5,090$ psi).....	66
Series II, 32" Shear Span.....	76
Beam II-1 ($f'_c = 2,030$ psi).....	76
Beam II-2 ($f'_c = 2,450$ psi).....	76
Beam II-8 ($f'_c = 6,750$ psi).....	77
Series III, 44" Shear Span.....	86
Beam III-1 ($f'_c = 2,040$ psi).....	86
Beam III-2 ($f'_c = 3,210$ psi).....	86
Beam III-5 ($f'_c = 6,810$ psi).....	87
DISCUSSION OF TEST RESULTS.....	96
Repeated Beams.....	96
Harvey.....	96
Wehr.....	99
Spaman.....	99
Effect of Concrete Strength.....	100
Modes of Failure.....	100
Shear Span to Depth Ratio.....	101
Concrete Strength.....	102
Diagonal Crack Location.....	103
Bar Cutoff.....	104
Steel Strains.....	106
ANALYSIS OF TEST RESULTS.....	107
Shearing Stress at Diagonal Cracking.....	107
Ultimate Shear Strength.....	107
Limiting Moment.....	111
SUMMARY AND CONCLUSIONS.....	115

TABLE OF CONTENTS (continued)

	Page
BIBLIOGRAPHY.....	117
APPENDIX A: STRESS-STRAIN PROPERTIES OF THE REINFORCEMENT.....	119
APPENDIX B: TEST DATA.....	121

LIST OF TABLES

Table	Page
1. Properties of Repeated Specimens.....	18.
2. Properties of Concrete Strength Test Specimens...	19
3. Properties of Longitudinal Reinforcement.....	22
4. Properties of Soft Web Reinforcement.....	23
5. Summary of Repeated Test Results.....	30
6. Summary of Test Results for Concrete Strength....	31
7. Comparison of Repeated Beam Strengths with A.C.I. Building Code Requirements.....	97
8. Comparison of Repeat Beam Strengths with AASHTO Standard Specifications.....	98
9. Effect of Shear Span to Depth Ratio.....	101
10. Comparison of Concrete Strength Test Results with A.C.I. Building Code Requirements.....	108
11. Comparison of Concrete Strength Test Results with AASHTO Specifications.....	110
12. Comparison of Ultimate Moment to Flexural Moment.....	113
Appendix	
Tables	
B1. Test Data, Beam IA-4.....	121
B2. Test Data, Beam IIB-5.....	122
B3. Test Data, Beam IIT-1.....	123
B4. Test Data, Beam IA.....	124
B5. Test Data, Beam IE.....	125

LIST OF TABLES (continued)

Appendix Table	Page
B6. Test Data, Beam IIA.....	126
B7. Test Data, Beam IID.....	127
B8. Test Data, Beam I-1.....	128
B9. Test Data, Beam I-2.....	129
B10. Test Data, Beam I-3.....	130
B11. Test Data, Beam I-4.....	131
B12. Test Data, Beam II-1.....	132
B13. Test Data, Beam II-2.....	133
B14. Test Data, Beam II-8.....	134
B15. Test Data, Beam III-1.....	135
B16. Test Data, Beam III-2.....	136
B17. Test Data, Beam III-5.....	137

LIST OF FIGURES

Figure	Page
1. Beam with Diagonal Tension Crack.....	4
2. Beam Capacity versus a/d Ratio for Simply Supported Rectangular Beams.....	10
3. Details of Specimens.....	17
4. Forms Prior to Casting.....	24
5. Test Set-up.....	26
6. Repeat Beams of Spaman After Test.....	32
7. Beams After Test Series I.....	33
8. Beams After Test Series II.....	34
9. Beams After Test Series III.....	35
10. Load versus Deflection - Harvey.....	39
11. Concrete Strain Distribution - Beam IA-4.....	40
12. Load versus Steel Strains - Harvey.....	41
13. Pictorial Representation of Beam on Crack Pattern Sheet.....	42
14. Beam IA-4.....	43
15. Beam IIB-5.....	44
16. Beam IIIB-5.....	45
17. Beam IIIB-6.....	46
18. Graphs for IIT-1.....	48
19. Strain Distribution, IIT-1.....	49
20. Beam IIT-1.....	50

LIST OF FIGURES (continued)

Figure	Page
21. Load versus Deflection, Spaman.....	54
22. Concrete Strain Distribution, IA.....	55
23. Concrete Strain Distribution, IE.....	56
24. Concrete Strain Distribution, IIA.....	57
25. Concrete Strain Distribution, IID.....	58
26. Steel Strain Distribution, IA and IE.....	59
27. Steel Strain Distribution, IIA and IID.....	60
28. Beam IA.....	61
29. Beam IE.....	62
30. Beam IIA.....	63
31. Beam IID.....	64
32. Load versus Deflection, Series I.....	68
33. Concrete Strain Distribution, I-1 and I-2.....	69
34. Concrete Strain Distribution, I-3 and I-4.....	70
35. Load versus Steel Strain, Series I.....	71
36. Beam I-1.....	72
37. Beam I-2.....	73
38. Beam I-3.....	74
39. Beam I-4.....	75
40. Load versus Deflection, Series II.....	78
41. Concrete Strain Distribution, II-1.....	79
42. Concrete Strain Distribution, II-2.....	80
43. Concrete Strain Distribution, II-8.....	81
44. Load versus Steel Strain, Series II.....	82

LIST OF FIGURES (continued)

Figure	Page
45. Beam II-1.....	83
46. Beam II-2.....	84
47. Beam II-8.....	85
48. Load versus Deflection, Series III.....	88
49. Concrete Strain Distribution, III-1.....	89
50. Concrete Strain Distribution, III-2.....	90
51. Concrete Strain Distribution, III-5.....	91
52. Load versus Steel Strain, Series III.....	92
53. Beam III-1.....	93
54. Beam III-2.....	94
55. Beam III-5.....	95
56. Shearing Stress versus Concrete Strength.....	112
57. Typical Stress-Strain Properties, Longitudinal Steel.....	119
58. Typical Stress-Strain Properties, Stirrup Steel.....	120

LIST OF SYMBOLS

A_s	nominal area of tension steel
A_v	cross-sectional area of one stirrup
a	length of critical shear span (distance from section of maximum moment to point of inflection)
b	width of beam section
C	total internal compression force in concrete
d	effective depth (measured to centroid of tension steel)
d'	distance from compression face to centroid of compression steel
E_s	modulus of elasticity of steel
E_c	initial tangent modulus of concrete
f'_c	concrete compressive strength, 6" x 12" standard cylinder
f_{st}	split tensile strength, 6" x 12" standard cylinder
f_y	yield stress of longitudinal steel
jd	internal moment arm, straight-line theory
M	moment at any section

M_{f1}	ultimate flexural moment
M_u	ultimate moment carried by beam
M_1	maximum negative moment
M_2	maximum positive moment
P	total load
P_{cr}	total load at formation of diagonal tension crack
P_{sp}	total load at splitting along steel
P_u	total load at failure
P_1, P_2	load on the overhang and load between supports, respectively
p	A_s/bd percentage of longitudinal steel
R	reaction
r	A_v/b_s web reinforcement ratio
s	horizontal spacing of stirrups
T	total force in tension steel
V	total shear at any section
V_a	shear in critical shear span
V_c	shear force carried by concrete

V'_u	ultimate shear force carried by web reinforcement
v	nominal shearing stress = V/bjd or V/bd as defined in text
v_a	allowable nominal shearing stress = V/bjd
v_c	shear stress carried by concrete
v_{cr}	shear stress at diagonal cracking
v_s	portion of shearing stress carried by stirrups
v_{sp}	shearing stress at splitting along steel
v_u	ultimate shear strength
α	inclination of stirrups with respect to longitudinal axis
ϕ	capacity reduction factor
D.T.	diagonal tension failure
S.C.	shear-compression failure
MII	strain in micro-inches per inch

ABSTRACT

Borchelt, J. Gregg. M.S.C.E., Purdue University, August 1968. THE EFFECT OF CONCRETE STRENGTH ON THE SHEAR STRENGTH OF REINFORCED CONCRETE BEAMS WITH BAR CUTOFF. Major Professors: M. J. Gutzwiller and R. H. Lee.

This is an experimental study of the ultimate behavior of reinforced concrete beams which fail in shear. The objectives of this investigation were:

- 1) to repeat certain beam tests of earlier studies here at Purdue in order to clarify and supplement their investigation,
- 2) to determine the effect of concrete strength upon the behavior and failure mode of beams with different shear span to depth ratios,
- 3) to use all of the data available in order to draw conclusions.

Nine beams from the earlier reports were retested in accordance with the original procedure. Ten additional beams were cast to complete the study of the concrete strength. All specimens had a 6" x 13" rectangular cross-section and were loaded to simulate a portion of a continuous girder. The beams were designed to restrict failure to a shear type failure in the length between maximum negative moment and zero moment -- commonly called the shear span.

Failure occurred in two modes, shear compression and diagonal tension. It was found that the type of failure depended upon the position of the diagonal crack when it crossed the neutral axis. The location of the critical crack depended upon the shear span to depth ratio and the concrete strength.

Detailed discussion of individual beam behavior and the failure patterns are presented along with the summary of test results.

INTRODUCTION

The behavior of reinforced concrete members has been the subject of extensive experimental and analytical research. The basic fundamentals of mechanics provide reasonable limits for design, but it is well known that the true response of reinforced concrete structures does not strictly conform to standard design methods. In recent years the ultimate load behavior of reinforced concrete has been under investigation in an effort to remove the impositions of elastic behavior.

Sufficient test data has been correlated with theoretical hypotheses so that a reasonable understanding of the ultimate strength of such members in pure bending and axial compression has been obtained. Although much work has been performed on beams subjected to the combined action of bending and shear, the behavior of such members cannot be predicted with sufficient accuracy.

The effect of shearing stresses can be established by examining a simply-supported beam loaded with two symmetrical concentrated loads. In this case the region between loads is in a state of pure bending, while the length between the load and the support, commonly called the shear span, is subjected to a combination of shearing and bending stresses.

When the loads are placed near the center of the span, so that the shear span is greater than 6 to 7 times the beam depth, the effect of shear on the ultimate strength of the beam is small or negligible. The member fails by flexure with either crushing of the concrete or initial yielding of the tension steel followed by crushing of the concrete. This type of loading approaches the case of pure bending, for which an accurate prediction of the ultimate load can be made.

If the loads are moved closer to the supports the ratio of moment to shear is reduced as the shear span becomes smaller. The combination of shearing stresses and bending tensile stresses begins to affect the formation of cracks and the ultimate load. The flexure cracks will begin to incline toward the point of load application as the load is increased. Before sufficient bending moment is developed to produce failure in flexure, distinct diagonal tension cracks may form independently from the flexural cracks and closer to the supports. These cracks form near the neutral axis and at approximately forty-five degrees to the neutral axis. Although the diagonal tension crack may be an extension of the flexural crack it is distinct from the latter in that it penetrates deeply into the compression region. Following formation of the diagonal tension crack there are two typically observed types of behavior which may occur. One, the diagonal tension crack forms across the entire face of the beam from the tension

steel through the compression face. This may occur simultaneously or at a slightly higher load, essentially splitting the beam into two pieces and causing failure. This is the diagonal tension failure and is most frequently found with a shear span to depth ratio in the range from three to seven. Two, with smaller shear span to depth ratios, the diagonal crack enters the compression zone but does not reach the compression face. Increasing the load results in a deeper penetration, reducing the area of concrete available to resist compression until the beam fails by crushing of the concrete. This type of failure is commonly called the shear compression failure. In this case the beam has additional strength after the formation of the diagonal tension crack.

It can be concluded that shear affects the behavior of the beam through the formation of the diagonal tension crack. Prior to the formation of this crack the stress in the longitudinal steel and in the concrete is proportional to moment in the beam. The formation and growth of the diagonal tension crack causes a significant redistribution of the internal stresses. It is the ability of the beam to accept this stress redistribution that determines the ultimate strength of the beam.

A beam with no web reinforcement which has a diagonal tension crack is shown in Figure 1a. Figure 1b illustrates the section of the beam to the left of the crack. After

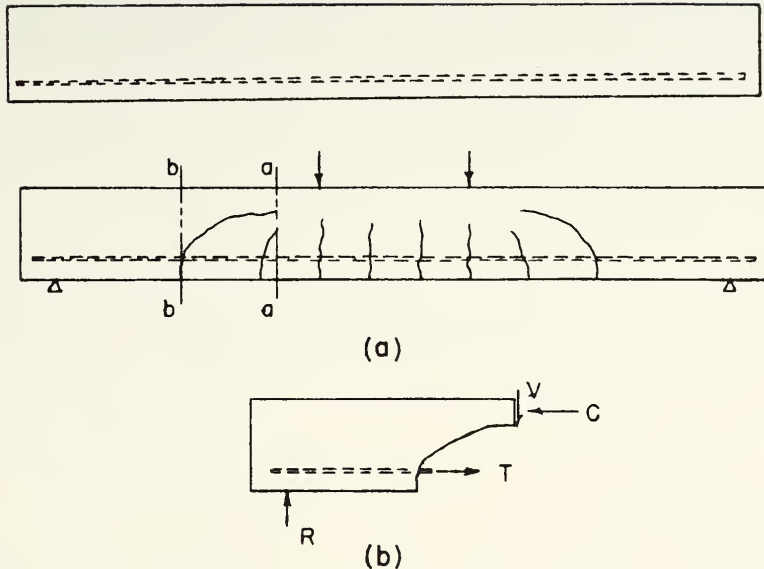


FIGURE 1. BEAM WITH DIAGONAL CRACK

the crack has formed the concrete above the crack is assumed to resist the entire shear force although a small portion of the shear is transferred by dowel action of the longitudinal steel. In order for the beam to adjust to this new form the steel at section b-b must be capable of resisting the moment at section a-a. This will cause an increase in stress of the steel at section b-b. If the beam is not able to reach a force equilibrium the steel will yield and cause a spontaneous collapse.

The resistance of the beam to diagonal tension cracking depends primarily upon the stability of the compression zone,

or the compressive strength of the concrete. However, the percentage of longitudinal reinforcement and the length of the shear span also affect the ability of the beam to reach a force equilibrium.

Thus, for beams without web reinforcement, failure may come immediately with the formation of the diagonal tension crack or at loads as much as 100 per cent higher than loads causing the critical diagonal tension crack. This erratic behavior indicates that the ultimate load of such a beam should be the diagonal cracking load.

Web reinforcement has little effect on the beams' behavior prior to formation of the diagonal crack. In fact, measurements have shown that there is no appreciable stress in the stirrups before cracking. Even after cracking has taken place only the stirrups crossed by the crack carry the stress originally transferred by the concrete. The stress level in these stirrups is increased as the load rises. If the beam is to fail by shear compression the web reinforcement would have to yield before the concrete crushes. A flexure failure would result if the percentage of web reinforcement were high enough to keep the stirrups from reaching yield stress. Presence of the stirrups also adds to the shear resistance by reducing the propagation of the diagonal tension crack into the compression zone. The beam will not fail suddenly unless the percentage of web reinforcement is so small that the stirrup yields upon formation of the diagonal tension crack.

The percentage of longitudinal reinforcement crossed by the diagonal tension crack is also of importance. Present design standards allow for a reduction in the amount of tension steel when it is no longer needed to resist the moment developed. It has been shown that the longitudinal steel near the support, where the moment is low, may be required to resist a higher moment after the formation of the diagonal tension crack. There are two consequences of terminating bars solely in accordance with moment requirements. A sudden increase in the stress of the tension steel where it is crossed by the diagonal tension crack could cause immediate yielding. A large differential in steel stress in a region of high shear may lead to very large bond stresses adjacent to tension cracks. The resulting splitting causes progressive destruction of bond of the concrete to the steel and failure.

Present Design Methods

Beams which are reinforced for flexure must be designed so that the shearing stresses that develop are below the critical value that would result in diagonal tension cracking of the beam. The maximum shear force, V , and therefore the maximum calculated shear stress, v , generally occur immediately adjacent to a support. However, the additional local stresses caused by the reaction counteract crack formation and the first crack occurs at a distance of the order of the depth of the beam, d , from the support. The ACI Code

[2]^{*} therefore specifies that the maximum shear stress for design is at a section a distance d from the face of the support, where d is the effective depth of the beam. It is also required that the concrete area and web reinforcement calculated at this section must be continued to the support.

The ultimate shear stress allowed in a beam without web reinforcement, as given by the ACI Code is:

$$v_c = \frac{V}{bd} = \phi (1.9\sqrt{f'_c} + 2500 \frac{pVd}{M}) \leq 3.5 \phi \sqrt{f'_c} \quad (1)$$

where ϕ is a capacity reduction factor which is 0.85 for shear and diagonal tension, $p = A_s/bd$, A_s is the area of tension reinforcement, b is the width of the web, M is the bending moment. This equation was developed after studying experimental results. Details can be found in the report of the ACI-ASCE Committee 326 [1]. It is seen that this equation contains all of the major factors influencing the shear strength of reinforced concrete beams.

When the shear stress exceeds that permitted for the concrete of an unreinforced web the Code allows for designing web reinforcement to carry the excess. The method for computing the required amount of web reinforcement is based on the truss analogy. The basis for the truss analogy has been well documented in earlier works and be found in both Harvey's

^{*} Bracketed numbers refer to items in the Bibliography.

thesis [9], pp. 9-12 and Wehr's thesis [19], pp. 5-9. The final result of this method is

$$A_v = \frac{V'_u s}{\phi f_y d (\sin \alpha + \cos \alpha)} \quad (2)$$

where A_v is the total area of web reinforcement in tension within a direction parallel to the longitudinal reinforcement, V'_u is the ultimate shear carried by the web reinforcement, s is the spacing of the stirrups on bent bars in a direction parallel to the longitudinal reinforcement, f_y is the yield strength of reinforcement, and α is the angle between inclined web bars and longitudinal axis of member. The committee could not recommend changes in the procedure for proportioning web reinforcement as given by the truss analogy. This is due to a lack of beam tests with shear reinforcement and the performance of beams designed in this way.

Thus, the shear strength of beams with web reinforcement is the sum of the shear carried by the uncracked concrete section, v_c , and that carried by the stirrups, v_s .

$$v = v_c + v_s \quad (3)$$

Review of the Literature

The complex nature of the distribution of internal stresses after diagonal cracking has prevented anyone from presenting a rational explanation of the mechanism of shear

failure. Efforts to unravel this mystery have been made since the beginning of the century, with intensified attempts over the last decade giving a much better understanding than previously available. A thorough synopsis of the developments prior to 1964 has been presented by Harvey in his thesis [9]. The following discussion will only cover the material written since this review.

Beams Without Web Reinforcement

Recent approaches have attempted to establish a basically rational theory to describe effects of shear and diagonal tension on the behavior of reinforced concrete members. The major difficulties in developing such a theory are due primarily to the indeterminacy of the internal force system after inclined cracking, the nonhomogeneity of concrete, and the nonlinearity of its stress-strain diagram. Further problems arise because of the number of parameters influencing the beam strength: percentage of steel, grade of steel, type and arrangement of web reinforcement, concrete strength, shape of cross-section, shear span to depth ratio, dimensions of the cross-section, type of loading, and type of beam. The large number of variables involved in the problem has prevented anyone from collecting and interpolating all of the data available and presenting the desired understanding.

The effect of the shear span to depth ratio on the shear capacity of rectangular beams with all other variables

constant can be illustrated as shown in Figure 2. This clearly shows two separate effects governing the ultimate capacity, shear compression and inclined cracking.

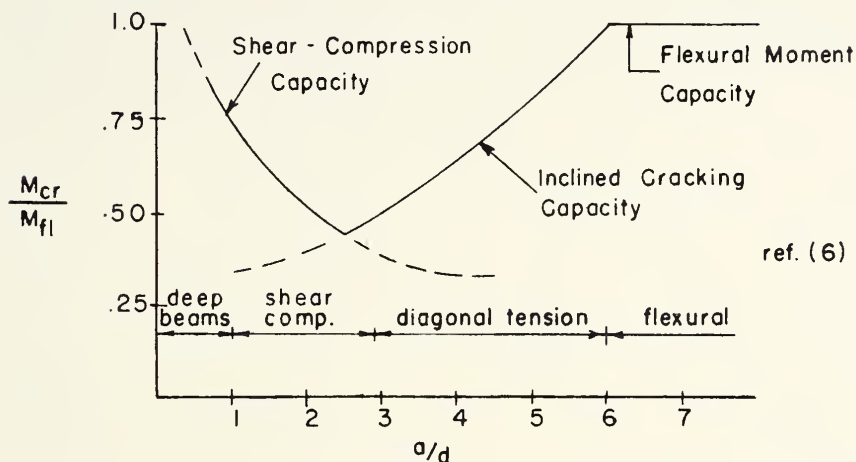


FIGURE 2. BEAM CAPACITY VS. A/D RATIO
FOR SIMPLY SUPPORTED RECTANGULAR BEAMS

The shear compression failure occurs after flexural cracks have formed. An inclined crack which is generally a continuation of a flexural crack progresses through the compression zone toward the nearest concentrated load. With an increase in load the inclined portion of the crack generally propagates downward to the reinforcement and extends along

it. This secondary horizontal crack is associated with either slip or dowel action of the reinforcement.

Once the inclined crack has developed failure may occur in one of two primary ways: (1) a crushing of the concrete at the end of the crack; and (2) anchorage failure due to loss of bond of the tension reinforcement. As noted in Figure 2 a shear compression failure always has a reserve strength after the formation of the inclined crack.

In beams of larger shear span to depth ratio, from about 2.5 to 7, the redistribution of stresses after diagonal tension cracking will exceed the strength of the member. Such a member fails immediately upon the formation of the inclined crack, with little or no indication of failure. The crack, which often splits the beam into two pieces, may be the rapid progression of a flexural crack or form independently in the web.

Several reports written in the past few years have observed the behavior of beams failing in shear [10,11,12,14, 16]. Other investigations [5,8,11,12,13] have examined single aspects of shear failure in order to give a more complete understanding. Particular attention has been paid to the contribution and effect of the tension reinforcement [5,13,15].

A method of analysis of beams subjected to the combined action of bending and shear stress that has been developed recently is the "tooth-failure cracking." This mechanism

of diagonal failure was presented by Kani [12], along with the transformation of the beam into a tied arch. Development along these lines resulted in a design basis which accounts for the changing behavior of the beam as the shear span to depth ratio changes. Comparison to test data proved very favorable. Investigations by other authors [6,8,15,16] have also examined this and similar behavior.

The importance of the inclined crack upon the behavior and shear strength of reinforced beams has long been known. Since the inclined crack is essential to shear failure it is important to be able to define the load which will cause the diagonal cracking. Several attempts have been made to study the formation of inclined cracks and determine their effect on the beam [6,7,8,13,16,17].

The result of this research has been several semi-empirical design criteria for reinforced concrete beams [11,12,14,15,17]. The accuracy of these proposed theories varies, but each was developed for a particular beam size with a limited range of variables. Often the results are contradictory. It has been concluded in nearly all of these studies that more work must be done [6,14,17].

Beams with Web Reinforcement

Research concerning beams with stirrups is much more limited. This is due to the introduction of another variable with the addition of one more material to handle and the associated difficulties.

Behavior of beams with stirrups prior to diagonal cracking is essentially the same as that of beams without stirrups. Once inclined cracking occurs the stirrups carry part of the stress and even small percentages of web reinforcement shows some increase in carrying capacity. Tests by Krefeld and Thurston [14] have shown that there is a minimum value of transverse steel necessary to develop the flexural capacity of beams.

Presence of stirrups adds to the beams shear capacity in several ways. As might be expected, the web steel carries part of the shear in tension when it is crossed by an inclined crack. The width of the crack is reduced as well as the relative displacement of the segments in the crack zone. Propagation of the critical diagonal tension crack is thus reduced and the compression zone of the beam remains larger. Crack patterns remain nearly the same as for beams without stirrups, but the inclined cracks are flatter. Dowel action of the longitudinal reinforcement is greatly increased because the stirrups tie the tension steel to the uncracked concrete.

The effect of web reinforcement is most pronounced in beams which would fail in diagonal tension if the stirrups were not present. Failure does not occur upon formation of the inclined crack because the stirrups carry the shear and allow the internal stresses to redistribute.

Several methods have been presented which attempt to analyze the behavior of a concrete beam with stirrups. The

most popular of these are the truss analogies but a frame analogy is also available. Limit analysis mechanisms, both rigid-simple mechanism and rigid-elasto-plastic models have been used. Each of these approaches has been reviewed by Bresler and MacGregor [6]. Any of the above procedures which is relatively clear and easy to use does not give results which agree with test data.

PURPOSE AND SCOPE

The object of this study was to observe the behavior of beams with different shear span-to-depth ratios as a function of concrete strength. The effect of the concrete strength on the ultimate shear strength of beams without web reinforcement was examined.

It was also the intent of this study to assemble the results of recent studies here at Purdue. All of the previous test data were combined and examined. Certain beam tests were repeated in order to clarify, supplement and continue the investigation. In this manner a more comprehensive study was obtained.

The data included in this report come from the following Joint Highway reports:

1. "A Study of Diagonal Tension Failure in Reinforced Concrete Beams" by W. N. Harvey [9].
2. "Shear Strength of Reinforced Concrete T-Beams" by K. E. Wehr [19].
3. "A Study of the Effect of Bar Cut-off on the Shear Strength of Restrained Reinforced Concrete Beams" by G. R. Spaman [18].

TEST SPECIMENS AND PROCEDURE

All beams were simply supported with an overhang on one end. One concentrated load, P_1 , was applied to the cantilevered portion and a second load, P_2 , to the region between supports. These two loads were applied to the specimens as reactions from a steel I-section. A specific ratio of maximum negative moment to maximum positive moment was obtained by positioning the load applied to the I-section. The details and dimensions of the specimens, along with the applied loads, shears and moments, are found in Figure 3 and Tables 1 and 2.

Each of the repeated tests was made to conform as close as possible to the original test. Changes were made only in the position of the strain gages on the steel when it was felt that their position affected the behavior of the beam. Strains were measured with the type of gages presently available in place of the strain measuring devices originally used.

The same 6" x 13" rectangular cross-section was used for all beams. The two variables in the study were the compressive strength of the concrete and the length of the shear span "a." Two No. 6 bars were used for the top reinforcement while two No. 5 bars were used as the bottom steel. All of the longitudinal reinforcement was terminated where it

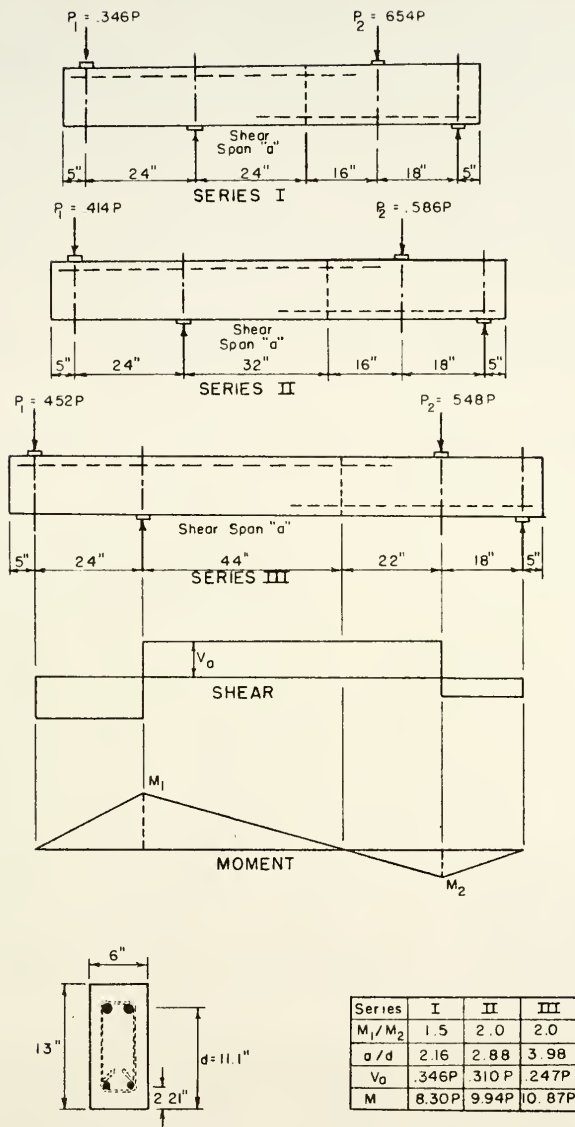


FIGURE 3. DETAILS OF SPECIMENS

Table 1. Properties of Repeated Beam Specimens.

Beam Designation	d in.	d' in.	a in.	Longitudinal Reinforcement		p _u (A _s /bd)	Reinforcement		Compressive Strength f _c psi	Split Tensile Strength f _t psi	Modulus of Elasticity E × 10 ⁶ psi	
				Top	Bottom		Size & Spacing	Web (A _v /bs)				
Harvey												
IA-4	10.2	2.3	24	2-#5, 2-#6	2-#5	.0167	-----	----	3957	404	3.05	
Repeat	10.2	2.3	24	2-#5, 2-#6	2-#5	.0167	-----	----	4420	446	4.00	
II8-5	11.1	2.2	32	2-#8 2-#6	2-#5	.0132	-----	----	4360	416	3.25	
Repeat	11.1	2.3	32	2-#8 2-#6	2-#5	.0132	-----	----	4440	432	4.23	
II18-5	11.1	2.3	44	3-#6 2-#6	2-#5	.0132	#4 wire at 4"	.00316	4425	429	2.98	
Repeat	11.1	2.3	44	3-#6 2-#6	2-#5	.0132	#4 wire at 4"	.00316	4500	446	4.40	
II18-6	11.1	2.3	44	3-#6 2-#6	2-#5	.0132	-----	----	4550	380	3.19	
Repeat	11.1	2.3	44	3-#6 2-#6	2-#5	.0132	-----	----	4570	538	4.06	
Wehr												
II1-1	11.2	2.25	44	3-#3 2-#6	2-#5	.0132	-----	----	3950	428	3.80	
Repeat	11.2	2.3	44	3-#3 2-#6	2-#5	.0132	-----	----	3870	411	3.75	
Spanan												
IA	11.1	2.3	32	2-#8 2-#6	2-#5	.0132	-----	----	3600	354	3.84	
Repeat	11.1	2.3	32	2-#8 2-#6	2-#5	.0132	-----	----	5130	557	4.06	
IE	11.1	2.3	32	2-#8 2-#6	2-#5	.0132	-----	----	4380	356	3.55	
Repeat	11.1	2.3	32	2-#8 2-#6	2-#5	.0132	-----	----	4740	454	3.79	
IIA	11.1	2.3	32	2-#8 2-#6	2-#5	.0132	#4 wire at 3½"	.00362	4090	450	3.63	
Repeat	11.1	2.3	32	2-#8 2-#6	2-#5	.0132	#4 wire at 3½"	.00362	4870	405	4.17	
IID	11.1	2.3	32	2-#8 2-#6	2-#5	.0132	#4 wire at 3½"	.00362	4590	477	3.94	
Repeat	11.1	2.3	32	2-#8 2-#6	2-#5	.0132	#4 wire at 3½"	.00362	4880	489	4.49	

Table 2. Properties of Concrete Strength Test Specimens.

Beam Designation	Compressive Strength f'_c psi *	Split Tensile Strength f_{st} psi	Modulus of Elasticity $E_c \times 10^6$ psi
I-1	2740	341	3.17
I-2	3600	379	3.61
I-3	3820	301	3.33
I-4	5090	460	3.47
II-1	2030	269	2.78
II-2	2450	305	3.07
II-3	3340	290	3.84
II-4	3620	279	3.44
II-5	4360	416	4.06
II-6	4380	478	3.91
II-7	4440	432	4.23
II-8	6750	618	4.62
III-1	2040	278	3.03
III-2	3210	306	3.19
III-3	4550	380	3.19
III-4	4570	538	4.06
III-5	6810	471	4.38

All specimens have as longitudinal reinforcement with AASHTO Cutoffs: Top 2-#6, Bottom 2-#5. The percentage of longitudinal reinforcement is $p = 0.0132$. The modulus of elasticity is the initial tangent modulus.

* Average of 3 cylinders chosen at random from 6.

was no longer needed to resist tension in accordance with the governing criteria of the ACI or AASHTO Codes. Failure was restricted to the shear span, "a," by placing an excessive amount of web reinforcement in the cantilever and the region outside the load P_2 .

The specimens were grouped into three series according to the length of the shear span, "a."

Series I a = 24"

Series II a = 32"

Series III a = 44"

Further classification was obtained by numbering the beams in proportion to their increasing concrete strength. All repeated specimens have the same designation as in the original theses and are also included with the data to determine the effect of the concrete strength if they had the longitudinal reinforcement terminated according to AASHTO.

Materials

Concrete Mix

All concrete was made with Type 1 portland cement, ASTM C29. The mixes were proportioned according to ACI Standard 613-54, "Recommended Practice for Selecting Proportions for Concrete," to give a slump of 3-4 inches. The water-cement ratios were selected to give the desired strength and ranged from 0.71 to 0.645.

Aggregates

The aggregates used were purchased from a local supplier. The coarse aggregate was a natural gravel of 1" maximum size. At the laboratory it was sieved into two sizes to minimize segregation during handling. Using Fuller's Maximum Density Curve 48 per cent of No. 4 to 1/2" was combined with 52 per cent of 1/2" to 1" size, by weight. Average properties of the fine and coarse aggregates are shown below.

<u>Type</u>	<u>Sp. Gr..*</u>	<u>Absorption</u>	<u>Fineness Modulus</u>
Fine	2.83	1.26 per cent	2.87
Coarse	2.65	1.37 per cent	-1" max. size

*Based on saturated-surface-dry weight

Gradation of Fine Aggregate

<u>Sieve Size</u>	<u>Per Cent Retained</u>
No. 4	1.4
8	16.6
16	36.8
30	48.0
50	87.8
100	96.6

Reinforcing Steel

The longitudinal steel was a high strength steel with average properties as shown in Table 3. The No. 5 and 6 deformed bars were rolled from the same heat and specially selected to give the required yield strength. The properties shown are averages for several coupons chosen at random. A representative stress-strain curve is shown in Figure 57, Appendix A. The deformations met the requirements of ASTM-A305.

Table 3. Properties of Longitudinal Reinforcement.

Yield Stress	72,100 psi
Ultimate Stress	113,000 psi
Modulus of Elasticity	29.6×10^6 psi
Elongation in 8"	16.6 %

The 1/4" diameter plain bars used for stirrups in the 18" interior span and the overhang were of hard grade steel, ASTM-A15 having an average yield stress of 52,000 psi and an average ultimate strength of 81,700 psi.

The web reinforcement used in the shear span "a" was a very soft No. 4 wire, diameter = .225". Coupons of this steel were selected to give the average properties shown in Table 4. A representative stress-strain curve is found in Figure 58, Appendix A.

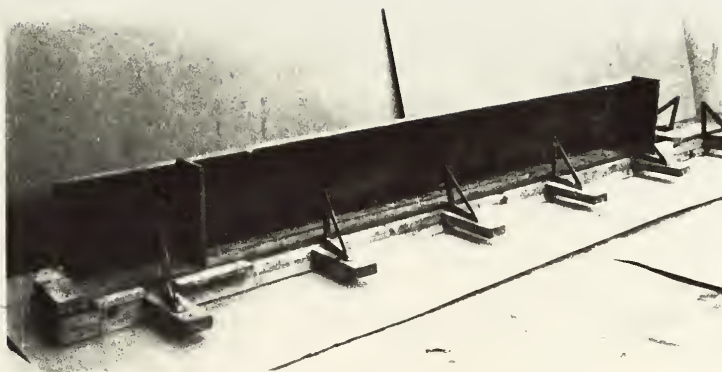
Table 4. Properties of Soft Web Reinforcement.

Yield Stress	24,100 psi
Ultimate Stress	43,700 psi
Modulus of Elasticity	27.2×10^6 psi

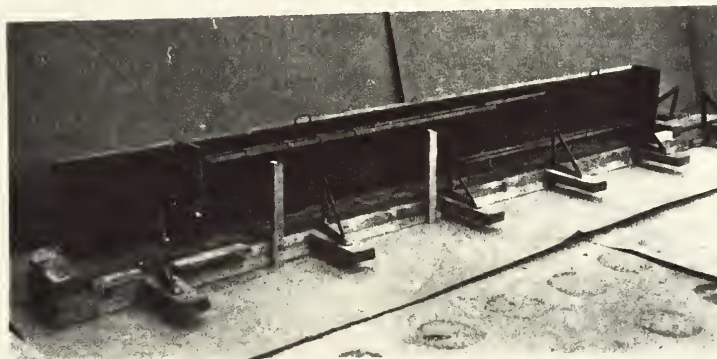
Fabrication and Curing

All specimens were cast in 3/4" plywood forms which were treated to reduce deterioration due to the repeated wetting and drying. The forms are shown partially assembled in Figure 4. Bracing was supplied by the 1" x 1" angles bolted to wooden 2 x 4's. Tie rods were placed through angles on the bulkheads to keep the bulkheads in place during casting.

The reinforcement was wired into a rigid cage with the stirrups wrapped around the longitudinal steel. A minimum of 1.4" clear between the longitudinal steel was obtained by wiring the bars to the stirrups. Cover of 1.5" was maintained on the sides by using wooden blocks which were removed as the concrete was placed. The reinforcement was placed on rigid steel chairs to provide 2" clear cover on the bottom under the interior load. The steel to resist the negative moment was supported on steel bars fitted through the forms to provide the proper effective depth. These bars were removed after the concrete attained initial set. Handles made from the 1/4" plain bars were wired to the stirrups at each



(a) FORMS ONLY



(b) FORMS AND REINFORCEMENT

FIGURE 4.
FORMS PRIOR TO CASTING

end of the beam to facilitate moving the beam after the concrete hardened.

The concrete was mixed for about 10 minutes in a stationary rotating drum mixer with a maximum capacity of eleven cubic feet. All of the materials were weighed before mixing was started. Six 6" x 12" control cylinders were cast with each specimen. The concrete was placed by shovel and consolidated with a 3/4" internal vibrator.

Several hours after placing the concrete the top of the forms and the cylinder molds were covered with moist burlap. A sheet of plastic was then placed over the burlap. Forms were kept on as long as possible to promote better curing. During this time the burlap was kept moist. Two days prior to testing the covering and forms were removed so the beam could be prepared for testing. Specimens cast during the summer months were taken from the forms as soon as possible and placed in a moist room along with the control cylinders in order to control the curing. These were removed two days before testing.

Instrumentation and Testing Procedures

A Baldwin hydraulic testing machine of 600,000 lb. capacity was used to provide the load for testing the repeats from Harvey's thesis [9], and Wehr's thesis [19]. The load for the specimens from Spanan's thesis [18] and the study of variable concrete strength was from a remote hydraulic jack actuated by an Amsler Pendulum Dynamometer with automatic load maintainer. Figure 5 gives a general view

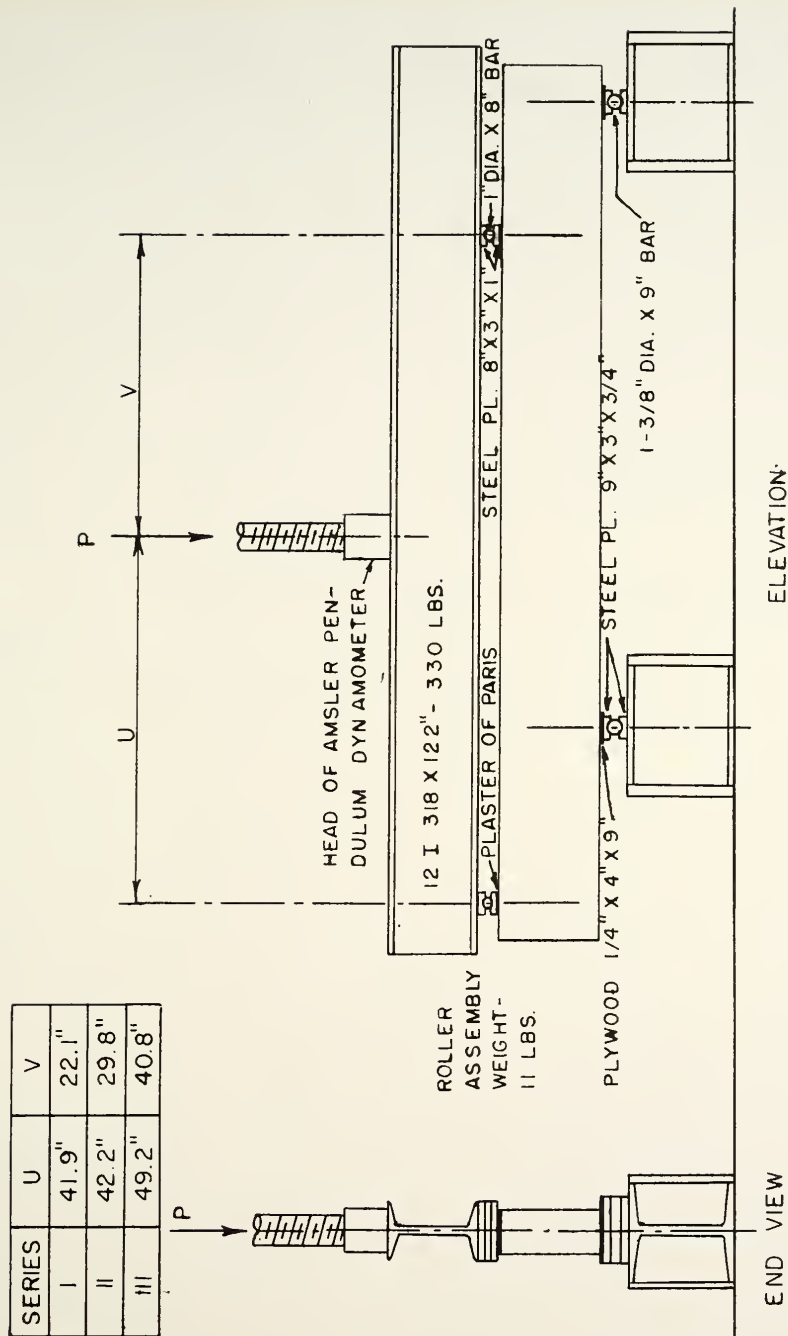


FIGURE 5. TEST SETUP

and details of the setup respectively. Steel strains were measured with foil type electric strain gages (Budd Metal-film C6-141B). The gages were affixed to the reinforcement at prepared locations with Eastman 910 adhesive. The gages and their lead wires were waterproofed and protected with an epoxy compound (Epoxylite No. 222). Strain in the longitudinal steel was measured at the point of maximum moment and in the critical shear span. Strains were also measured on some of the stirrups located within the critical shear span. The actual location of each of the gages is shown on the crack pattern sheets.

Surface strains in the concrete compression zone were measured at 3 1/2" from the interior support into the shear span "a." Paperback SR-4 wire gages (BLH A-1-S6) were cemented to the concrete surface using Duco cement. The concrete surface had been smoothed with a wire brush, cleaned with acetone, and sealed with Duco cement one day prior to the application of the gages. The vertical position of these gages varied from beam to beam and the actual location is shown on the individual crack pattern sheets.

Deflections under the overhang were measured with two 0.001" Federal dial gages supported by two ringstands. An aluminum angle was clamped onto the bottom of the beam with the movable stem of the gages compressed and resting upon it. In this manner the deflected beam moved away from the gage.

The sides of each beam were painted white and gridded so that the crack pattern was easily visible and could be drawn. After each load increment the crack penetration was traced and the load marked on the beam. After the test the beams were photographed and the crack pattern recorded.

The beam was loaded in increments of one to five kips, with decreasing increments as the load approached ultimate. Strains and deflections were recorded at each load increment. To monitor the strains, A Honeywell Digital Voltmeter, model 623 and Honeywell 620 Converter were used with a D.C. power supply of approximately 4.0 volts.

Three control cylinders were tested in compression for each specimen with the remainder in split tension. Two of the compression cylinders were used to determine the modulus of elasticity of the concrete with the aid of a 10 inch extensometer.

TEST RESULTS

Table 5 summarizes the pertinent test results of the repeated specimens along with the original tests. A tabular summary of the test results for the effect of concrete strength is found in Table 6. Photographs of some of the beams are shown in Figures 6 through 9. Strain and deflection data are shown graphically in this section and can be found in complete form in Appendix B. A brief description of each test is given to correlate the strains and deflection with the observed behavior of the beam. Scale drawings of each beam showing the crack pattern and gage locations are included. Figure 13 is a pictorial explanation of the way in which the crack patterns are presented. The loads recorded are applied loads only and do not include the weight of the loading apparatus and the dead weight of the specimen.

In beams without web reinforcement the formation of the diagonal crack was in most cases easy to determine. When web reinforcement was present and in some of the longer specimens the formation of the diagonal tension crack was more difficult to detect. For this reason the diagonal cracking load is defined as the load at which the critical diagonal crack was observed to reach the neutral axis, using the cracked-section theory. The neutral axis was nominally four inches from the compression face.

Table 5. Summary of Repeated Test Results.

Beam Designation	Diagonal		Ultimate Load P_u kips	Diagonal		Ultimate Shear Stress v_u psi	Failure Mode*	Remarks
	Cracking Load P_{cr} kips	Cracking Shear Stress v_{cr} psi		Cracking Shear Stress v_{cr} psi	Cracking Shear Stress v_{cr} psi			
<u>Harvey</u>								
IA-4	32	181	34	181	192	DT	gages in shear span	
Repeat	40	226	50	226	271	Combined		
IIB-5	25	116	29.1	116	135	DT		
Repeat	32	149	34	149	158	DT		
IIB-5	30	111	59.6	111	221	DT		
Repeat	40	148	53	148	185	DT		
IIB-6	30	111	30	111	111	DT		
Repeat	34	126	34	126	126	DT		
<u>Wehr</u>								
II-1	49	226	49	226	226	DT		
Repeat	46	212.2	47.6	212.2	219.5	DT	splitting along bottom steel	
<u>Spaman</u>								
IA	15	70	31	70	98			
Repeat	24	112	29	112	182	DT	extensive splitting along steel	
IE	34	158	48	158	223	SC		
Repeat	38	177	44	177	204	SC		
IIA	20	93	42	93	195			
Repeat	20	93	42	93	186	DT		
IID	35	163	67	163	311	SC		
Repeat	40	186	72	186	344	SC		

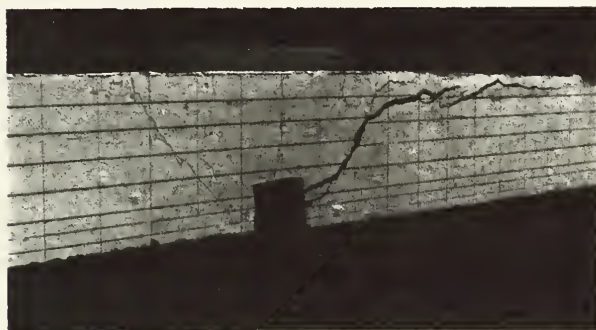
* DT = Diagonal Tension, SC = Shear Compression, Combined =

Table 6. Summary of Test Results for Concrete Strength.

Beam Designation	Concrete Strength f'_c psi	Diagonal Cracking Load P_{cr} kips	Steel Splitting Load P_s kips	Ultimate Load P_u kips	Diagonal Cracking Shear Stress v_{cr} psi	Steel Splitting Shear Stress v_s psi	Ultimate Shear Stress v_u psi	Failure Mode	Remarks
I-1	2740	20	24	34	104	125	177	SC	splitting after DT Formed
I-2	3600	36	36	46	187	187	239	SC, splitting	
I-3	3820	34	32	52	177	166	260	SC, splitting	
I-4	5090	39.8	39.8	39.8	206	206	206	DT	little splitting
II-1	2030	26	26	32	121	121	149	SC	followed by crushing and splitting
II-2	2450	33	33	33	154	154	154	DT	little splitting
II-3	3340	29	29	29	135	135	135	DT	Spanan IIC
II-4	3620	32	32	32	149	149	149	DT	Spanan IIC
II-5	4360	25	29.1	29.1	116	135	135	DT	Harvey IIB-5
II-6	4380	23	29	31	107	135	144	SC	Spanan IIC (18)
II-7	4440	32	30	34	149	140	158	DT	IIB-5 repeat splitting
II-8	6750	40	40	40	186	186	186	DT	
III-1	2040	32	28	34	119	104	126	DT	splitting
III-2	2210	28	28	28	104	104	104	Combined	DT and splitting
III-3	4550	30	30	30	111	111	111	DT	Harvey IIB-6
III-4	4570	34	34	34	126	126	126	DT	
III-5	6810	40	40	40	148	148	148	DT	



(a) BEAM I A

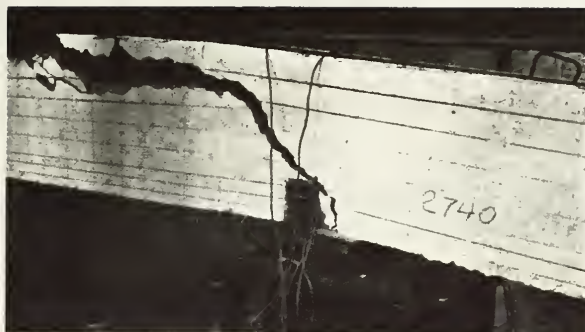


(b) BEAM I E



(c) BEAM II A

FIGURE 6.
REPEAT BEAMS OF SPAMAN AFTER TEST



(a) BEAM I-1



(c) BEAM I-3

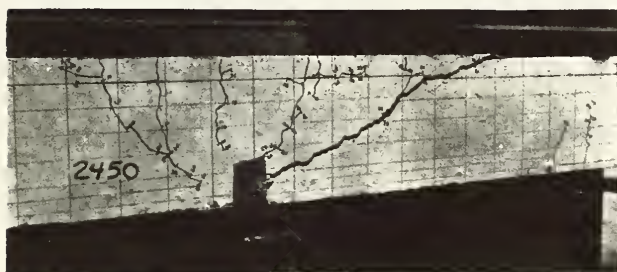


(d) BEAM I-4

FIGURE 7.
BEAMS AFTER TEST - SERIES I



(a) BEAM II - 1



(b) BEAM II - 2

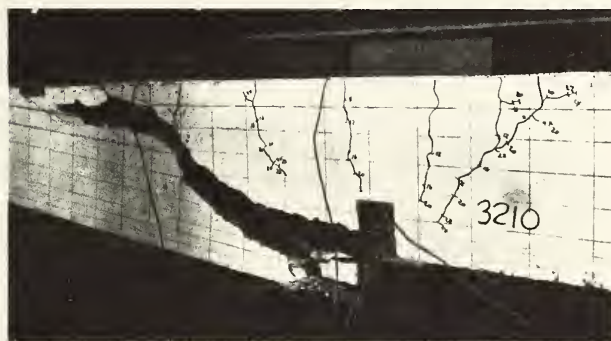


(c) BEAM II - 8

FIGURE 8.
BEAMS AFTER TEST - SERIES II



(a) BEAM III - 1



(b) BEAM III - 2



(c) BEAM III - 5

FIGURE 9.
BEAMS AFTER TEST - SERIES III

Repeated Tests

Harvey

Beam IA-4 (No Stirrups - 2 Layers of Tension Steel).

The original beam had strain gages in the shear span, 18" and 24" from the support, and failed suddenly at 34^k after the diagonal crack formed at 32^k . It was thought that the presence of these gages had an effect on the ability of the beam to reach a force equilibrium after diagonal cracking.

The repeat beam had strain gages on the steel only 3 1/2" from the support. The critical diagonal crack (Figure 14) formed at 40^k and penetrated to about 3" from the compression face. The concrete strain (Figure 11) showed the presence of the diagonal tension stress at 36^k . Splitting along the two rows of steel also began at 40^k and continued to failure. The development of the diagonal crack continued and it began to open wide at the failure load of 50^k . Failure seemed to be from the combined action of the splitting along the steel and the diagonal tension crack.

The crack pattern of the repeated beam was very similar to the original, but with more extensive flexural cracking due to the higher load. The critical crack was located in essentially the same position in both beams. The deflection of the repeat beam was larger than the original. Harvey's hypothesis about the presence of the gages in the shear span was evidently true.

. Beam IIB-5 (No Stirrups - AASHO Cutoff). What proved to be the critical crack (Figure 15) began to incline about 24^k and reached the compression zone at 32^k . Cracks on the side of the beam with the longer tension bar penetrated sooner than on the side with the shorter bar. Failure came suddenly at 36^k when the beam split into two pieces along the diagonal crack and the reinforcement. The critical crack was 2" from the compression face at 34^k and only minor splitting along the reinforcement had occurred.

The crack patterns of the repeat and original beams are remarkably similar and failure occurred in the same manner.

Beam IIIB-5 (4" Stirrup Spacing - AASHO Cutoff). While preparing the beam for testing a crack developed near mid-span in the shear span. The crack was primarily in the compression zone and did not seem to affect the behavior of the beam.

Several flexural cracks (Figure 16) inclined toward the support as the load was increased but did not penetrate the compression zone. The critical crack appeared at 40^k and reached the top of the compression zone. It was at the load of 40^k that the instrumented stirrup nearest this crack registered its first reading, 650 MII. The crack continued to penetrate and was nearly horizontal after 50^k . This crack continued traveling at a flat slope at 55^k but was still more than 14" from the support. An attempt to increase the load resulted in a diagonal tension failure when the crack split to the support.

Beam IIIB-6 (No Stirrups - AASHTO Cutoff). The failure crack formed suddenly at 34^k and was not visible at 32^k (Figure 17). Complete diagonal tension failure occurred with the appearance of this crack. The critical crack developed from a flexural crack which initiated at the cutoff point of the shorter longitudinal bar. After reaching the compression zone it became nearly horizontal. Splitting along the continuing tension bar was evident.

Both beams IIIB-5 and IIIB-6 failed in nearly the same manner as the original beams at approximately the same loads. In both cases the crack patterns, deflections and steel strains were similar to those of the original.

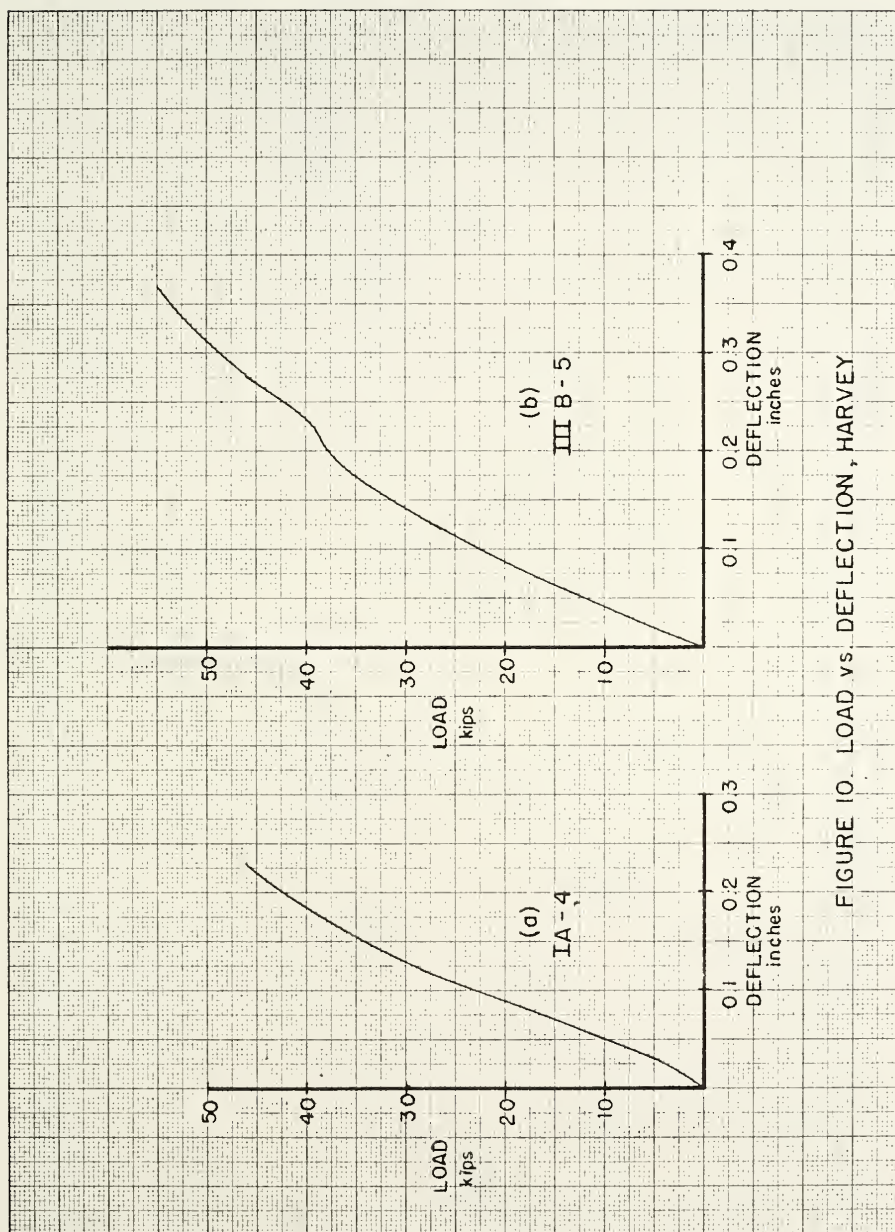
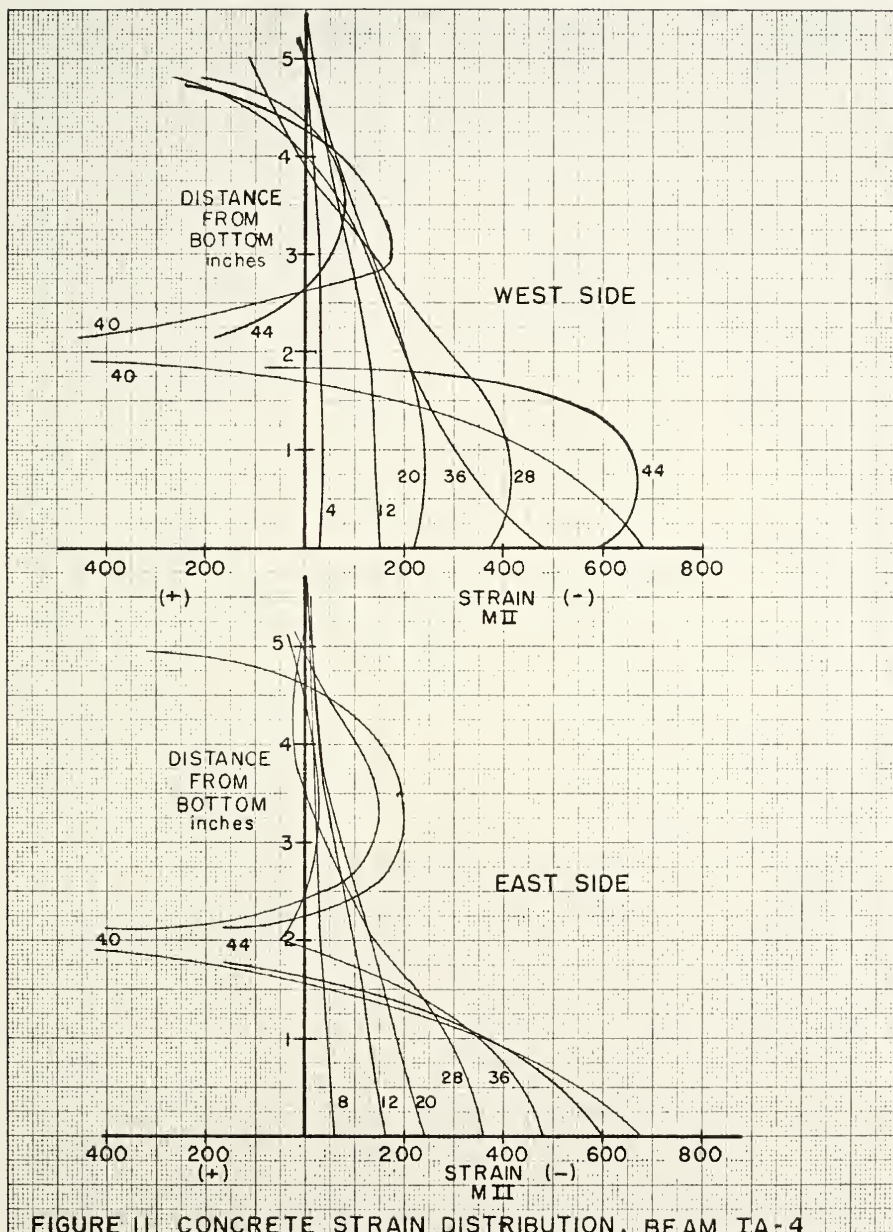


FIGURE 10. LOAD vs. DEFLECTION, HARVEY



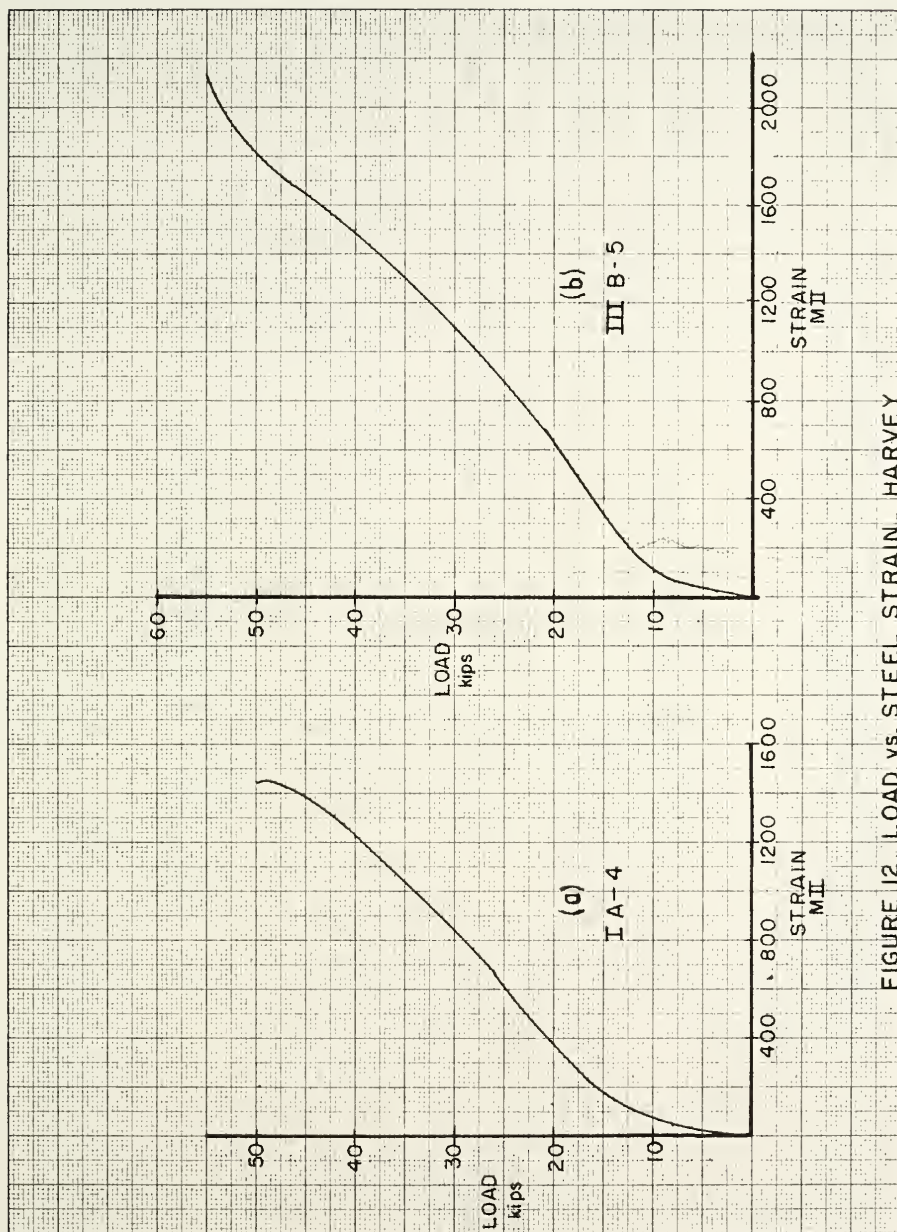


FIGURE 12. LOAD vs. STEEL STRAIN, HARVEY

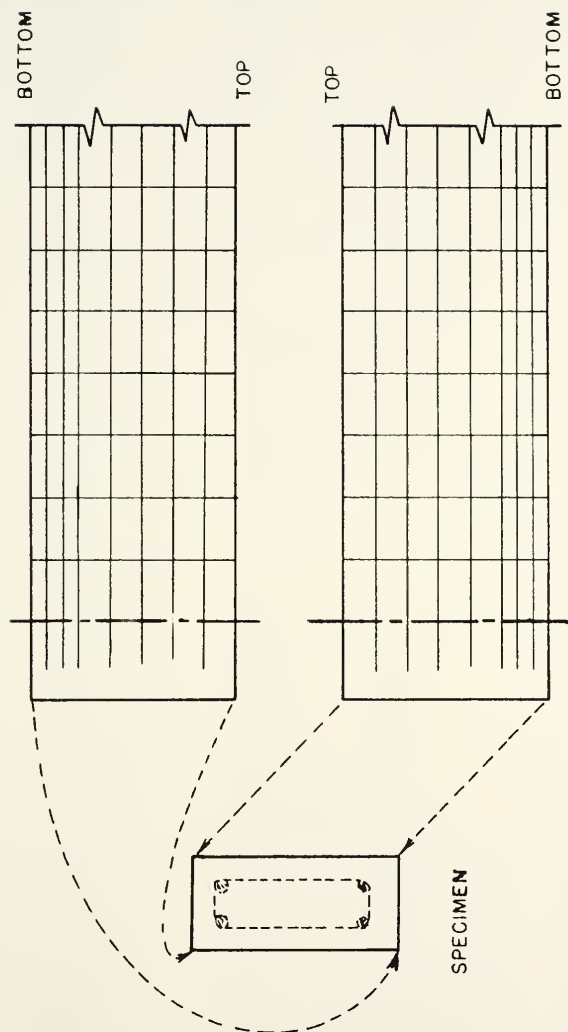


FIGURE 13.
PICTORIAL REPRESENTATION OF BEAM ON CRACK PATTERN

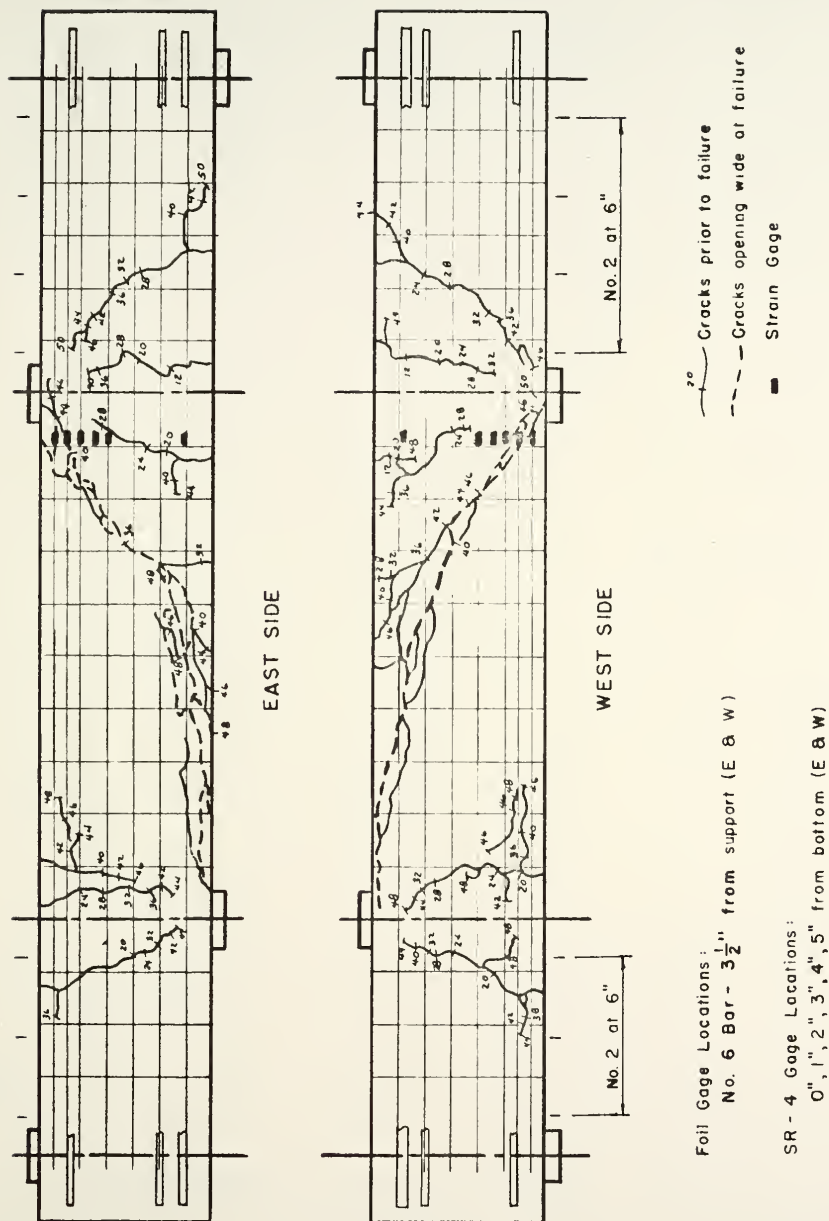


FIGURE 14. BEAM IA - 4

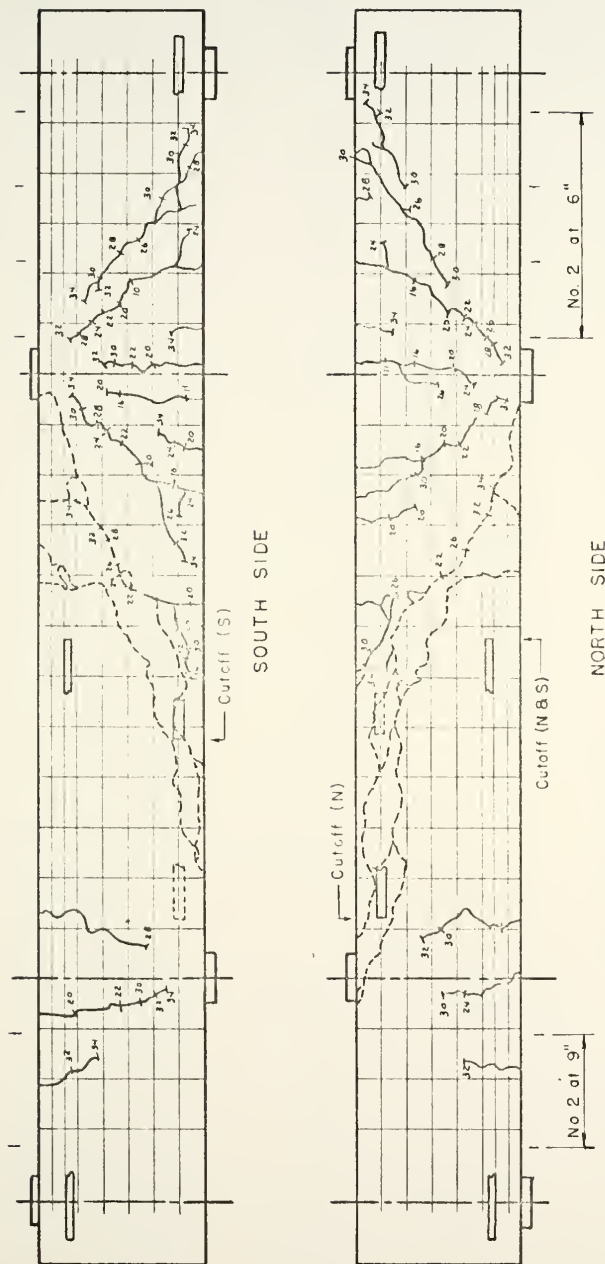


FIGURE 15. BEAM IB-5

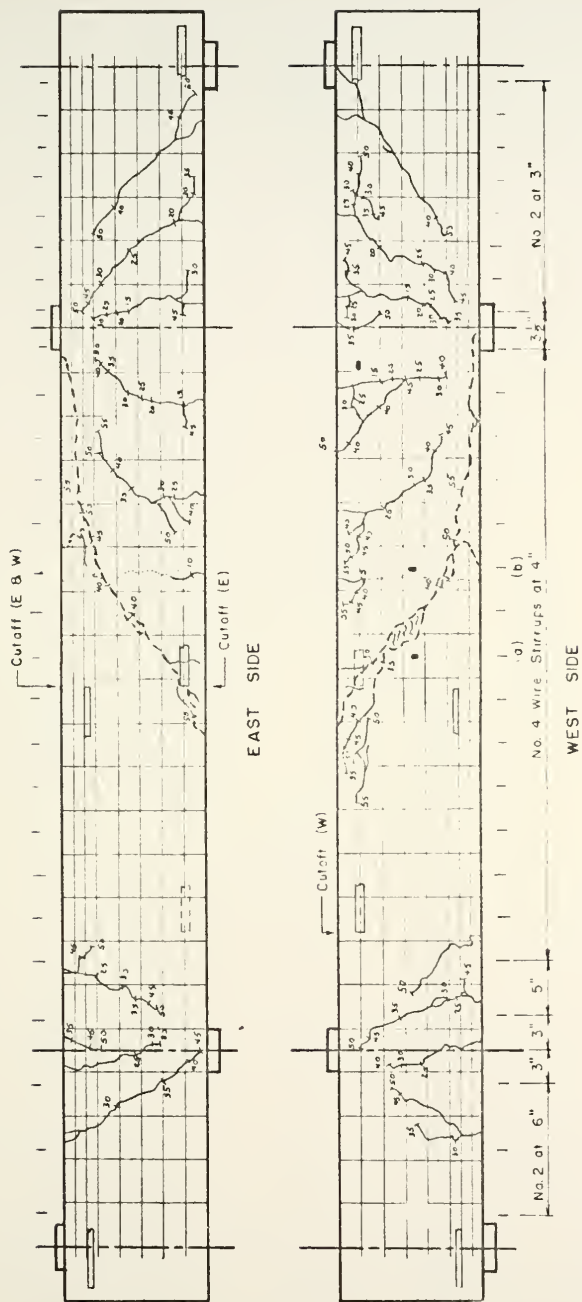


FIGURE 16. BEAM III 8-5

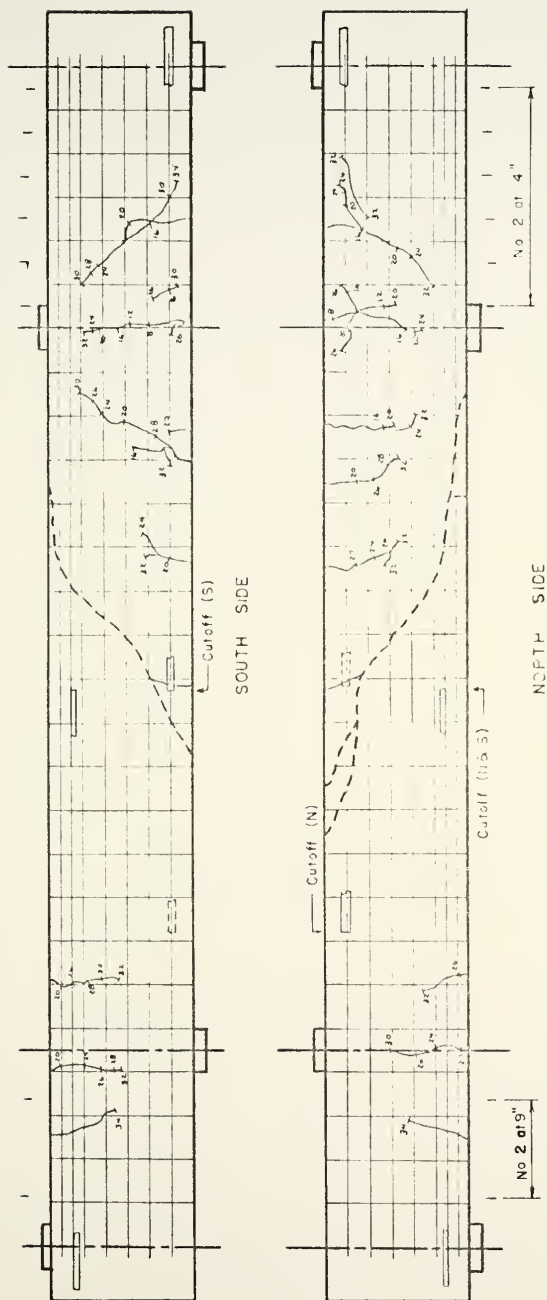
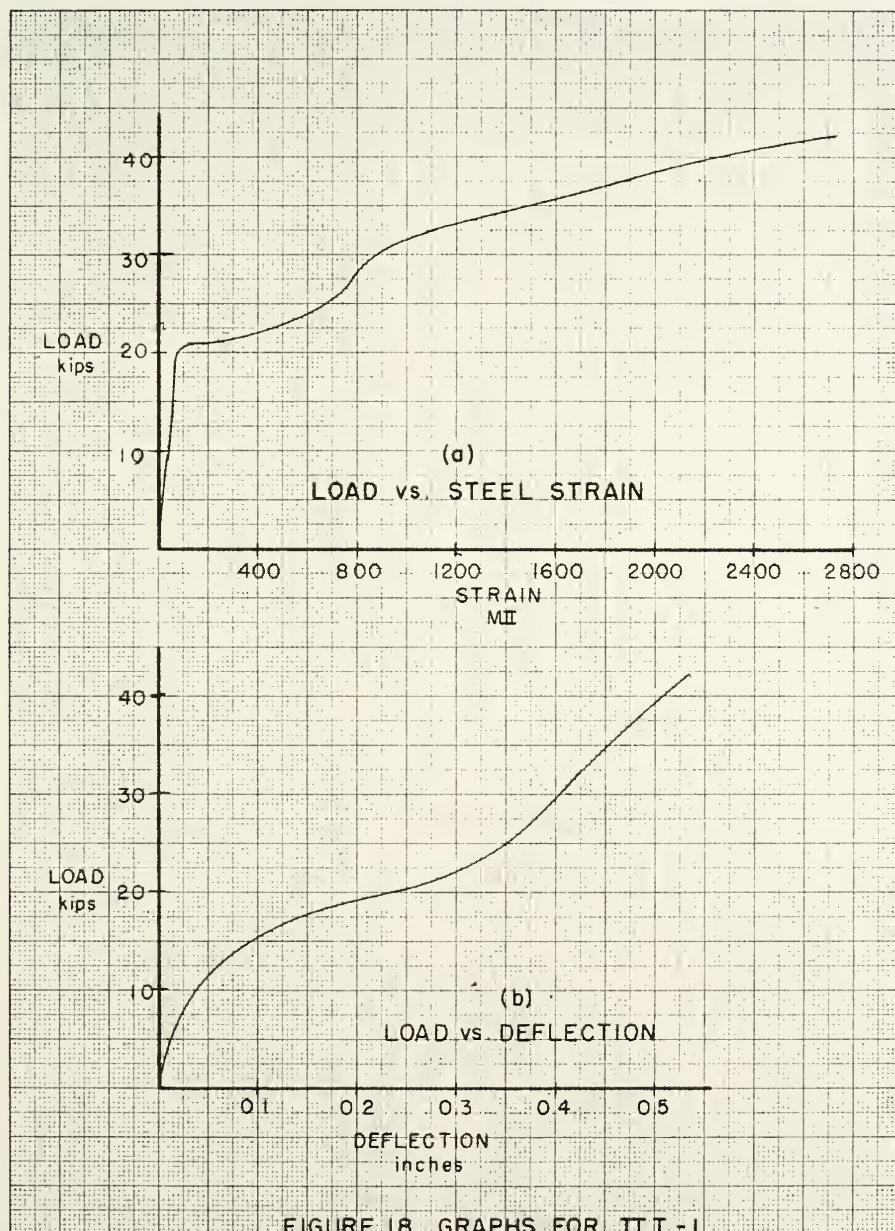


FIGURE 17. BEAM III B-6

Wehr

Beam IIT-1 (No Stirrups - No Cutoff). Steel strains and deflection (Figure 18) increased very slowly until the formation of the first tension crack through the flange at 25^k . This crack (Figure 20) penetrated to within 4" of the interior support and opened about $1/4$ ". The first diagonal crack formed at 40^k and on the south side this crack penetrated into the flange. This crack did not open wide at failure but served as the starting point for a crack which formed at 44^k , ran along the chamfer and opened wide at failure. On both sides parallel diagonal cracks opened wide at failure, with the latter splitting along the bottom reinforcement.

The strain distribution (Figure 19) shows that the neutral axis is about 3" from the compression face as opposed to 4" in the original beam. The failure cracks in the repeat beam formed farther from the support than that of the original beam even though the behavior and failure loads were similar.



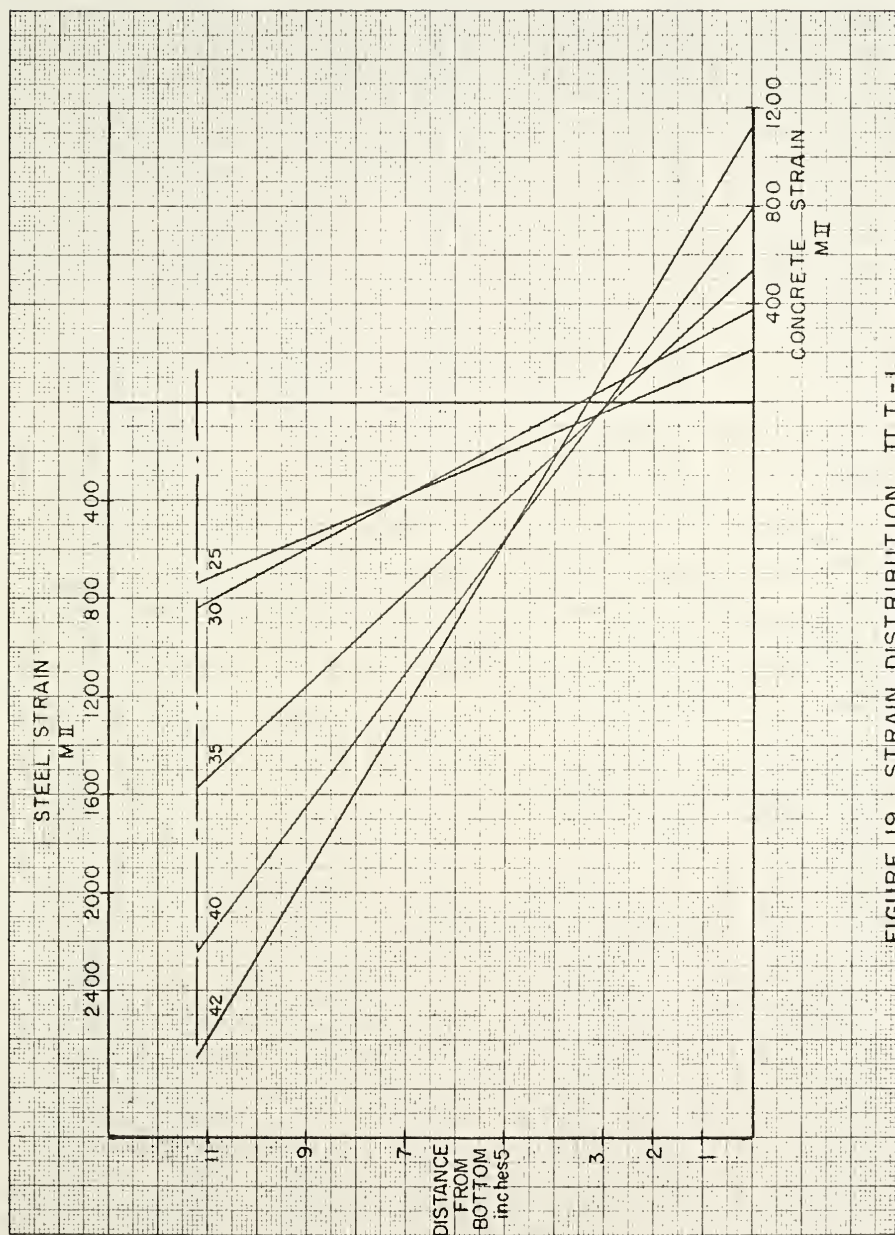


FIGURE 19. STRAIN DISTRIBUTION, II T-1

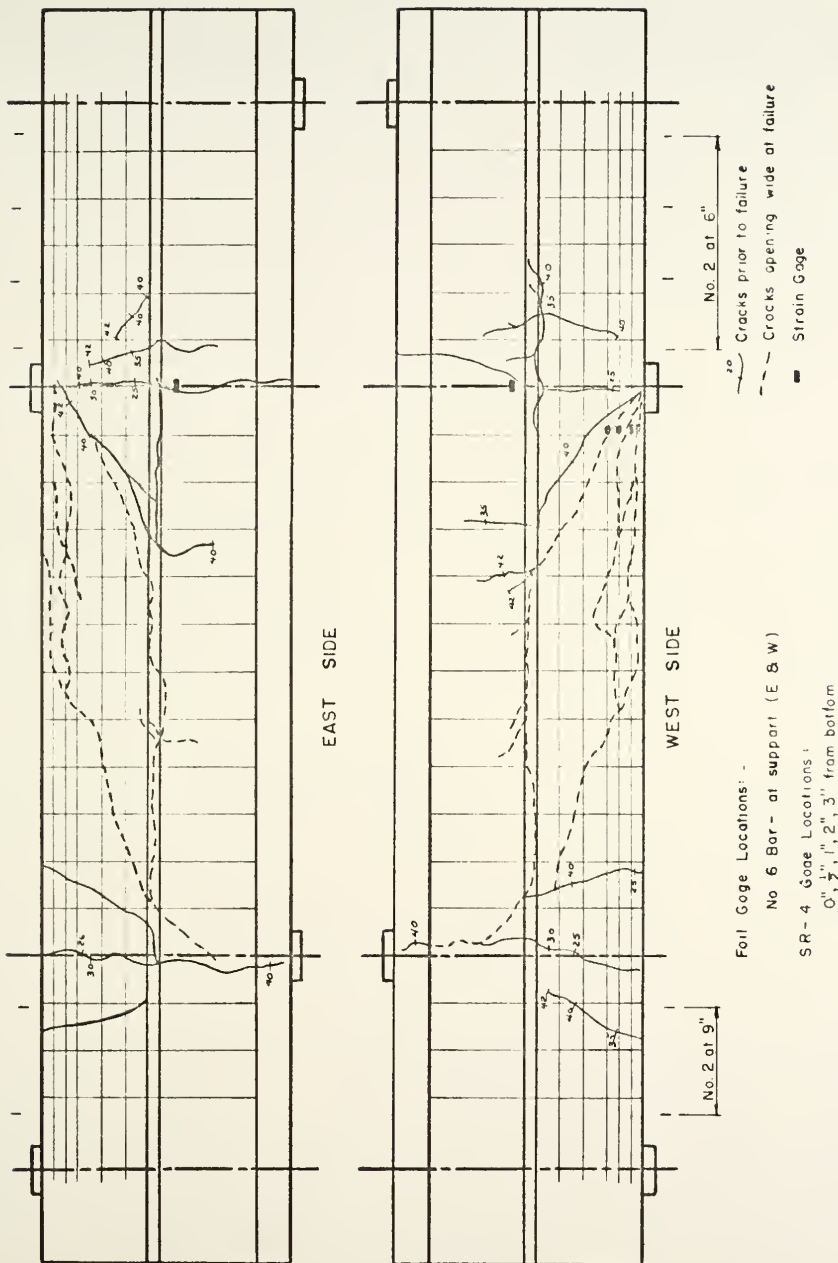


FIGURE 20. BEAM II T-1

Spaman

Beam IA (No Stirrups - Theoretical Cutoff). The critical crack (Figure 28) developed from the flexural crack nearest the cutoff point of the shorter bar. Progression of the crack was deeper on the south side of the beam which was the side with the shorter bar. It reached the compression zone at 24^k on this side and at 26^k on the north side. The concrete strain distributions (Figure 22) shows the effect of diagonal tension stresses at a load of 28^k . Splitting along the steel began at 22^k and is reflected in the greater increase of the strain in the second steel gage (Figure 26a). As splitting progressed the steel strain grew and the strain in the last gage increased fastest as failure approached. Diagonal tension failure and extensive splitting occurred at a load of 39^k .

The original beam failed in the same manner but at a load much lower, 21^k . The deflection of the original beam was nearly double that of the repeat. In both beams the strain in the central steel gage was the largest of the three after the formation of the diagonal tension crack.

Beam IE (No Stirrups - No Cutoff). The critical diagonal tension crack (Figure 29) began to incline at 34^k and reached the compression zone at 38^k . Also at 38^k the load deflection curve (Figure 21b) lost its linearity and deviated from that of the original beam. The concrete strain

distribution (Figure 23) became nonlinear about 25^k as the strain 2" from the compression face failed to increase. Failure came after holding 46^k long enough to record the steel strains. A sharp increase in the strain at the third gage (Figure 26b) was noted at 46^k .

Failure load, beam behavior and crack patterns were similar to those of the original.

Beam IIA (3 1/2" Stirrup Spacing - Theoretical Cutoff).

The critical crack (Figure 30) formed suddenly at 20^k and penetrated to within 3" of the compression face on the south side. Development on the north side was much slower and did not reach the compression zone until 34^k . The load was being applied unsymmetrically due to a misalignment of the I-beam and was removed after 28^k . Reapplication of the load showed a decrease in strain on the south side and an increase on the north side. The critical crack began to open wide at 32^k on the south side and penetrated through the compression face on that side at 36^k . Splitting along the continuing bar began at 34^k . At this load the steel strain at the third gage (Figure 27a) nearly equaled that of the second gage. Both were greater than that of the first gage. Again the strain in the last gage increased sharply as failure approached. Failure occurred at 39^k . The concrete strain distribution (Figure 24) was much more linear than that of its companion beam without stirrups (Figure 22).

The beam behaved as the original beam, except that the stress at the middle gage was greater on the original. This was probably due to the location of the critical crack.

Beam IIB (3 1/2" Stirrup Spacing - No Cutoff). The load was noted to be unsymmetrically applied at 35^k so it was removed and reapplied through a different I-section. All of the recorded steel strains were slightly larger while the concrete strains were slightly smaller after reapplication. The critical diagonal crack (Figure 31) entered the compression zone at 52^k about 9" from the support. This crack began to open wide at 64^k and resulted in a diagonal tension failure at 72^k when the load dropped to 51^k .

The concrete strain distribution (Figure 25) on the south side shows markedly the effect of the diagonal tension stresses beginning at a load of 58^k and continuing to failure. Strain at the third steel gage (Figure 27b) increased rapidly only after the critical crack opened wide.

The behavior of the original and repeat beam was very similar.

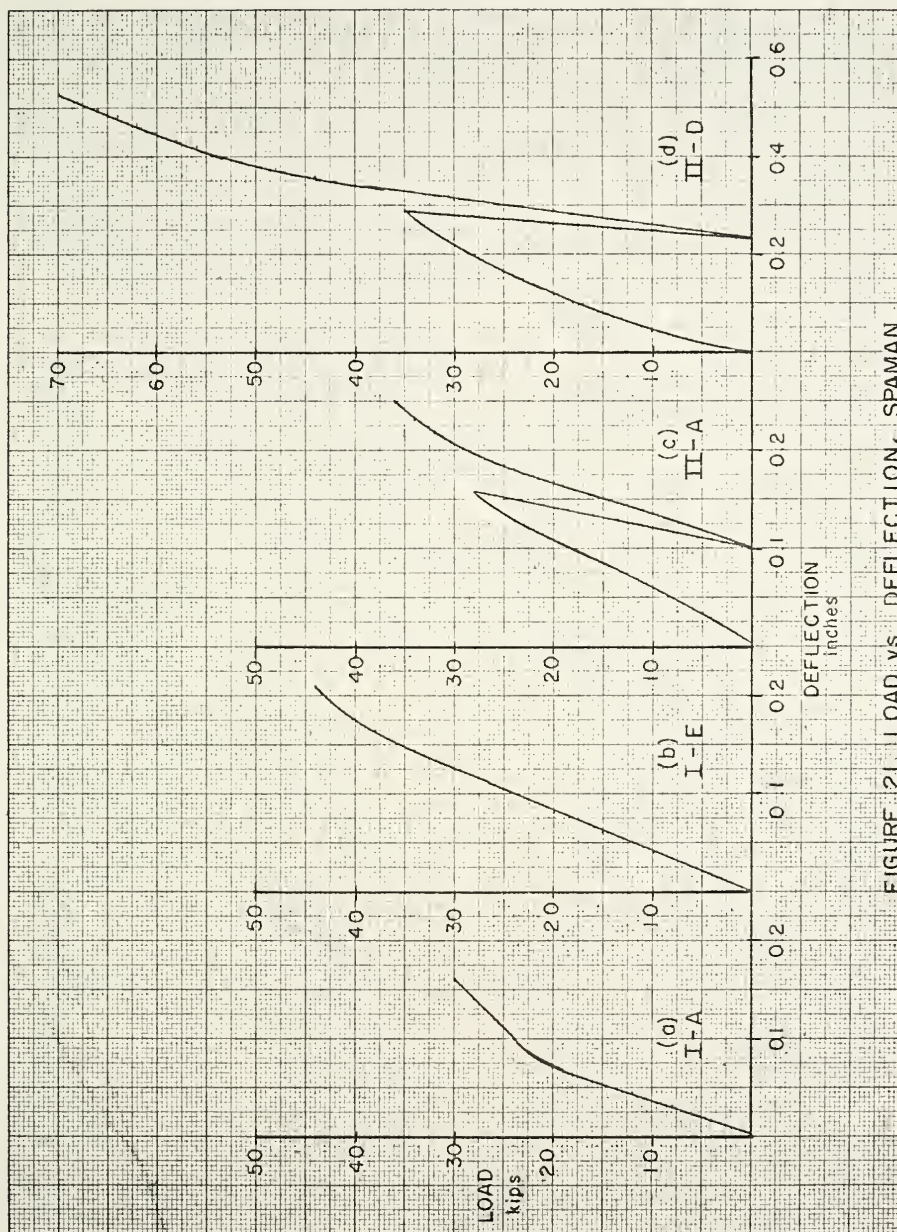


FIGURE 21. LOAD VS. DEFLECTION, SPAMAN

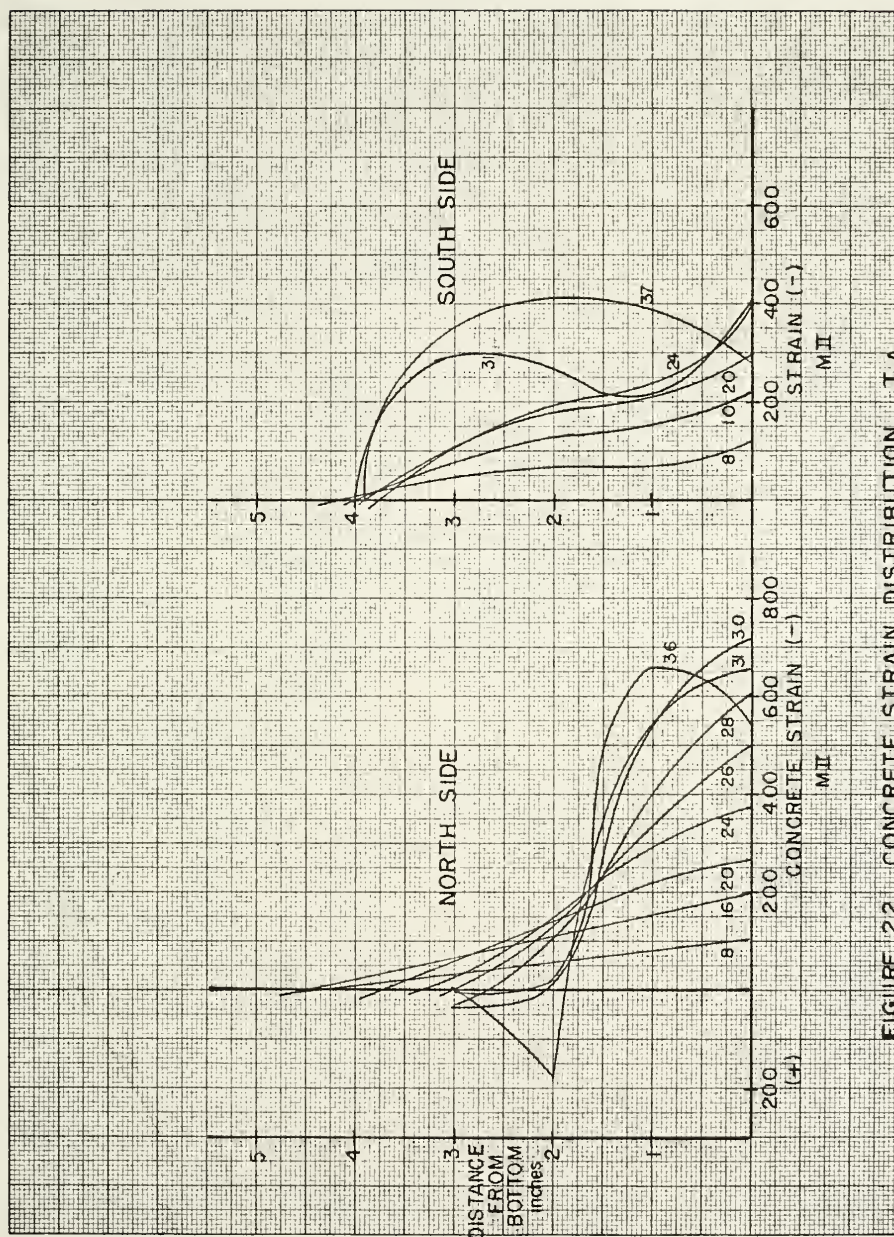
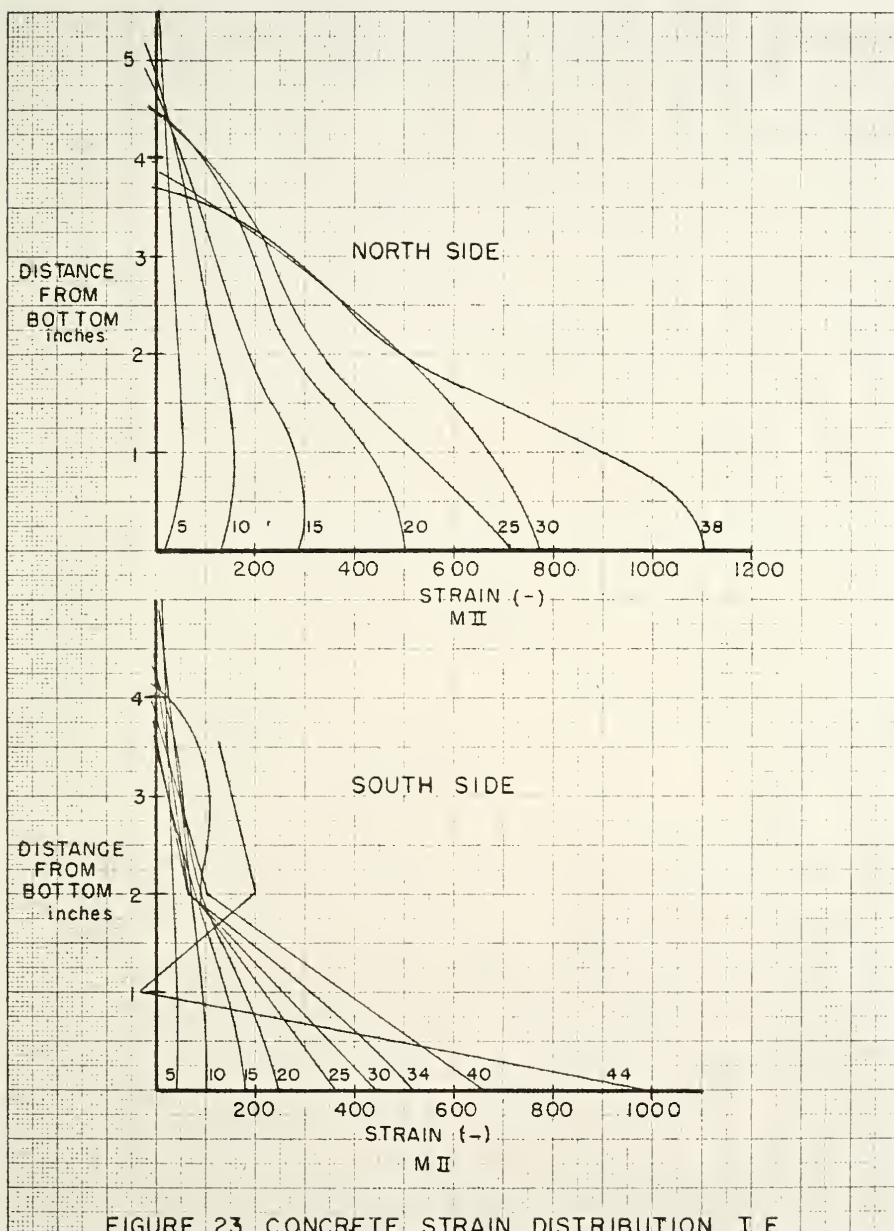
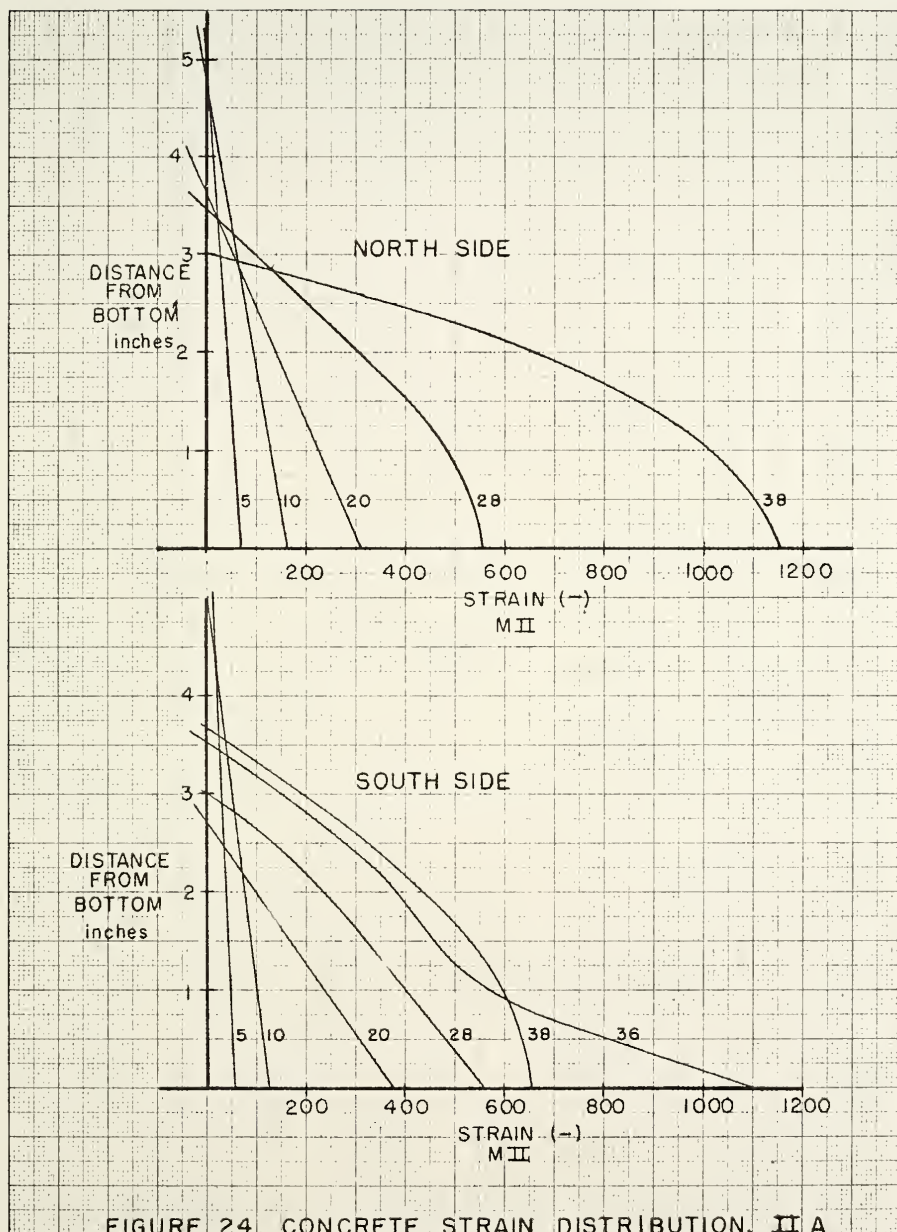


FIGURE 22. CONCRETE STRAIN DISTRIBUTION, I.A.





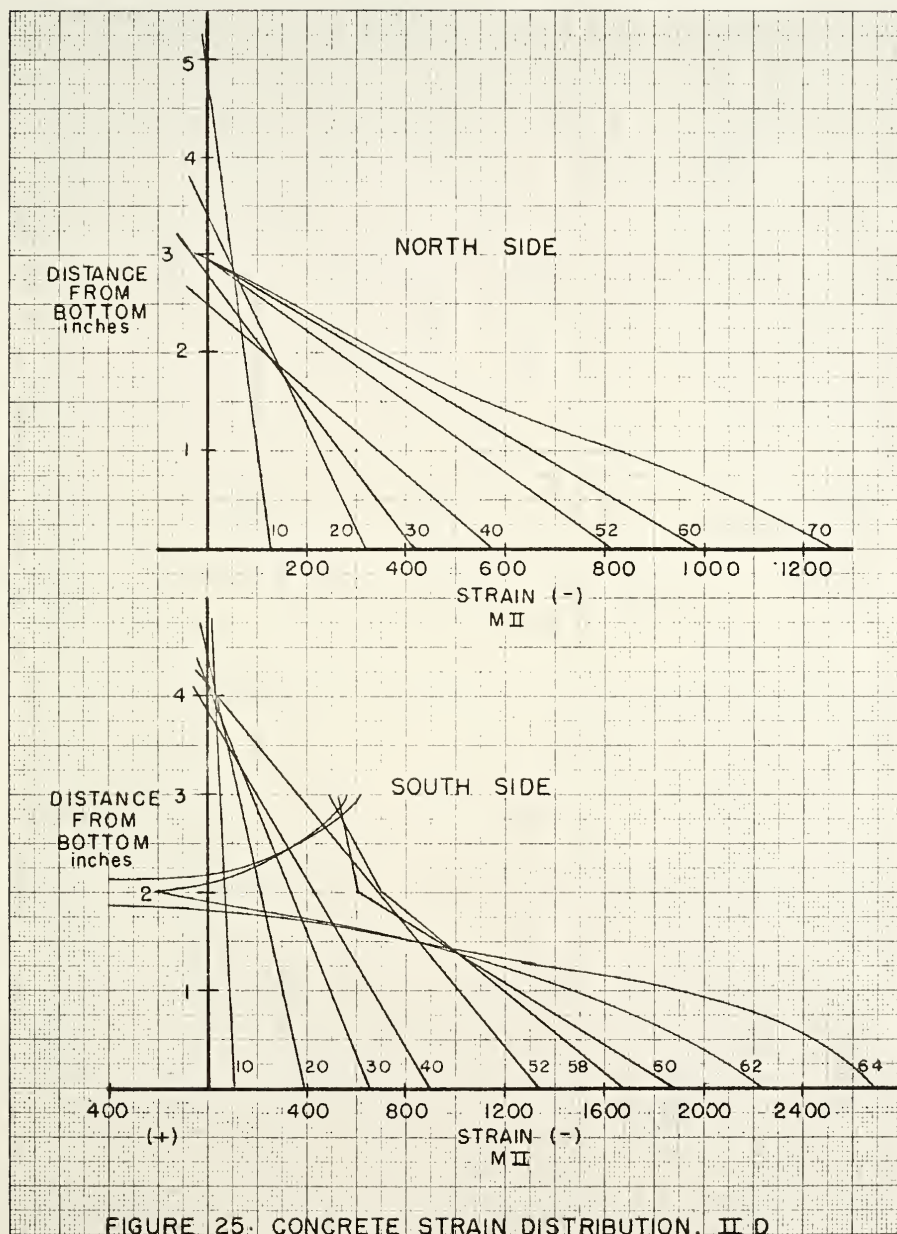


FIGURE 25. CONCRETE STRAIN DISTRIBUTION, II D

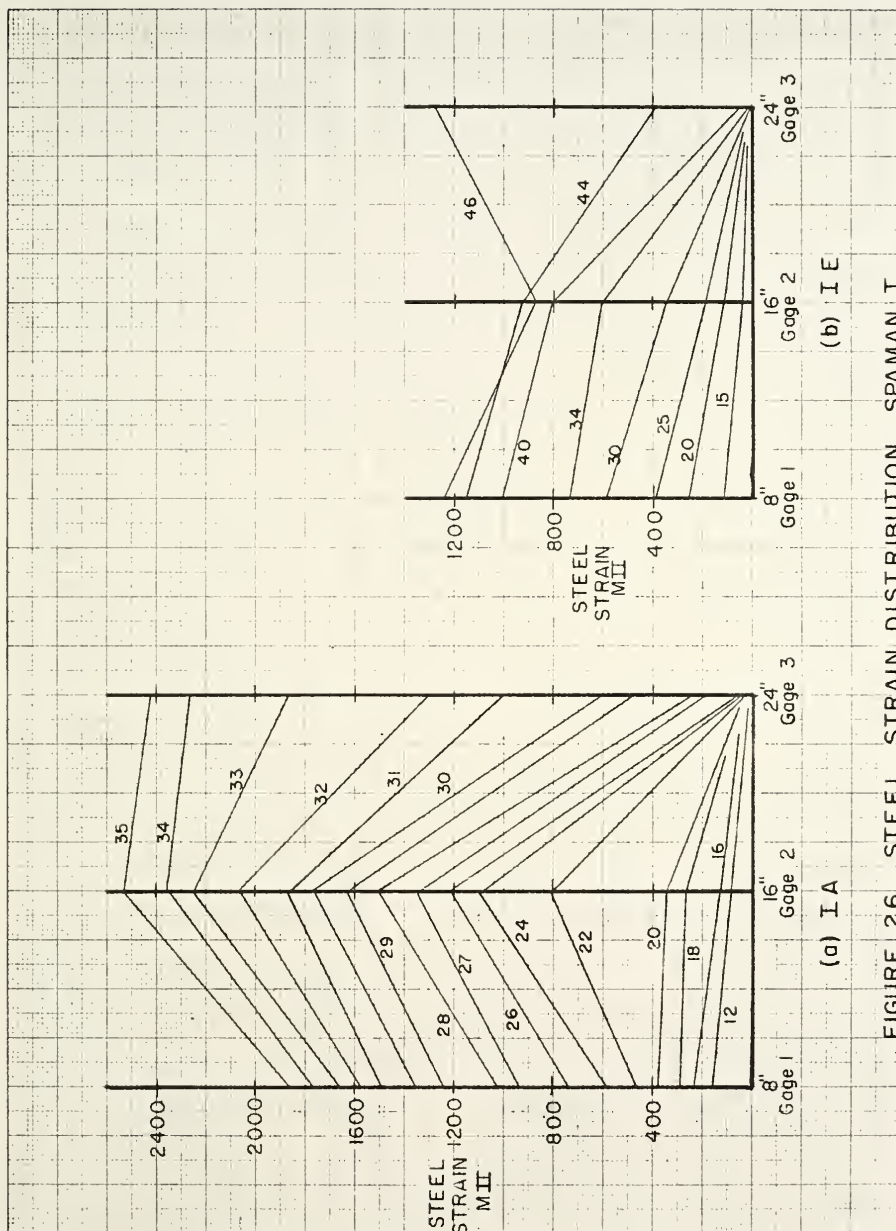
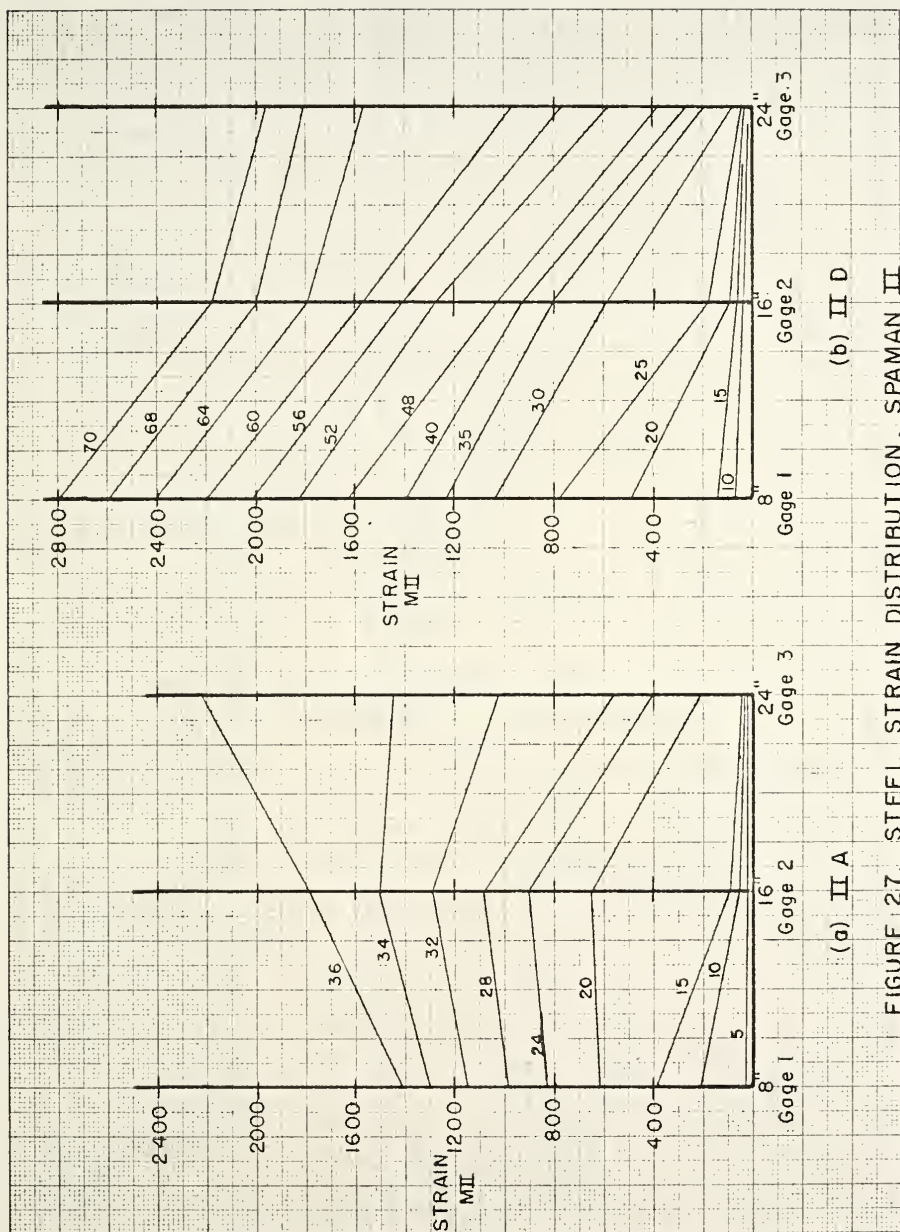


FIGURE 26. STEEL STRAIN DISTRIBUTION, SPAN I



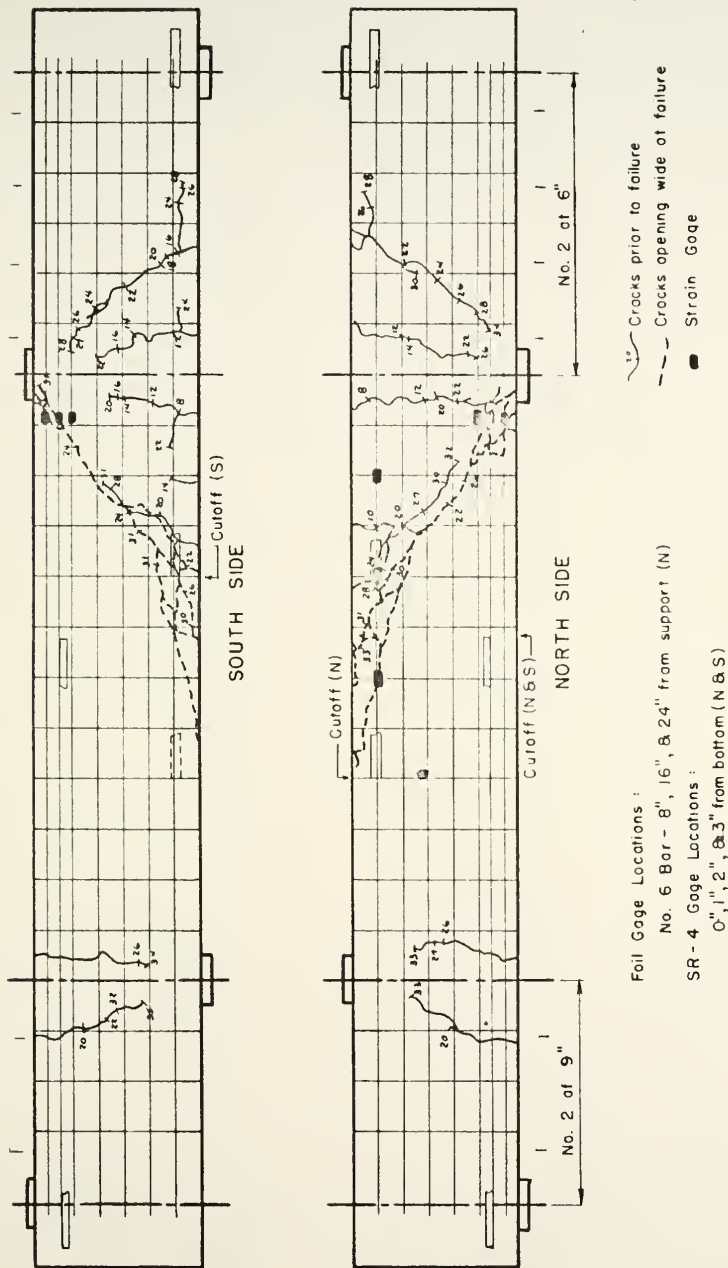
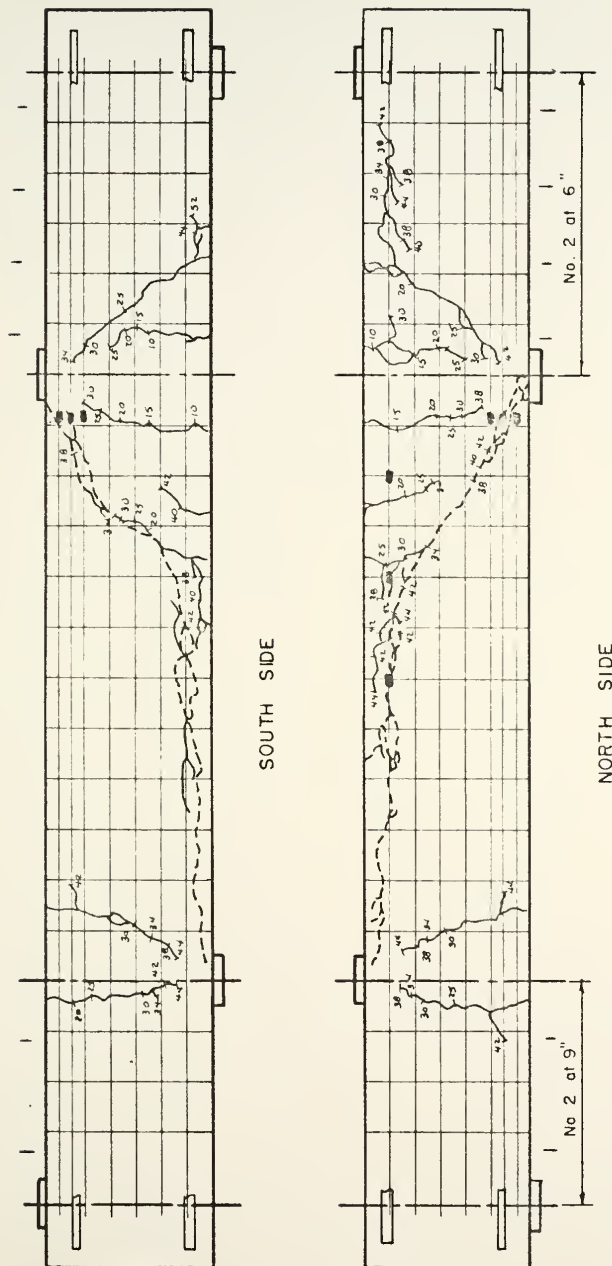
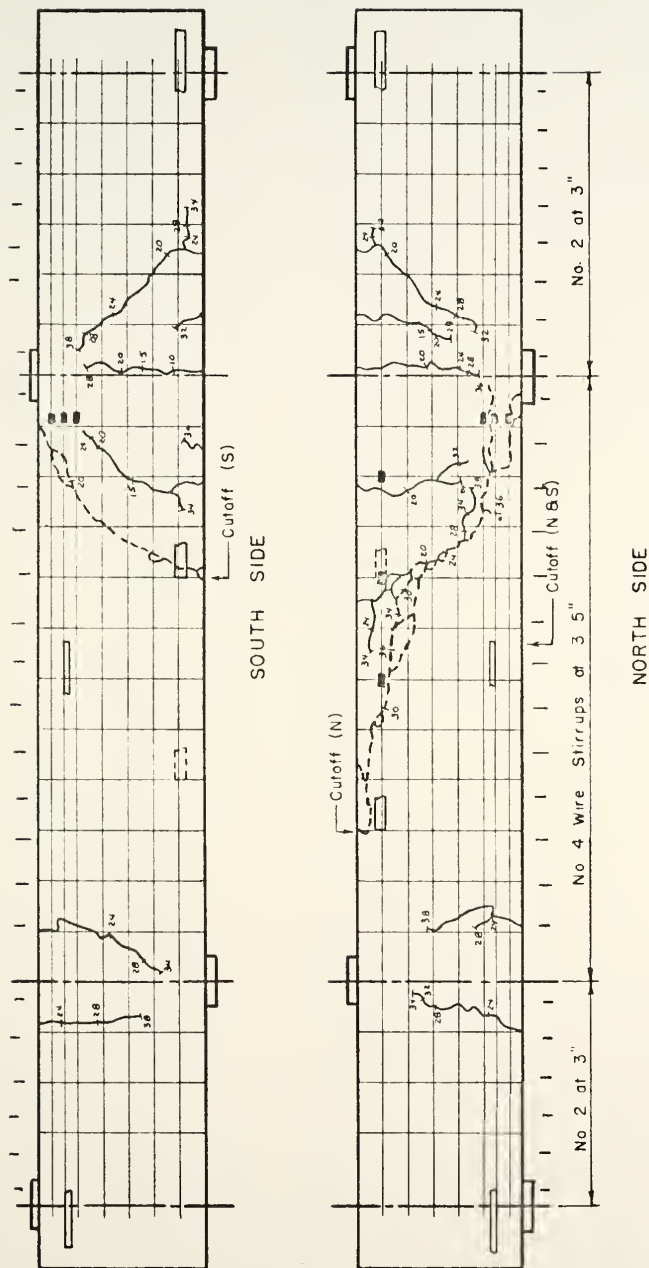


FIGURE 28. BEAM IA



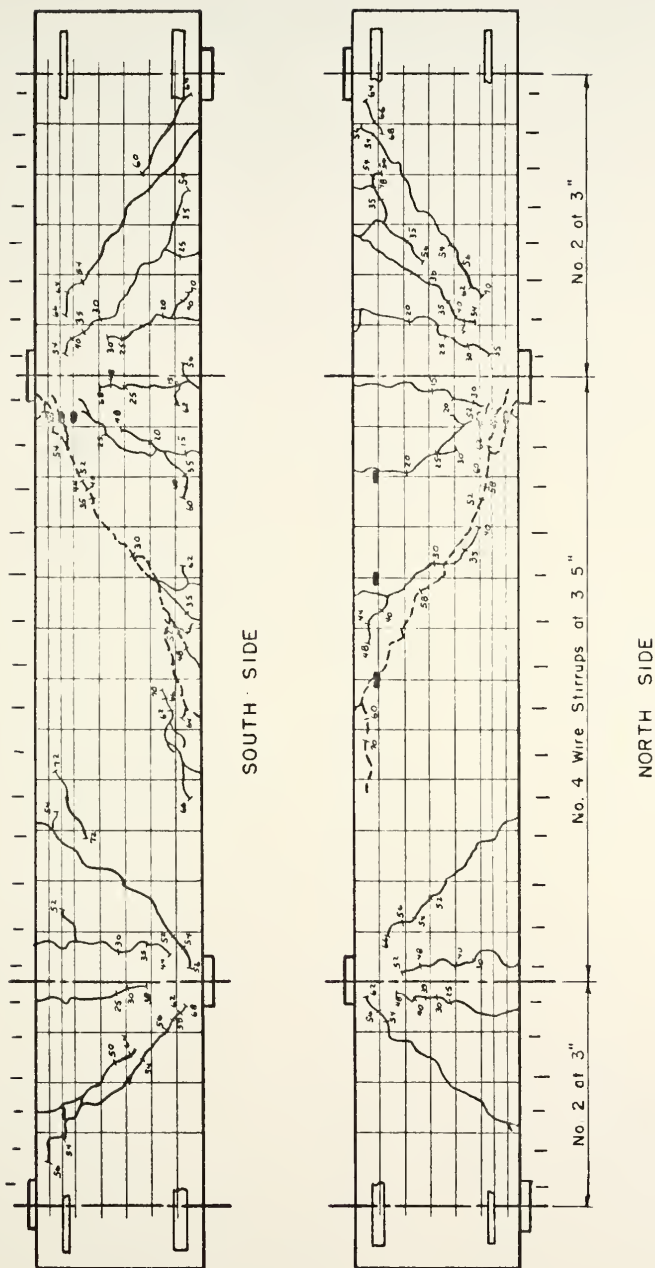
All gages as on Beam I A

FIGURE 29. BEAM I E



All gages as on Beam I A

FIGURE 30. BEAM II A



All gages as on Beam I A

FIGURE 31. BEAM II D

The Effect of Concrete Strength

All beams in the remainder of the investigation were similarly made with no stirrups and the longitudinal steel terminated in accordance with the AASHO requirements. The variables were the shear span and concrete strength. The beams were divided into three series by shear span and numbered with increasing concrete strength.

Series I, 24" Shear Span

Beam I-1 ($f'_c = 2,740$ psi). What proved to be the critical crack (Figure 36) began as a tension crack about 9" into the shear span. Penetration of this crack was much faster on the south side of the beam, the side with the shorter bar. This crack began to incline at 20^k and was 3" from the bottom on the south side. By 24^k splitting along the steel began on both sides. The diagonal tension crack began to open on the south side at a load of 30^k . The beam held 34^k long enough to take all readings. Splitting along the steel accounted for failure after the diagonal crack penetrated into the compression zone near the support. Extensive splitting existed.

The concrete strain distribution (Figure 33a) clearly shows that the north side of the beam had higher stress levels than the south side at loads after the diagonal crack formed.

Beam I-2 ($f'_c = 3,600$ psi). The critical crack (Figure 37) again developed from a flexural crack about 9" from the support but did not reach the compression region until 36^k . Splitting along the steel also began at 36^k . Failure came at 46^k by splitting along the steel causing extensive and explosive breakup of the concrete along the continuing bar.

The strain in the continuing bar (Figure 35a) in the shear span decreased when splitting along the steel began. Again, the concrete strain distribution (Figure 33b) on the north side had higher stress levels.

Beam I-3 ($f'_c = 3,820$ psi). In this beam slight splitting along the steel (Figure 38) began at 32^k before the critical crack reached the compression zone, 34^k , even though it had inclined from the originating flexural crack. Progression of the diagonal crack ended at 34^k until failure at 52^k when it penetrated to the support. Splitting continued until the steel split out at a load of 52^k .

The concrete strain distribution (Figure 34a) was very symmetrical until 28^k when the strain 2" up on the south side began to drop. It was also at 28^k that the steel strains (Figure 35b) increased markedly.

Beam I-4 ($f'_c = 5,090$ psi). The critical crack (Figure 39) did not reach the compression zone until failure at 39.8^k although it did begin to incline at 36^k . Failure was sudden diagonal tension at 39.8^k . The tension steel did not

split out and little splitting along the steel was present.

The concrete strain distribution (Figure 34b) was relatively symmetrical at 36^k but the effect of the diagonal tension stresses can be noted on the south side. The deflection (Figure 32d) was still essentially linear until failure.

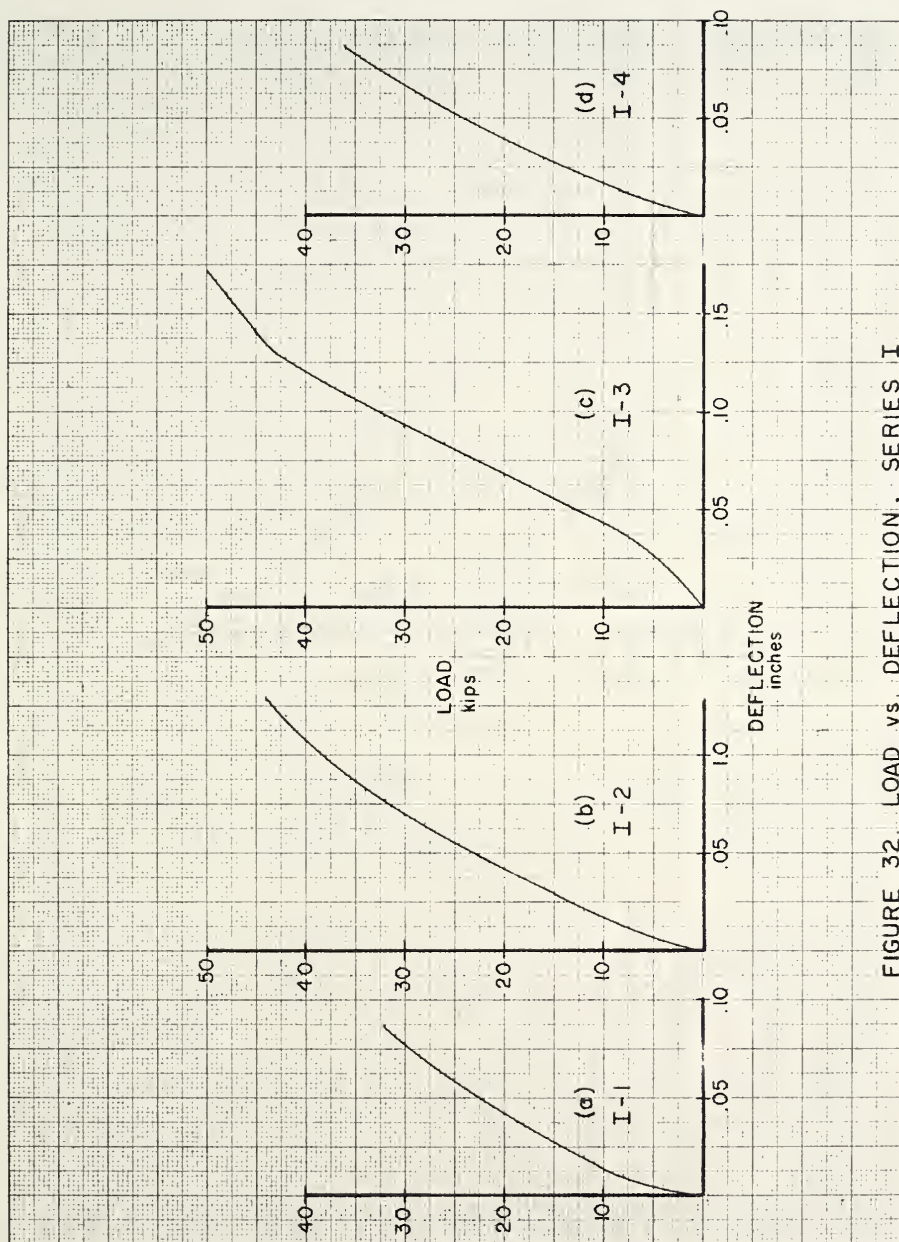


FIGURE 32. LOAD vs. DEFLECTION, SERIES I

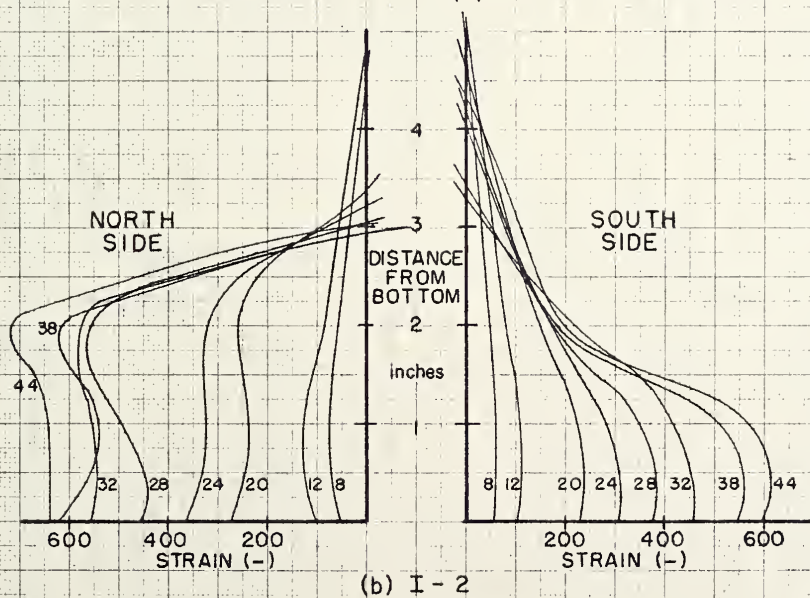
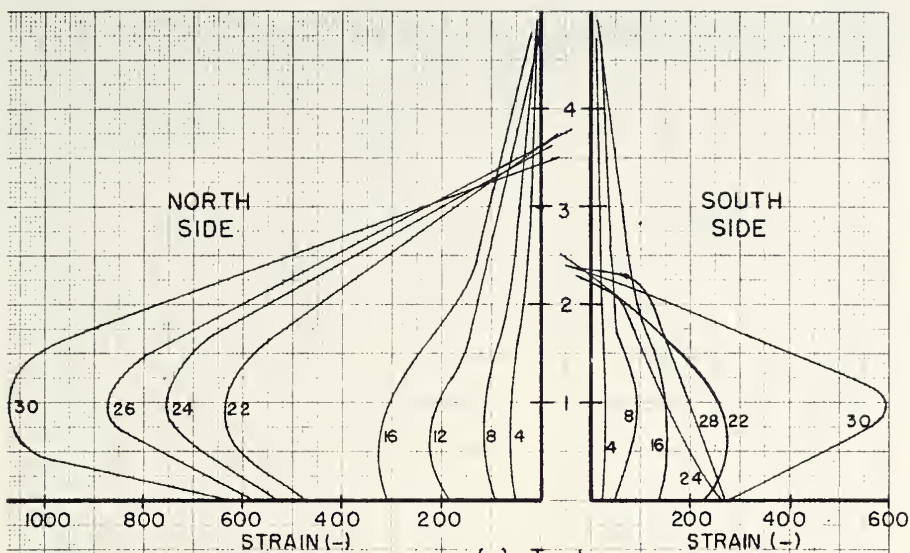


FIGURE 33. CONCRETE STRAIN DISTRIBUTION, I-1 & I-2

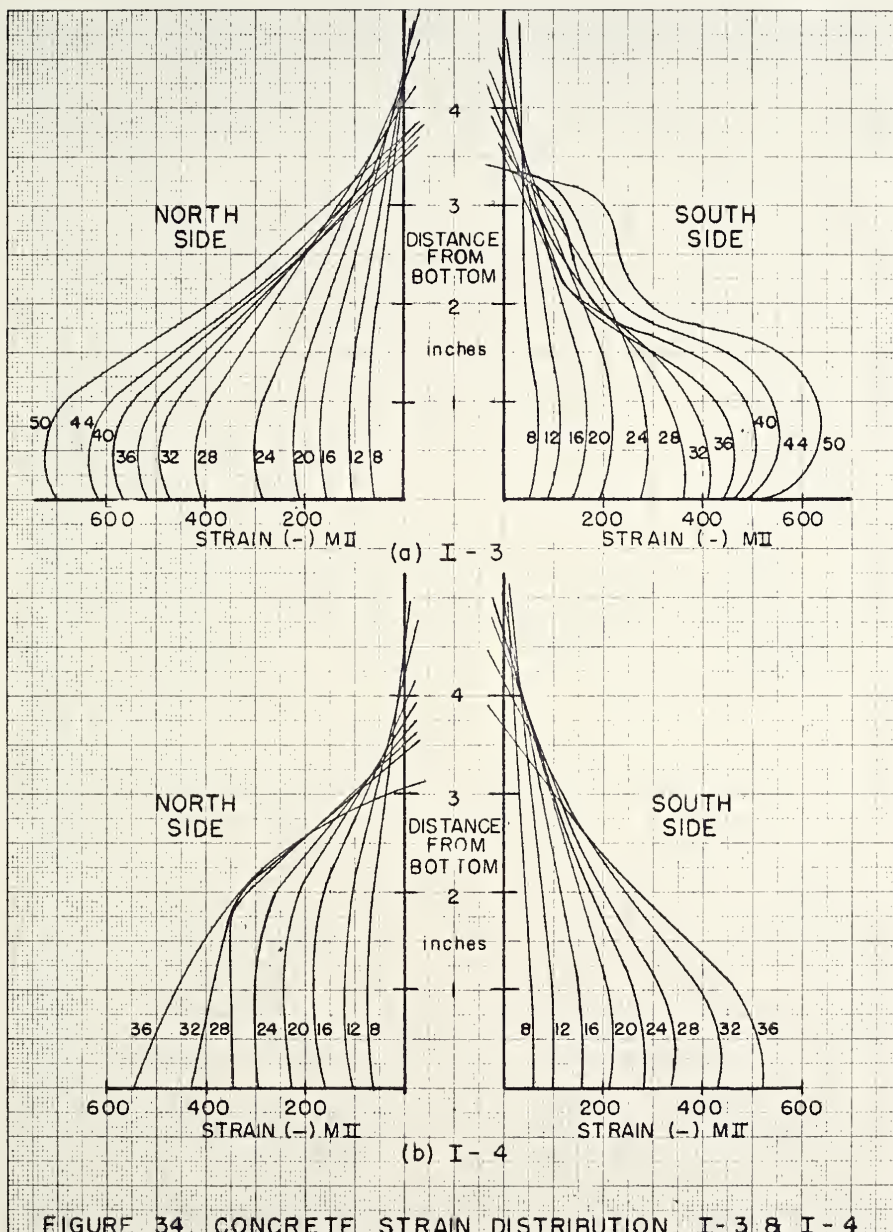


FIGURE 34. CONCRETE STRAIN DISTRIBUTION, I-3 & I-4

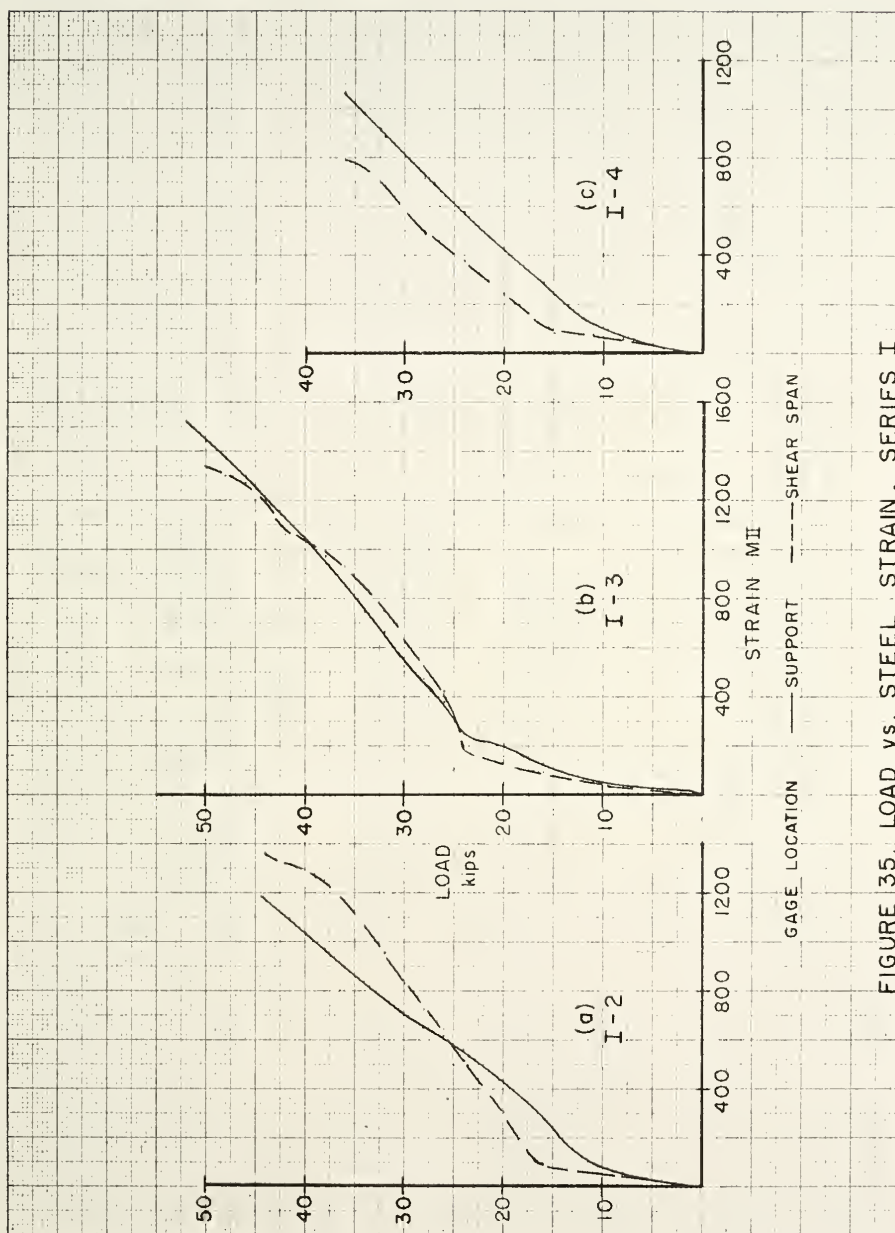


FIGURE 35. LOAD vs. STEEL STRAIN, SERIES I

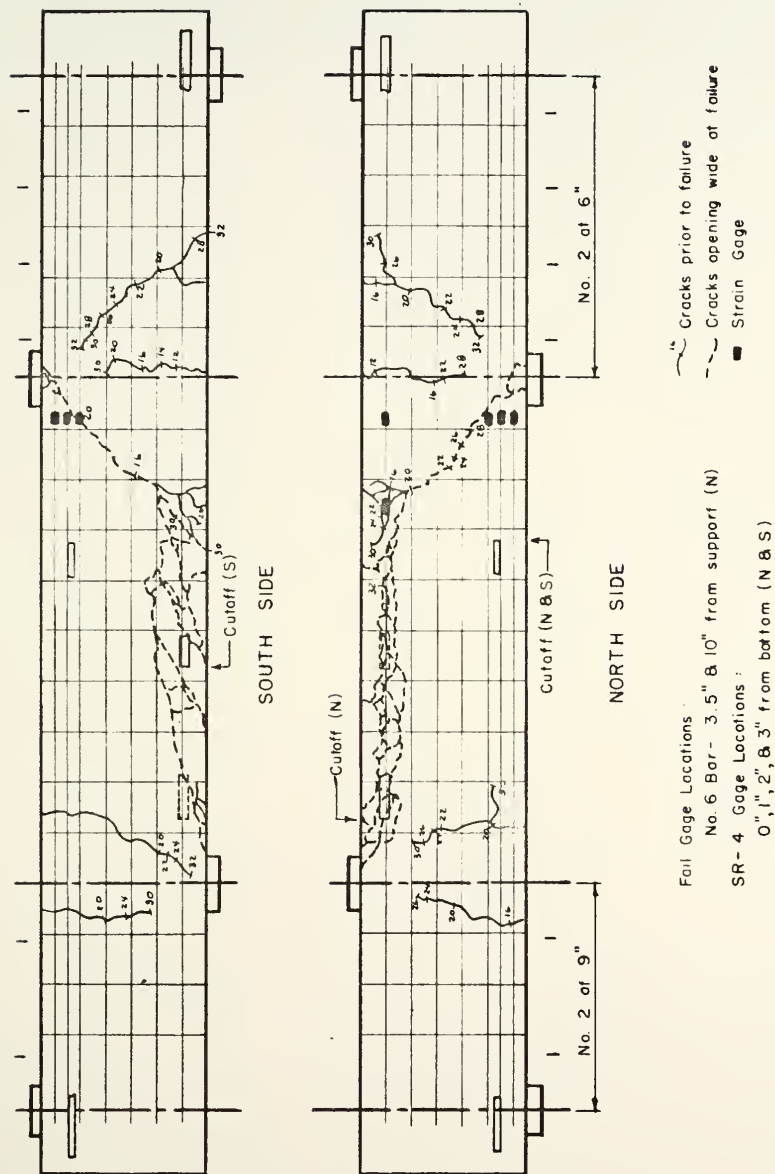
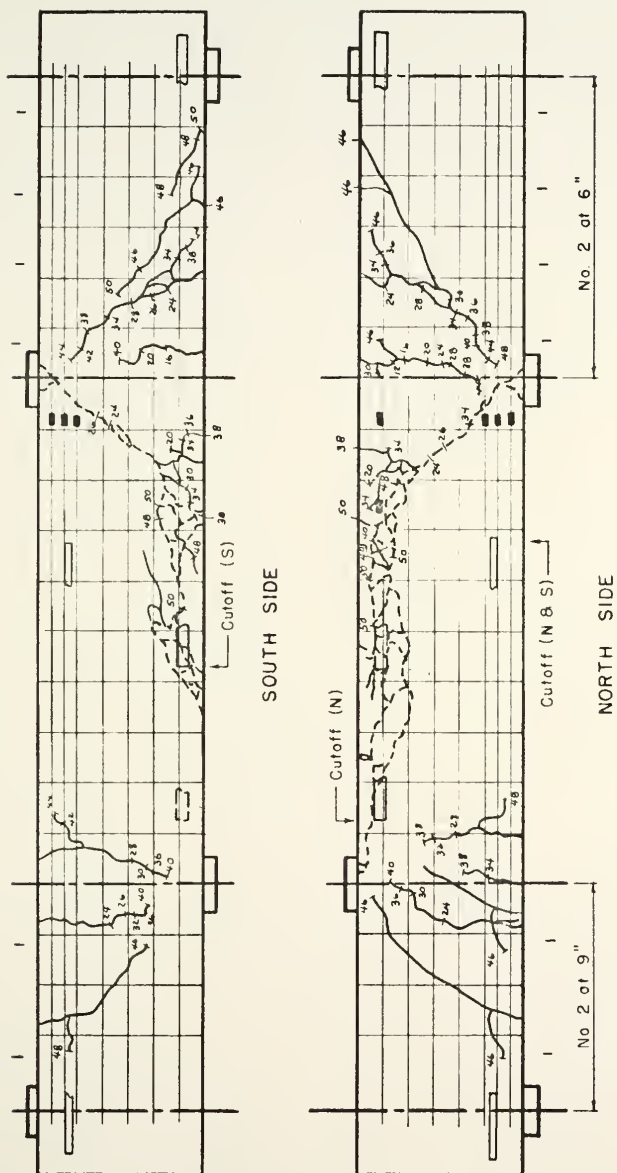
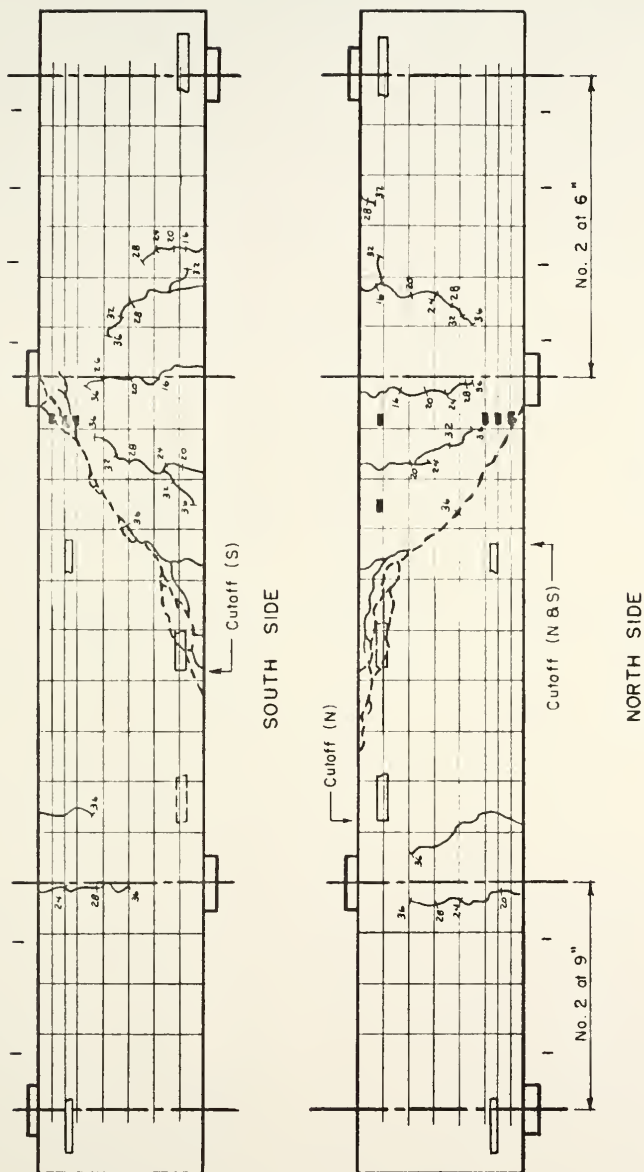


FIGURE 36. BEAM I-1



All gages as on Beam I - 1

FIGURE 38. BEAM I - 3



All gages as on Beam I-1

FIGURE 39. BEAM I - 4

Series II, 32" Shear Span

Beam II-1 ($f'_c = 2,030$ psi). The critical crack (Figure 45) formed from a flexural crack 12" from the support. It began inclining at 20^k and reached the compression zone at 26^k . Splitting along the steel also began at 26^k . At 32^k the diagonal crack formed and opened about 1/4" before crushing of the concrete at the support and splitting along the tension steel.

The deflection (Figure 40a) was nearly linear to the inclination of the critical crack. The steel strain (Figure 44a) in the shear span approached that at the support failure. The concrete strain (Figure 41) on the south side was greater than on the north.

Beam II-2 ($f'_c = 2,450$ psi). The beam (Figure 46) failed suddenly in diagonal tension at a load of 33^k . The critical crack just began to incline at 32^k and was still 7" from the compression face. Splitting associated with the critical crack occurred at failure.

Again the south side had higher concrete strains (Figure 42). The deflection (Figure 40b) was linear, with a kink at 20^k which corresponds to the formation of a non-critical inclined crack. The steel strain (Figure 44b) in the shear span was nearly equal to that at the support. There was no evidence of a decrease in steel strain due to splitting along the steel.

Beam II-8 ($f'_c = 6,750$ psi). The beam failed in diagonal tension after holding 40^k for about one minute. The critical crack (Figure 48) had formed as a flexural crack but had not begun to incline when failure occurred.

The concrete strain distribution (Figure 43) was very symmetrical. The deflection (Figure 40c) was essentially linear until failure.

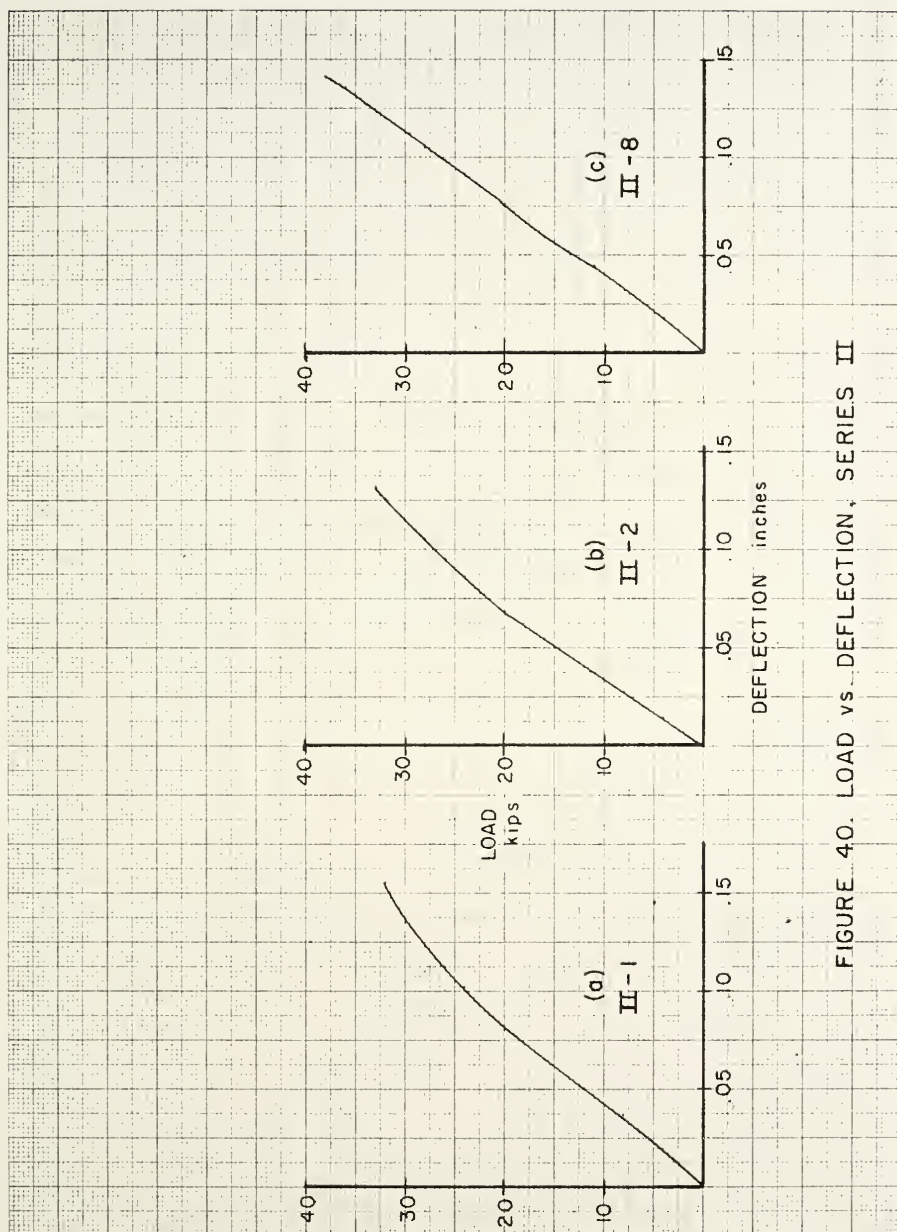


FIGURE 40. LOAD vs. DEFLECTION, SERIES II

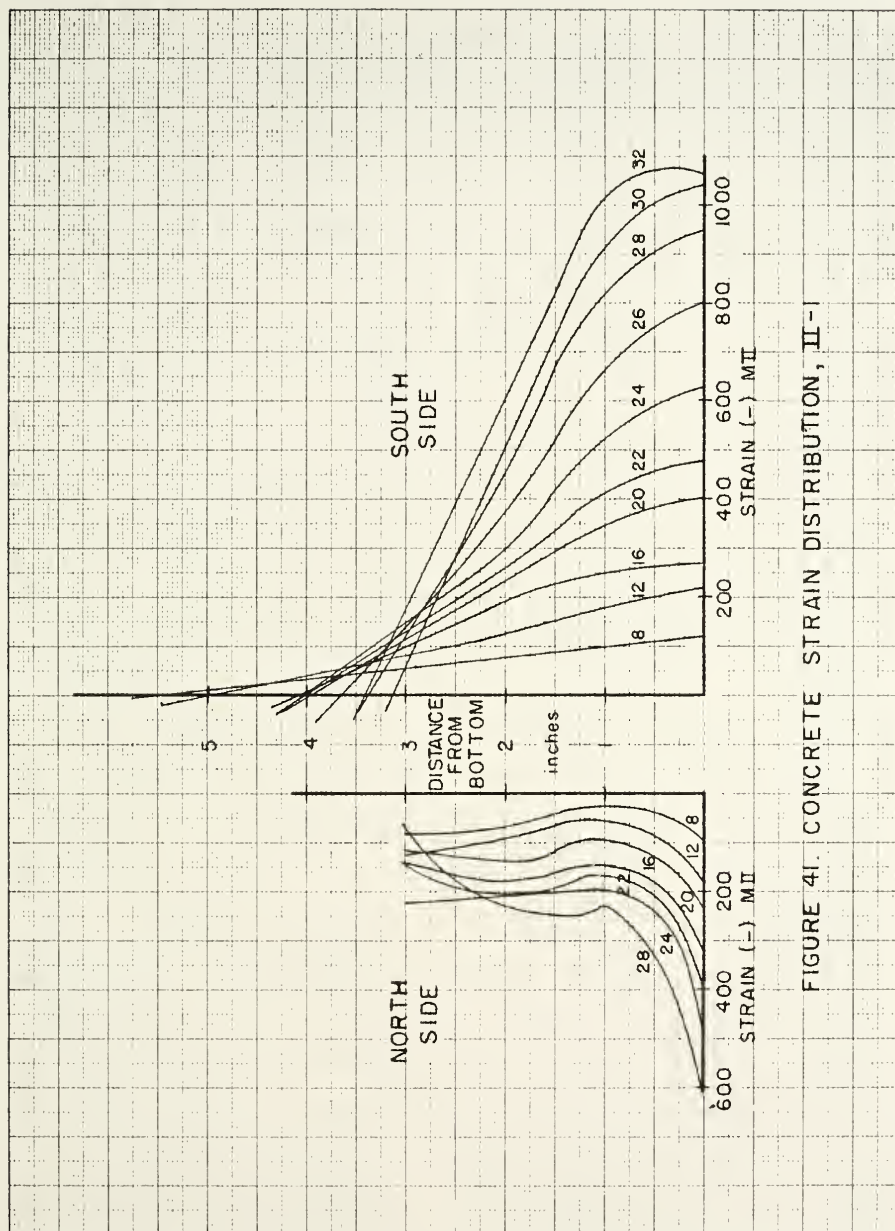


FIGURE 41. CONCRETE STRAIN DISTRIBUTION, II-

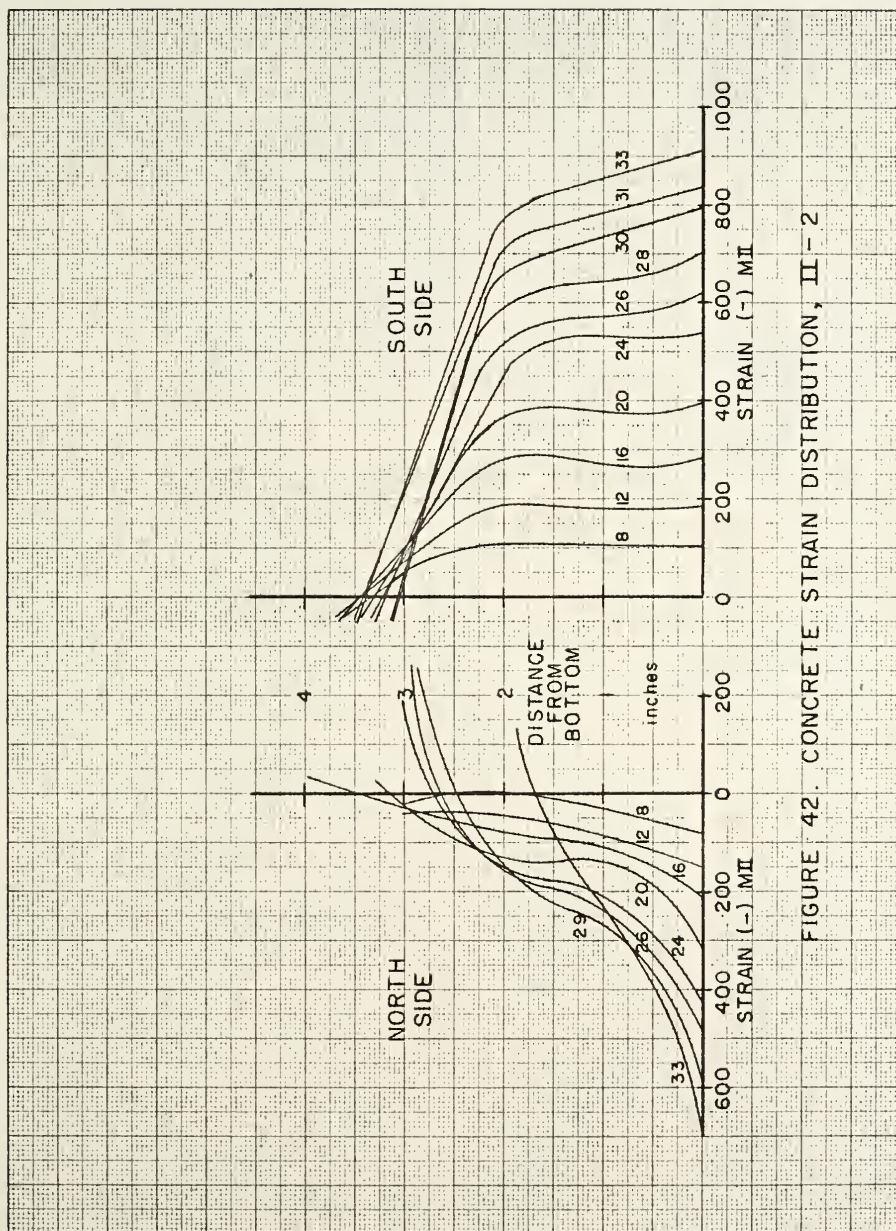


FIGURE 42. CONCRETE STRAIN DISTRIBUTION, II-2

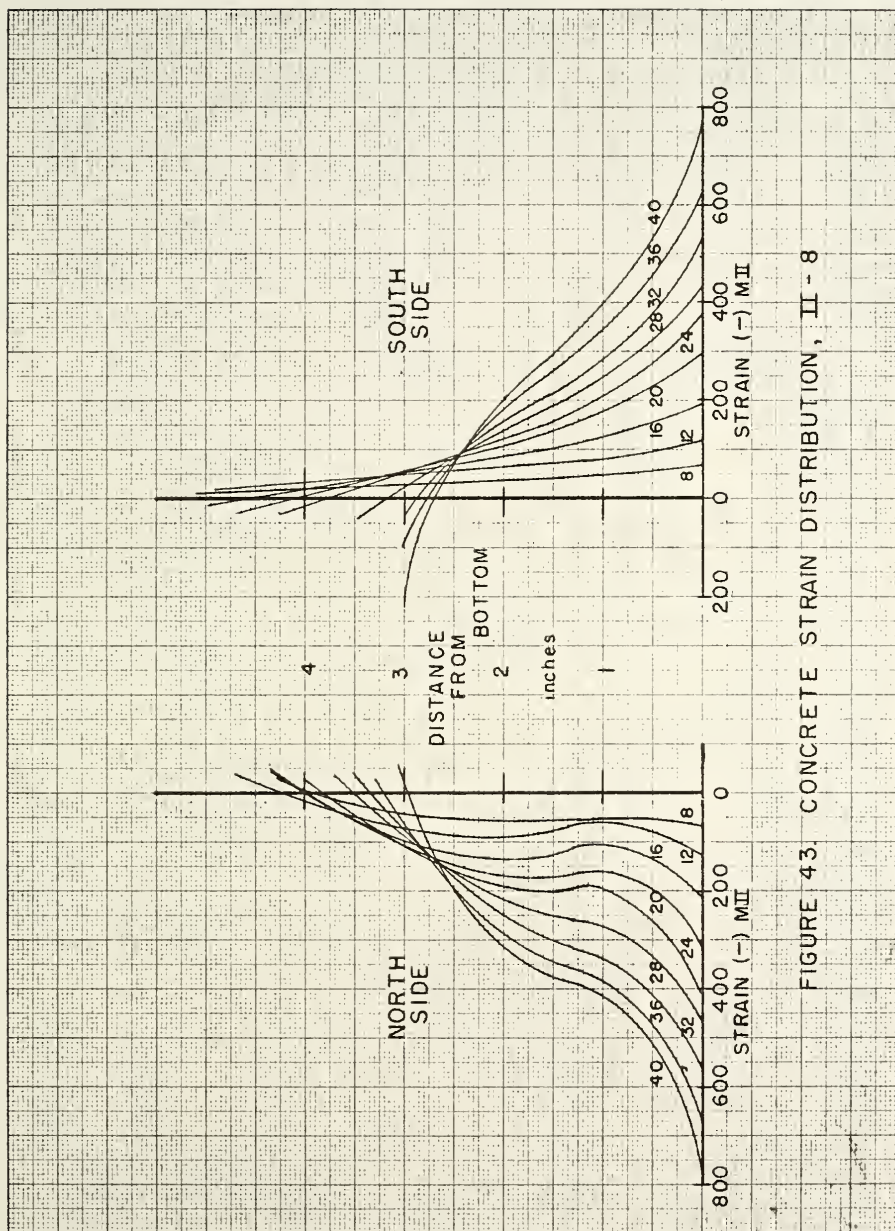


FIGURE 43. CONCRETE STRAIN DISTRIBUTION, II - 8

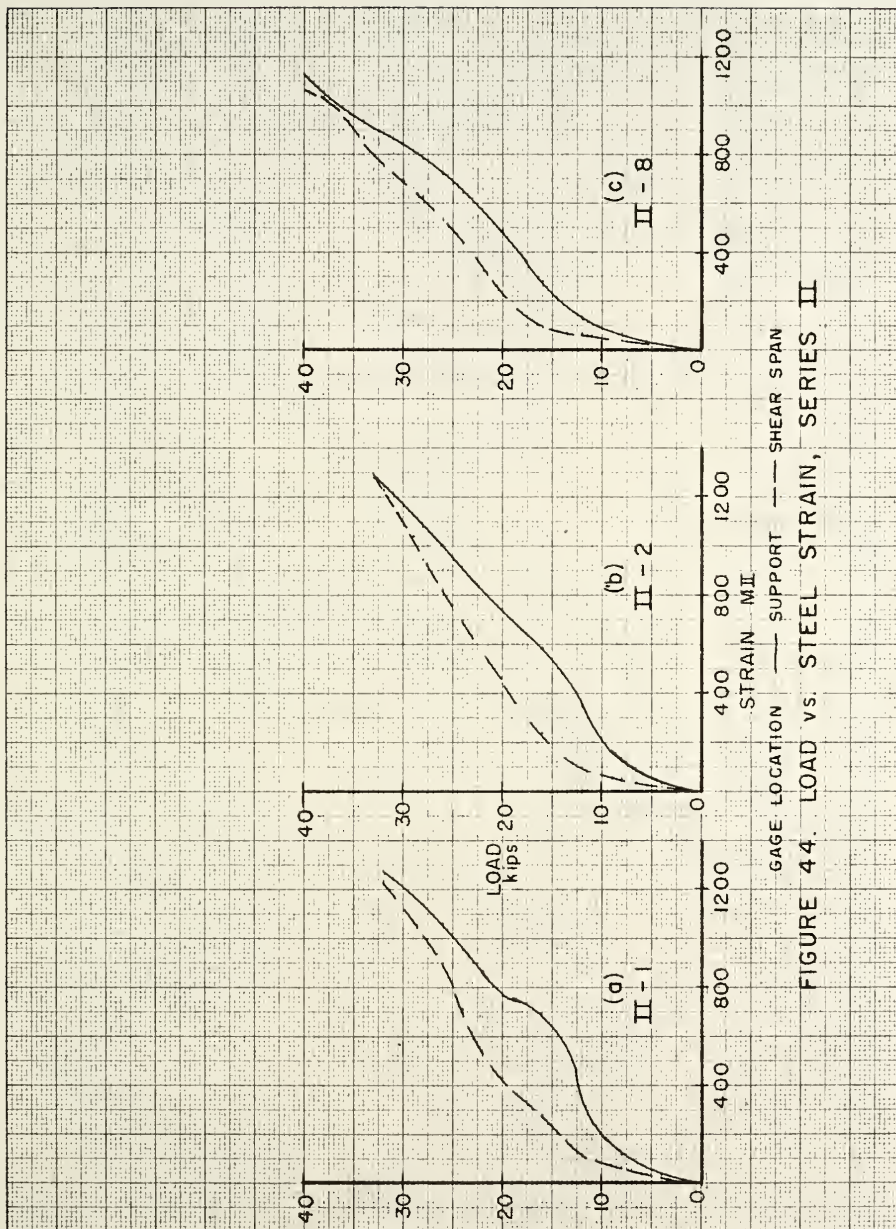


FIGURE 44. LOAD vs. STEEL STRAIN, SERIES II

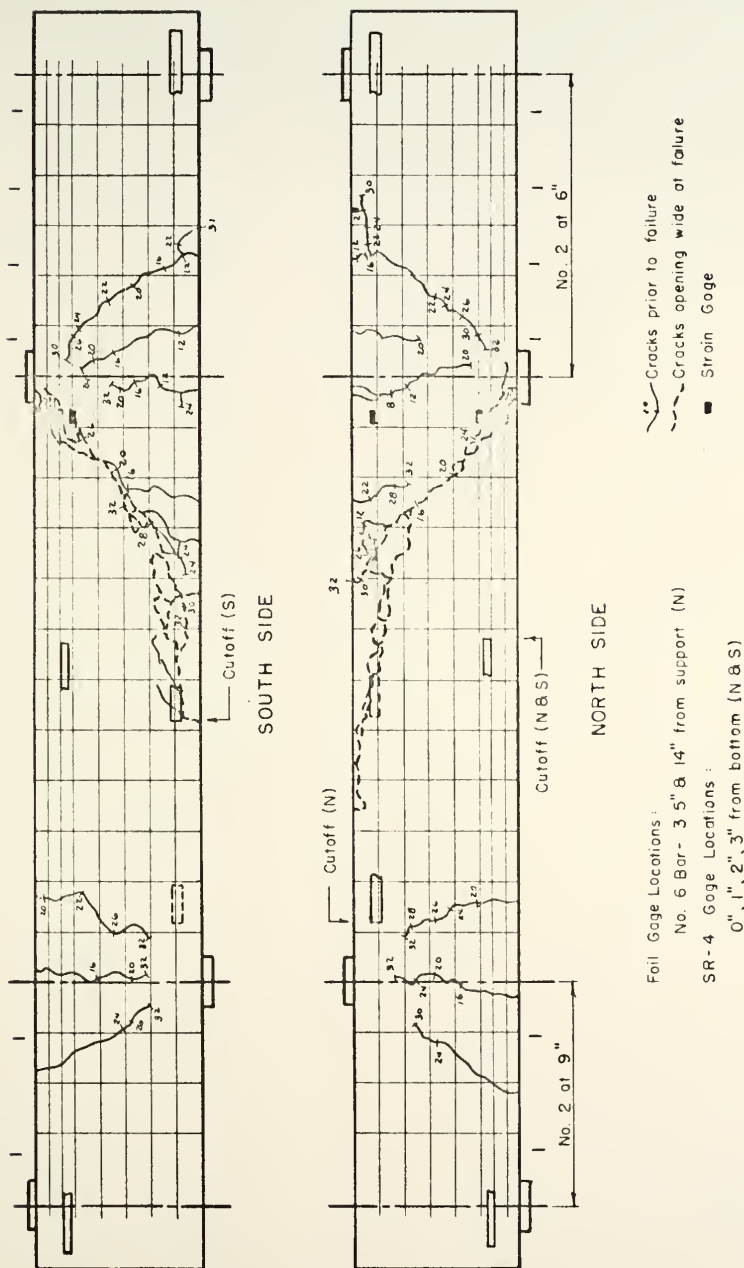
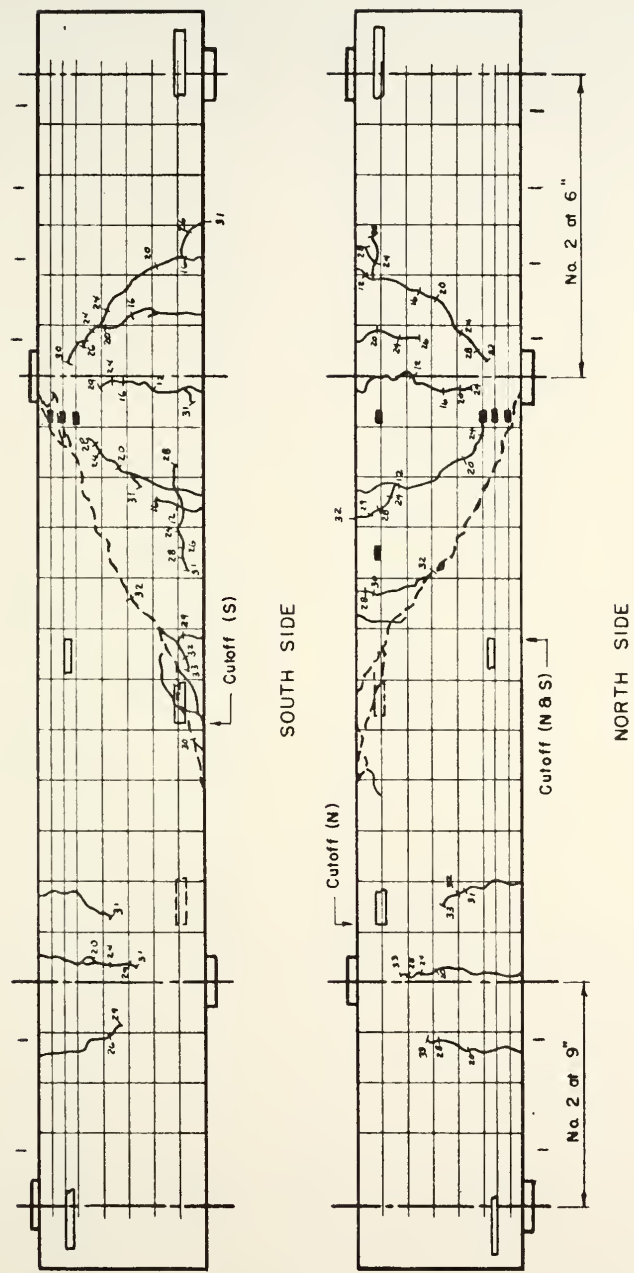
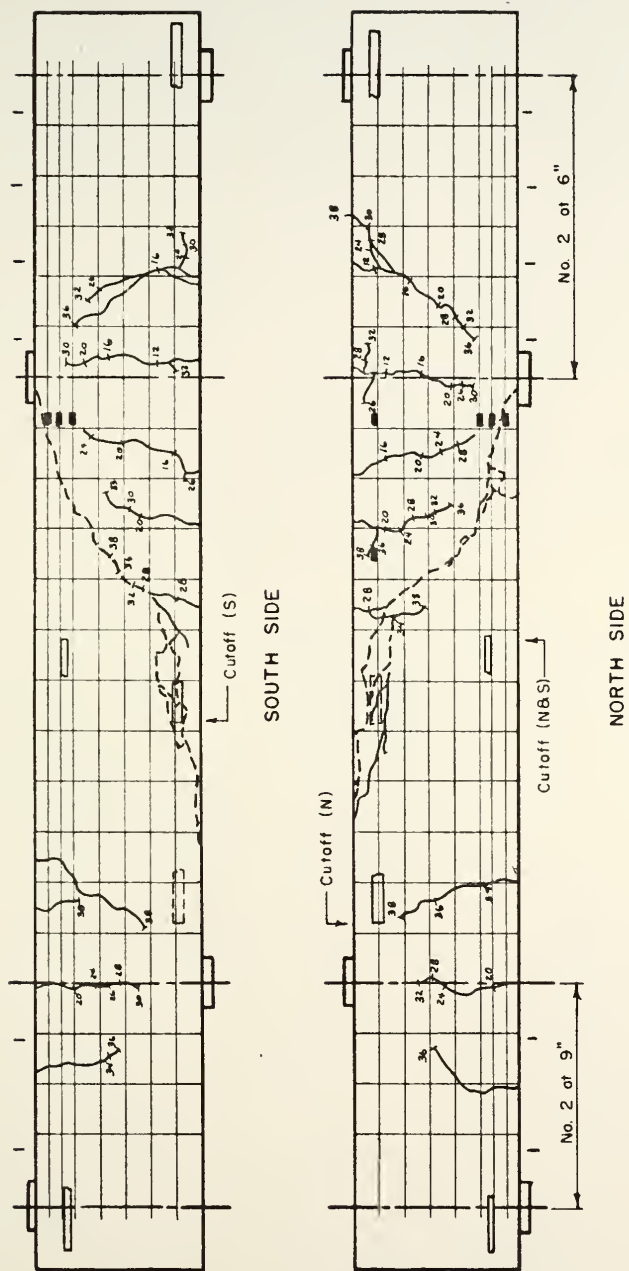


FIGURE 45. BEAM II - I



All gages as on Beam II-1

FIGURE 46. BEAM II - 2



All gages as on Beam II - 1

FIGURE 47. BEAM II - 8

Series III, 44" Shear Span

Beam III-1 ($f'_c = 2,040$ psi). The critical crack (Figure 53) began as a flexural crack at 20^k about 22" from the support. Inclining began at 22^k on the south side and 28^k on the north side. The compression zone was reached at 32^k . Diagonal tension failure occurred at 34^k when the critical crack penetrated the compression region to the support. The tension steel split out at failure.

The concrete strain (Figure 49) was higher at all gages on the north side than on the south. The steel strain (Figure 52a) in the shear span increased rapidly at a load of 34^k .

Beam III-2 ($f'_c = 3,210$ psi). The concrete around the continuing steel reinforcing bar on the north side began to crack and lose bond near the location of the strain gage in the shear span while the cracks were being traced after 28^k . The steel bar split out followed by rapid progression of the diagonal tension crack and total failure of the beam. The critical crack (Figure 54) had just begun to incline on the north side and had nearly reached the compression zone on the south side. Extensive splitting was present on the north side but little on the south. The presence of the strain gage in the shear span may have limited the strength of the beam.

The deflection (Figure 48b) was essentially linear to failure. As in III-1 the north side had higher concrete strains (Figure 50).

Beam III-5 ($f'_c = 6,810$). Failure came suddenly at 40^k when the diagonal tension crack (Figure 55) formed on the south side through the cutoff point of the short bar. This was followed by splitting of the continuing bar and rapid penetration of the diagonal tension crack on the north side.

The behavior of this beam (Figures 48, 51, 52) was the same as Beams III-1 and III-2.

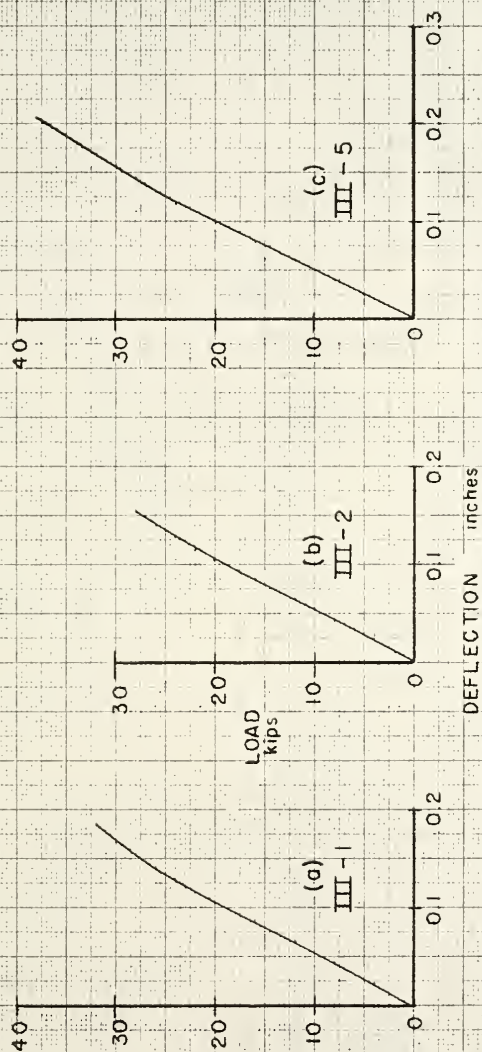


FIGURE 48. LOAD vs. DEFLECTION, SERIES III

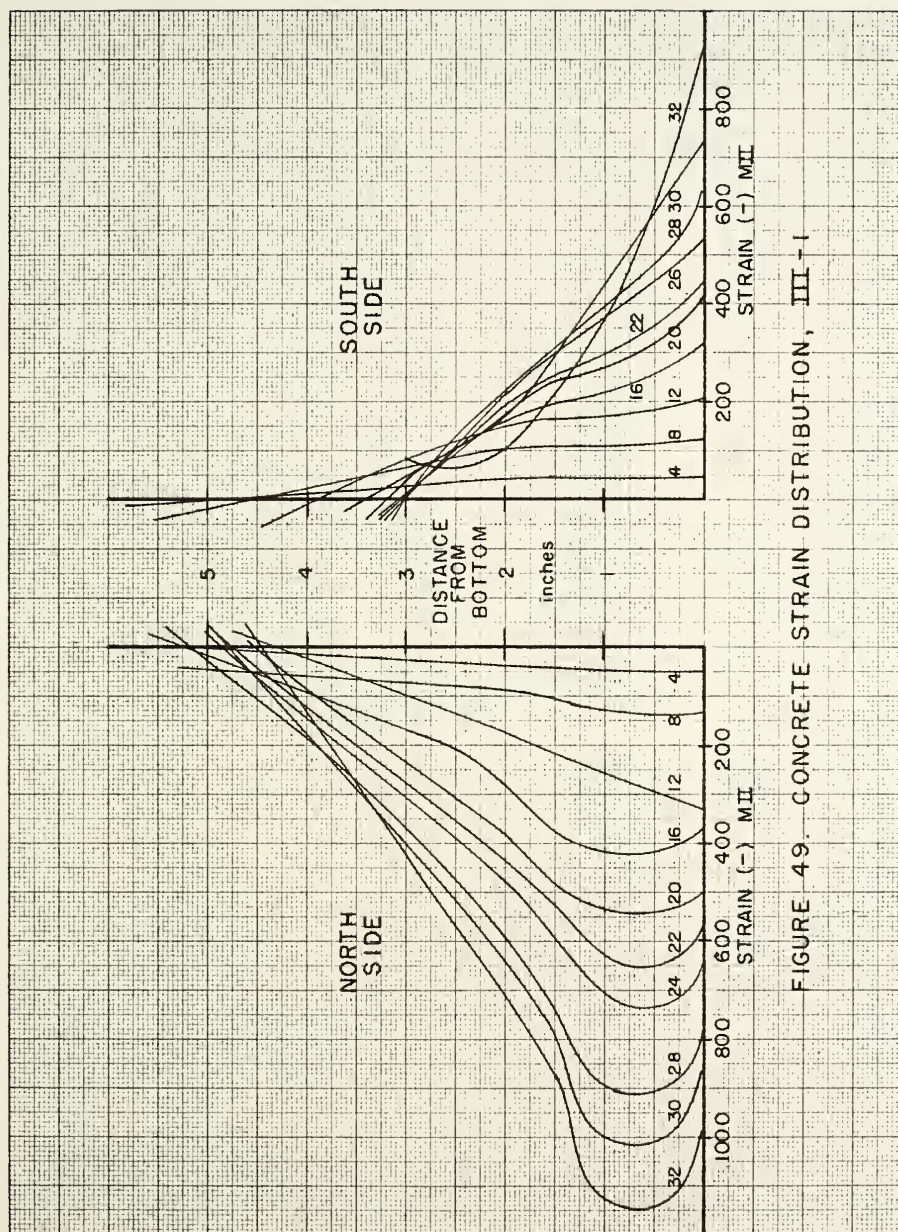


FIGURE 49. CONCRETE STRAIN DISTRIBUTION, III-1

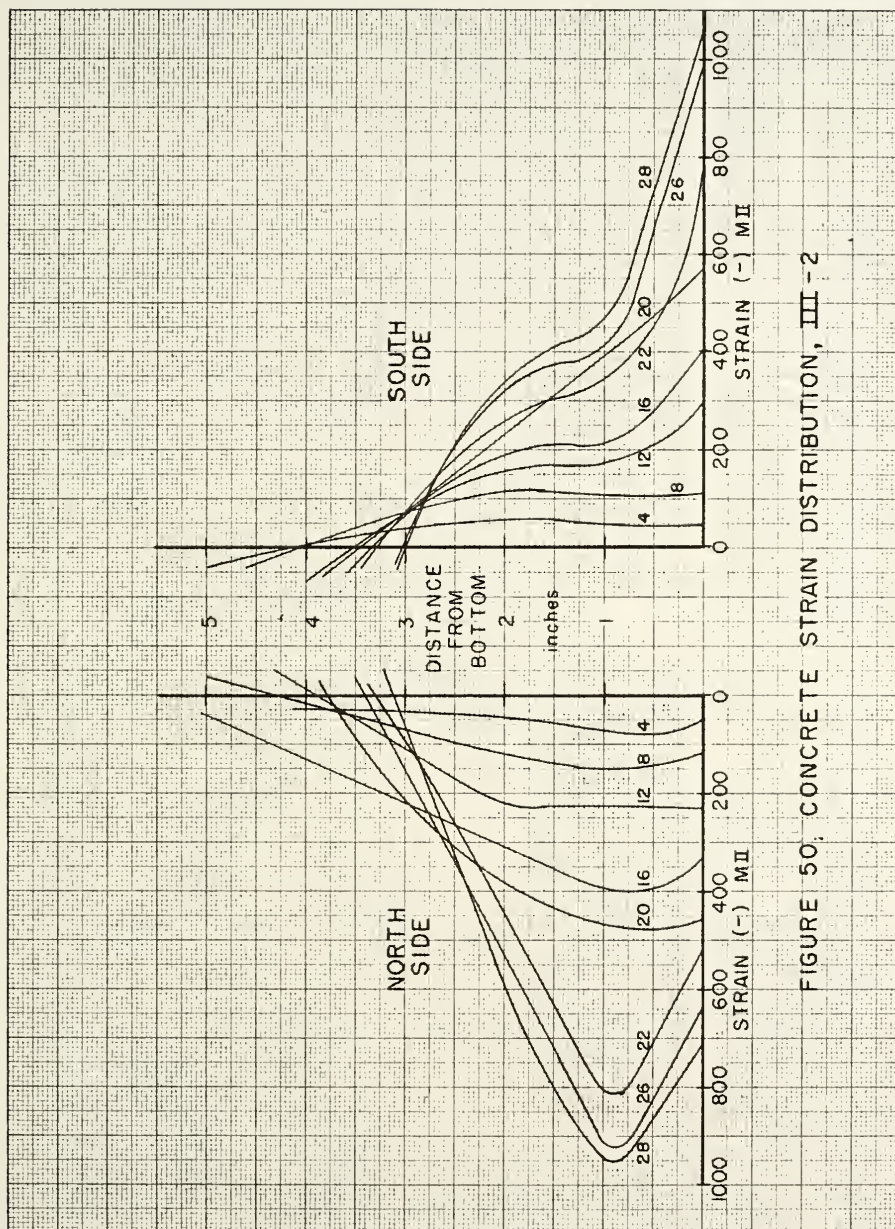


FIGURE 50. CONCRETE STRAIN DISTRIBUTION, III-2

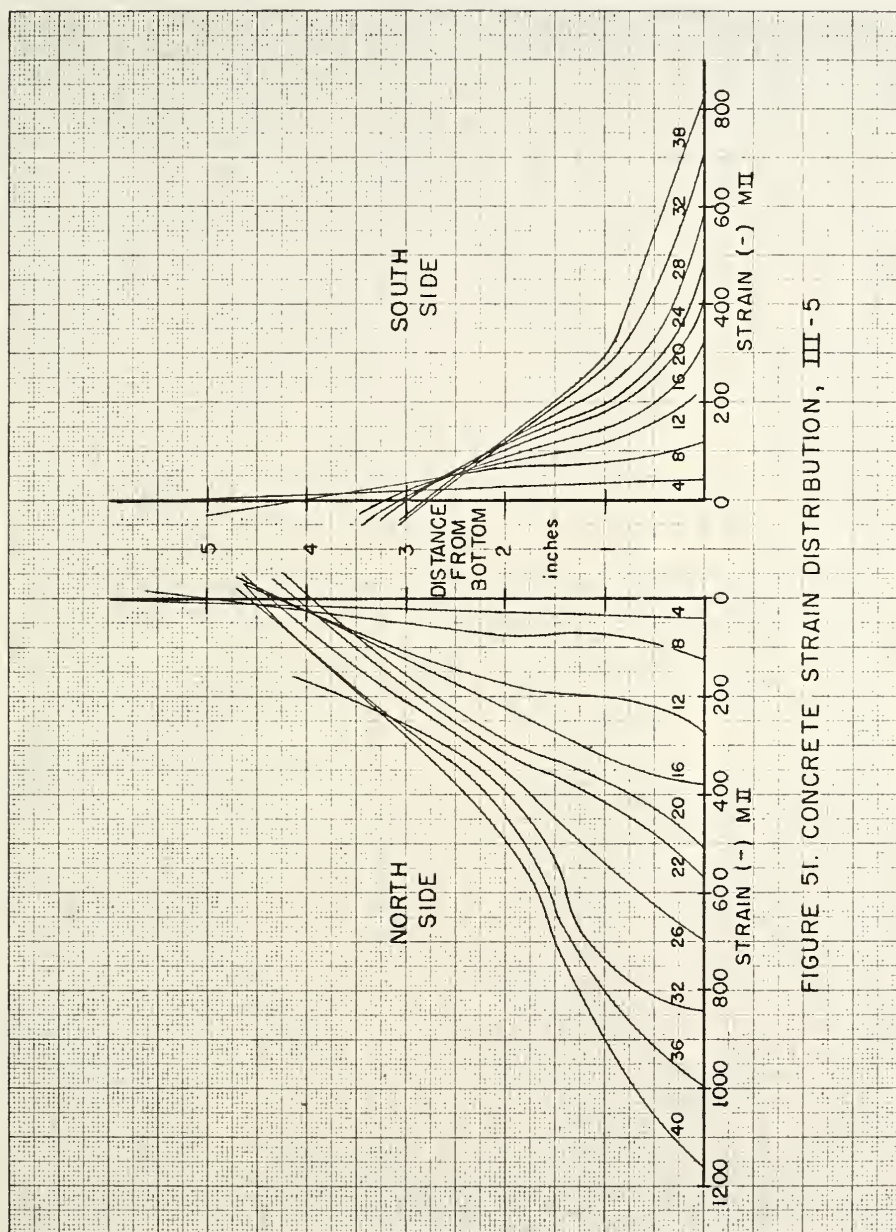


FIGURE 5I. CONCRETE STRAIN DISTRIBUTION, III-5

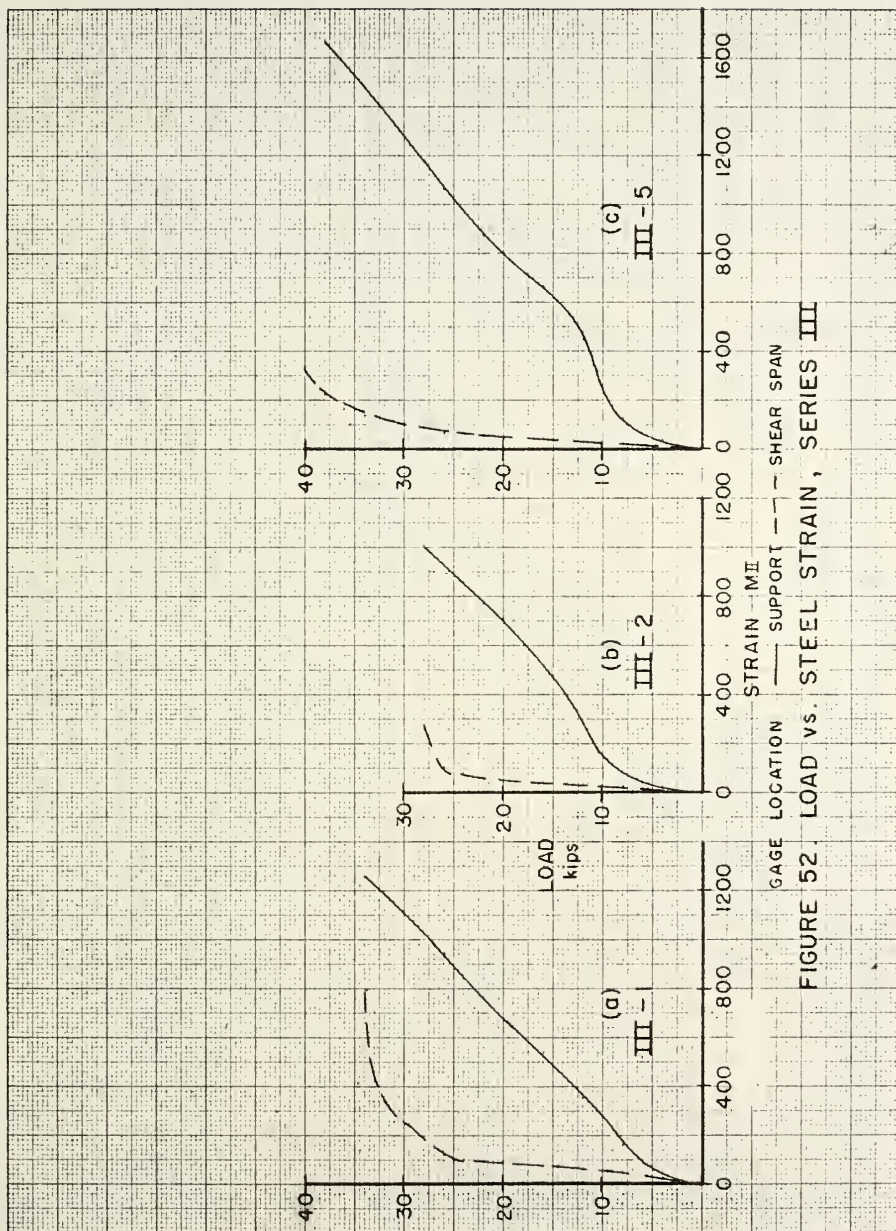


FIGURE 52. LOAD vs. STEEL STRAIN, SERIES III

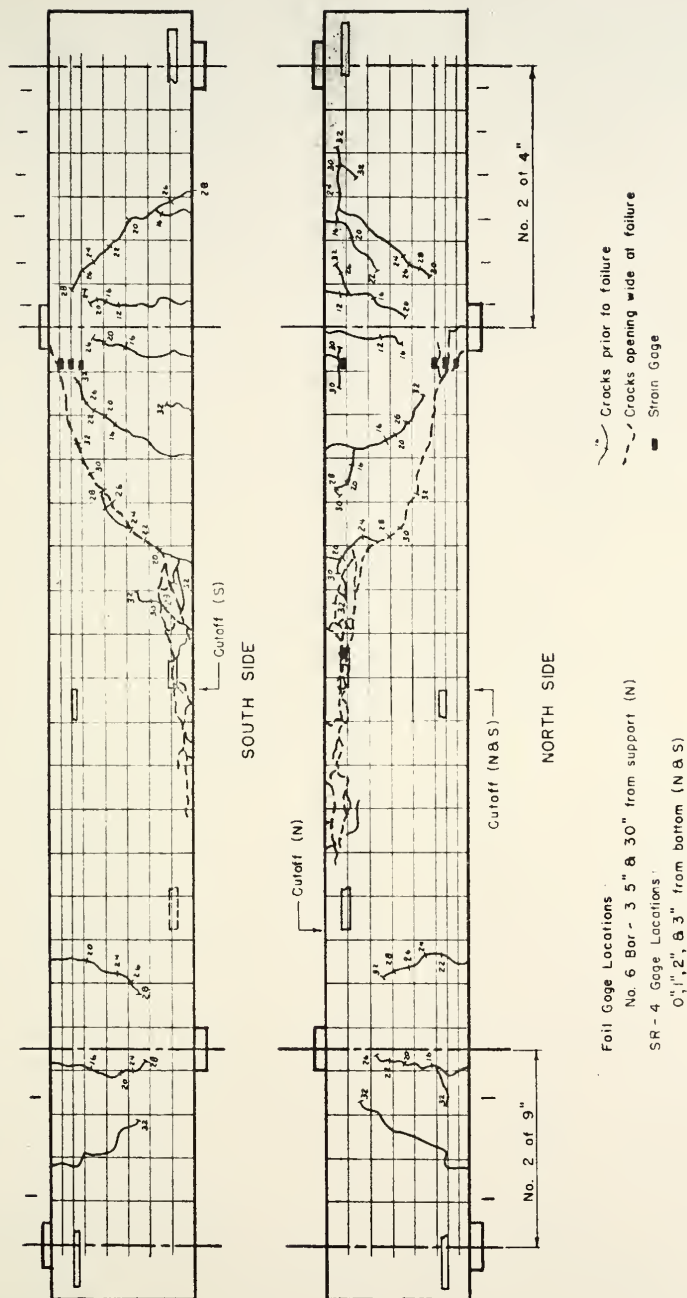
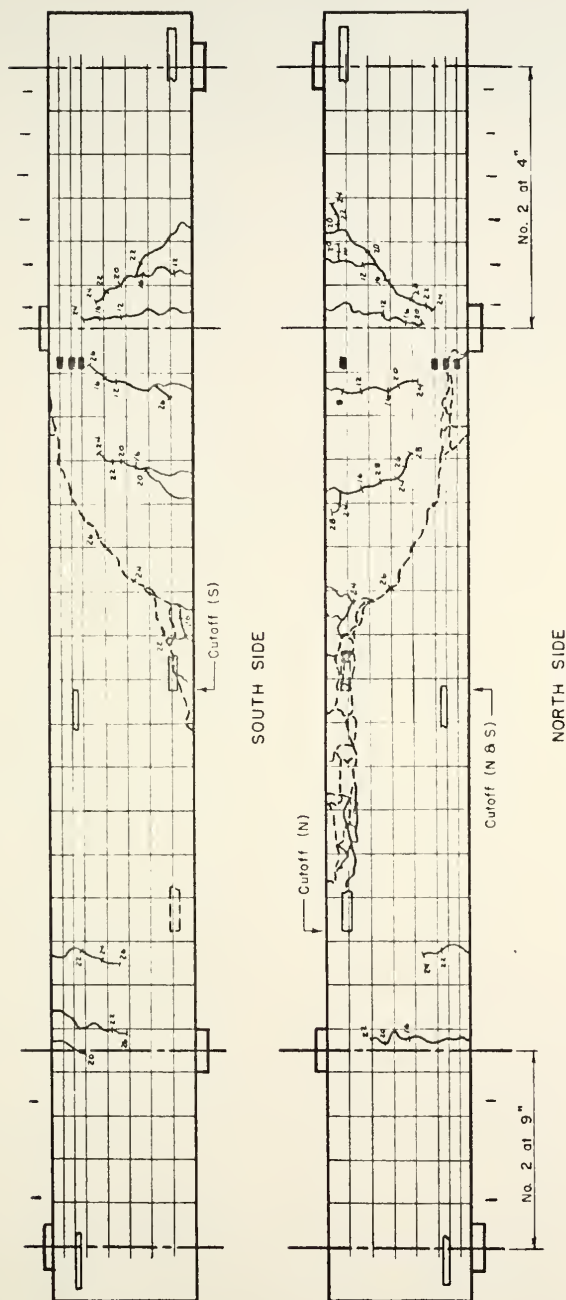
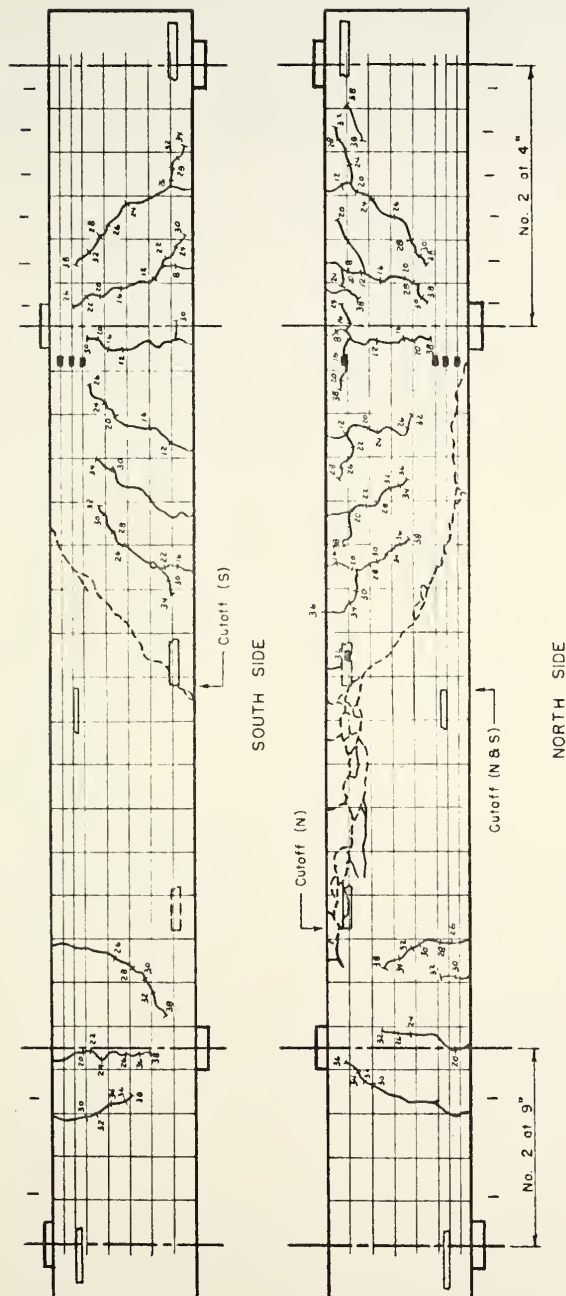


FIGURE 53. BEAM III - I



All gages as on Beam III - 1

FIGURE 54. BEAM III - 2



All gages as on Beam III - 1

FIGURE 55. BEAM III - 5

DISCUSSION OF TEST RESULTS

Repeated Beams

Harvey

Beam IA-4, when repeated without the strain gages in the shear span, followed the trend of the remainder of the beams in Series I and sustained a failure load substantially greater than the diagonal cracking load. The other repeats of Harvey's beams behaved very much like the originals, but with the diagonal cracking load increased in the duplicate beams. The ratio of the actual shearing stress at diagonal cracking to the shear stress calculated to cause diagonal cracking (Table 7) was approximately 0.80 for the original beams IIB-5, IIIB-5 and IIIB-6. In the repeat beams these values increased to 1.03, 1.06 and 0.92 respectively, when compared to the ACI Building Code Requirements. The ratio of the test value to calculated value of ultimate shearing stress also increased for all the beams when compared to both ACI and AASHO specifications (Tables 7 and 8). All of the repeated values fit well with the other values reported in Harvey's original work.

Table 7. Comparison of Repeat Beam Strengths with ACI Building Code Requirements.

Beam	Diagonal Cracking Strength			Ultimate Shear Strength		
	v_c^*	v_c^*	v_c test	v_u	v_u^{**}	v_u test
	test	calc	$\frac{v_c}{v_c}$ calc	test	calc	$\frac{v_u}{v_u}$ calc
IA-4	181	150	1.21	192	150	1.28
Repeat	226	158	1.43	271	158	1.71
IIB-5	116	143	0.81	135	143	0.94
Repeat	149	146	1.02	158	146	1.08
IIIB-5	111	138	0.80	221	254	0.87
Repeat	148	138	1.06	185	203	0.91
IIIB-6	111	139	0.80	111	139	0.80
Repeat	126	139	0.91	126	139	0.91
IIT-1	226	136	1.66	226	136	1.66
Repeat	212.2	135	1.57	219.5	135	1.62
IA	70	131	0.54	98	131	0.75
Repeat	112	154	0.73	182	154	1.18
IE	158	143	1.10	223	143	1.56
Repeat	177	148	1.20	204	148	1.38
IIA	93	139	0.67	195	212	0.92
Repeat	93	150	0.62	186	234	0.80
IID	163	146	1.12	311	279	1.12
Repeat	186	150	1.24	344	234	0.80

$$* \quad v_c = \frac{V}{bd} = 1.9 \sqrt{f'_c} + 2500 \frac{pVd}{M}$$

$$** \quad v_u = \frac{V_u}{bd} = v_c + Kr f_{vy}$$

Table 8. Comparison of Repeat Beam Strengths with AASHO "Standard Specifications."

Beam	v_u test	v_a	$\frac{v_u \text{ test}}{v_a}$
IA-4	192	79	2.44
Repeat	271	79	3.44
IIB-5	135	79	1.71
Repeat	158	79	2.00
IIIB-5	221	130	1.71
Repeat	185	102	1.81
IIIB-6	111	79	1.41
Repeat	126	79	1.60
IIT-1	226	79	2.86
Repeat	219.5	79	2.78
IA	98	79	1.24
Repeat	182	79	2.30
IE	223	79	2.83
Repeat	204	79	2.58
IIA	195	110	1.77
Repeat	186	117	1.59
IID	311	136	2.30
Repeat	344	117	2.94

$$v_a = \frac{8}{7}(.03 f'_c) < \frac{8}{7} \times 90 \text{ psi}$$

Wehr

Beam IIT-1 was repeated because it was the only one of the restrained T-beams tested that failed upon formation of the diagonal crack. The two T-beams of longer shear spans without stirrups sustained a failure load higher than the diagonal cracking load. The repeat of IIT-1 failed at a slightly greater load than the diagonal cracking load, but the ultimate shearing stress was only 3.4 per cent higher than the diagonal cracking shearing stress. However, in both cases the ratios of actual to calculated shearing stress at diagonal cracking at at ultimate were of the same order (Tables 7 and 8).

Spaman

The two beams with the longitudinal steel terminated at the theoretical points developed diagonal cracks at loads significantly lower than the calculated values. Even though both sustained a larger load at failure only IA, the beam without stirrups carried an ultimate stress greater than the calculated values (Tables 7 and 8). This was contrary to the original results, when both beams cracked and failed at stresses lower than the calculated values.

The beams with full length bars, IE and IID, cracked at slightly higher relative stresses than the original beams, but this trend did not hold for failure stresses (Tables 7 and 8).

Effect of Concrete Strength

Modes of Failure

The beams of Series I had an a/d ratio of 2.18. Failure of these four beams was instigated by penetration of the diagonal crack followed by splitting along the reinforcement. The amount of splitting was reduced in Beam I-4, which had the highest concrete strength. Only Beam I-4 failed upon formation of the diagonal tension crack, with the three remaining beams having reserve strength after the diagonal crack formed.

Beams of Series II failed in diagonal tension at stresses at or slightly above those causing diagonal cracking. Beams II-1, II-5, II-6 and II-7 had failure stresses 23 per cent, 14 per cent, 35 per cent and 5.4 per cent above their diagonal cracking stresses. The remainder of Series II failed upon formation of the critical crack. Splitting along the reinforcement was less evident than in Series I. The critical crack formed farther from the support than in Series I. Series II had an a/d ratio of 2.88.

Only Beam III-1 of Series III had failure stresses greater than the diagonal cracking stress and there was only 5.9 per cent difference in the two. All of Series III failed in diagonal tension but with more splitting present than in Series II. The critical crack formed much farther from the support, from 4" to 16" farther than Series II, and the distance increased with concrete strength. On the side of

the continuing bar the diagonal tension crack traveled nearly horizontally after entering the compression zone. The a/d ratio of Series III was 3.96.

The modes of failure in this investigation conform to those reported by others.

Shear Span to Depth Ratio

The effect of the shear span to depth ratio has been reported by Harvey [9] and others. This study shows that the diagonal cracking stress as well as the ultimate shear stress decreases as the a/d ratio increases. Table 9 summarizes the results.

Table 9. Effect of Shear Span to Depth Ratio.

Series	a/d	Average V_c (psi)	Average V_u (psi)
I	2.18	169	220
II	2.88	139	151
III	3.96	122	123

The behavior of the beam after diagonal cracking is of more importance. The beams of Series I were able to accept deeper penetration of the diagonal crack into the compression zone. Only Beam I-4 failed upon formation of the diagonal crack while half of Series II failed suddenly at

diagonal cracking and only Beam III-1 of Series III was able to carry a load greater than the cracking load.

The difference in behavior may be due to the location of the critical crack. In beams which sustained a greater load at failure than the cracking load the critical crack entered the compression zone much closer to the support. In Series II, which provides the best basis for comparison, the beams which carried an ultimate load higher than the cracking load the diagonal tension crack entered the compression region at an average of 8" from the support while it entered 14" from the support on the beams which failed at the crack's formation. It is thought that the vertical compression resulting from the proximity of the support reduces the principal tension at the end of the crack and thus delays the penetration of the crack.

This type of behavior is also true of the beams without stirrups in Harvey's thesis [9] and Spaman's report [18].

Concrete Strength

The compressive strength of the concrete seemed to have little effect on either the diagonal cracking load or the ultimate capacity of the beams. Classifying the beams according to increasing split tensile strength or Modulus of Elasticity did not show any trends either.

The splitting of the concrete along the tension reinforcement decreased as the concrete strength increased. Comparison of the crack patterns of Series I (Figures 37 to 40)

clearly show this behavior.

The strain distribution in the concrete becomes more symmetrical as the concrete strength becomes higher.

The location of the critical crack seemed to depend on the concrete strength. The flexural crack which served as the initiator of the diagonal crack moved farther from the support as the concrete strength increased. This was especially true in Series III where the initiator changed from 22" to 34" from the support.

Diagonal Crack Location

As mentioned previously the location of the diagonal tension crack has a definite effect on the beam behavior and failure mechanism. And, in turn, the location of the crack is dictated by the properties of the beam.

The shear span to depth ratio plays a large part in the location of the crack. As a/d increases the flexural crack which initiates the diagonal tension crack moves away from the support for beams of approximately the same concrete strength. For Example: 9" for Beam I-2 and 28" for Beam II-4, 18" for Beam II-8 and 34" for Beam III-5. Since the crack begins farther from the support it is also farther from the support when it enters the compression zone. In the beams of long shear spans the crack travels nearly horizontally

after penetrating the compression region (Figure 55). This is not the case in a shorter shear span where the crack continues nearly straight. However, for all three series the critical crack aims for the support after it enters the compression zone.

The effect of the concrete strength upon the location of the diagonal crack has been discussed and is found to be true for all shear spans studied. As the concrete strength increases the diagonal crack begins farther from the support.

The relative position of the diagonal tension crack when it enters the compression zone determines the behavior of the beam. This has also been discussed previously. Sudden failure results if the crack reaches the compression region far from the support. If the crack enters nearer the support the beam is able to carry additional load. Approximate values for this distance are:

Series I	3"-6"
Series II	13"-10"
Series III	12"-18"

where the first number indicates the largest distance from the support resulting in increased strength and the second indicates the closest with sudden failure.

Bar Cutoff

Terminating a portion of the longitudinal reinforcement within the tension zone results in a reduction of the shear

strength when compared to similar beams with extended steel. The reduction in both diagonal cracking loads and ultimate loads can be found in Tables 5 and 6 of Harvey's thesis [9].

The diagonal tension crack does not always initiate at the cutoff point, but the resulting failure crack does go through the cutoff. Splitting is, of course, less on the side of the beam with the shorter bar (Figure 55).

Another effect of terminating the steel is the loss of symmetry of the cracked section. On the side of the cutoff bar the cracks penetrate sooner for beam with the largest a/d ratio, Series III. This is also reflected in the concrete strain distribution of Beams III-1, -2, -5 all of which have the neutral axis higher on the North side of the beam. Neither of these observations are generally true for Series I and II.

For all the beams of Series I and Series III the concrete strains were higher on the side of the beam with the continuing bar. Over half of the beams of Series II, II-3, II-8, with concrete strains recorded also indicate this behavior. Spaman's results [18], also for beams of the type in Series II, had larger concrete strains on the side of the continuing bar. This could be explained by unsymmetrical bending resulting from the cross-section of the beam after terminating one of the reinforcing bars. However, the concrete strains were measured at least 18" from the point of bar cutoff and it seems more likely that the difference in strain

levels resulted only from the set-up.

Steel Strains

The steel strain (Figures 36, 45 and 53) in the shear span developed more slowly than that at the support for all series of beams. Once diagonal cracking began the strain in the shear span increased rapidly and in several cases: Beams I-2, I-3, II-2, III-1, III-2, increased more rapidly than that at the support. In Beams I-2 and I-3 the steel strain in the shear span exceeded the strain at the support. The increase in the shear span strain in Series III occurred closer to failure because the strain gage was placed farther from the support in order to be near the critical crack. The reinforcement at the top of the diagonal crack must resist the larger moment at the end of the crack as explained in the INTRODUCTION on page 4.

ANALYSIS OF TEST RESULTS

Shearing Stress at Diagonal Cracking

Semi-empirical expressions to predict the stress at which diagonal cracking will occur have been reported by several authors. The equation most often used is that recommended by the ACI Building Code [2]. The equation for ultimate strength design is:

$$v_c = \frac{V_c}{bd} = 1.9 \sqrt{f'_c} + 2500 \frac{pVd}{M} \quad (4)$$

The equivalent equation for working stress design has a factor of safety of approximately 2 applied to this equation. For beams of this study the critical section is a distance d from the section of maximum moment, and $V/M = 1/a - d$ for beams in this investigation. Test results are compared with the calculated values in Table 10.

The equation is conservative for all beams in Series I and II except Beam I-1, II-5 and II-6. However, only Beam III-1 of Series III exceeded the calculated value, indicating a definite lack of safety in this series.

Ultimate Shear Strength

ACI recommends the same equation for ultimate strength as for diagonal cracking in beams without web reinforcement

Table 10. Comparison of Concrete Strength Test Results with ACI Building Code Requirements.

Beam	Diagonal Cracking Strength			Ultimate Shear Strength		
	v_c^*	v_c^*	v_c	v_u	v_u^{**}	v_u
	test	calc	test v_c calc	test	calc	test v_u calc
I-1	104	128	0.81	177	128	1.38
I-2	187	143	1.31	239	143	1.67
I-3	177	146	1.21	260	146	1.78
I-4	206	164	1.26	206	164	1.26
II-1	121	103	1.17	149	103	1.45
II-2	154	111	1.39	154	111	1.39
II-3	135	128	1.05	135	128	1.05
II-4	149	132	1.13	149	132	1.13
II-5	116	143	0.81	135	143	0.94
II-6	107	144	0.74	144	144	1.00
II-7	149	146	1.02	158	146	1.08
II-8	186	174	1.07	186	174	1.07
III-1	119	97	1.23	126	97	1.30
III-2	104	119	0.87	104	119	0.87
III-3	111	139	0.80	111	139	0.80
III-4	126	139	0.91	126	139	0.91
III-5	148	168	0.88	148	168	0.88

$$v_c^* = \frac{V}{bd} = 1.9 \sqrt{f_c} + 2500 \frac{p_w V d}{M}$$

$$v_u^{**} = \frac{V}{bd} = 1.9 \sqrt{f_c} + 2500 \frac{p_w V d}{M}$$

due to the unreliable nature of the diagonally cracked beam. Comparison of ultimate test values and computed ultimate strengths is also given in Table 10. This equation is more conservative than the diagonal cracking strength because several of the beams had higher ultimate strength than cracking stress. In Series I and Series II only Beam II-5 failed at less than the predicted load (at 94 per cent of prediction). The beams of Series I were more conservative than those of Series II. However, only Beam III-1 of Series III failed at a stress greater than that estimated by Equation (4). For the rest of Series III the ultimate strength was also the stress at which diagonal cracking occurred.

The American Association of State Highway Officials recommends that Equation (5) be used for the working stress value of the shear strength of reinforced concrete beams.

$$v_a = \frac{V}{bjd} = 0.03 f'_c \leq 90 \text{ psi} \quad (5)$$

Multiplying Equation (5) by j , nearly $7/8$, allows a comparison of Equation (5) with Equation (4) of the ACI.

Table 11 contains the comparison of test results and the modified AASHO values. For the beams of Series I, shortest shear span, the stresses computed on this basis are quite conservative, from 2.45 to 3.30. Noting that these calculated values are meant to be safe working stresses, it is seen that half of Series II and all but one of Series III have factors

Table 11. Comparison of Concrete Strength Test Results
with AASHTO Standard Specifications for Highway Bridges.

Beam	v_u test	v_a	$\frac{v_u \text{ test}}{v_a}$
I-1	177	72	2.45
I-2	239	79	3.04
I-3	260	79	3.30
I-4	206	79	2.62
II-1	149	53	2.81
II-2	154	64	2.41
II-3	135	79	1.72
II-4	149	79	1.89
II-5	135	79	1.72
II-6	144	79	1.83
II-7	158	79	2.01
II-8	186	79	2.01
III-1	126	54	2.34
III-2	104	79	1.32
III-3	111	79	1.41
III-4	126	79	1.60
III-5	148	79	1.87

$$v_a = \frac{7}{8} [.03 f'_c < 90 \text{ psi}]$$

of safety less than two with respect to shear failure. The lowest factor of safety was 1.32 for Beam III-2.

Figure 56 provides a method of examining the effect of concrete strength upon the safety of the beams in each of the three series. Both working stress and ultimate strength are plotted for ACI and AASHTO equations. The trends indicated in Tables 10 and 11 are clearly indicated by the graphs. Increasing the concrete strength seems to have relatively little effect upon the ultimate shear strength although a slight increase is present. The square root dependency used by the ACI seems to more closely approximate the behavior of the beams.

Limiting Moment

Another method of evaluating the test data is to compare the ultimate moment to the flexural moment of the cross-section. The effect of shear span to depth ratio upon beam capacity was given in Figure 2.

The ultimate flexural moment of the beams in this investigation is the same for both ACI and AASHTO specifications and is given by

$$M_{f1} = A_s f_y \left(d - \frac{A_s f_y}{1.7 f'_c b} \right) \quad (6)$$

according to ACI. Table 12 contains the values of the ultimate moment and the flexural moment as well as their ratio.

Only Beams I-3 and III-1 attain over 70 per cent of their flexural moment with 71.7 per cent and 72.8 per cent

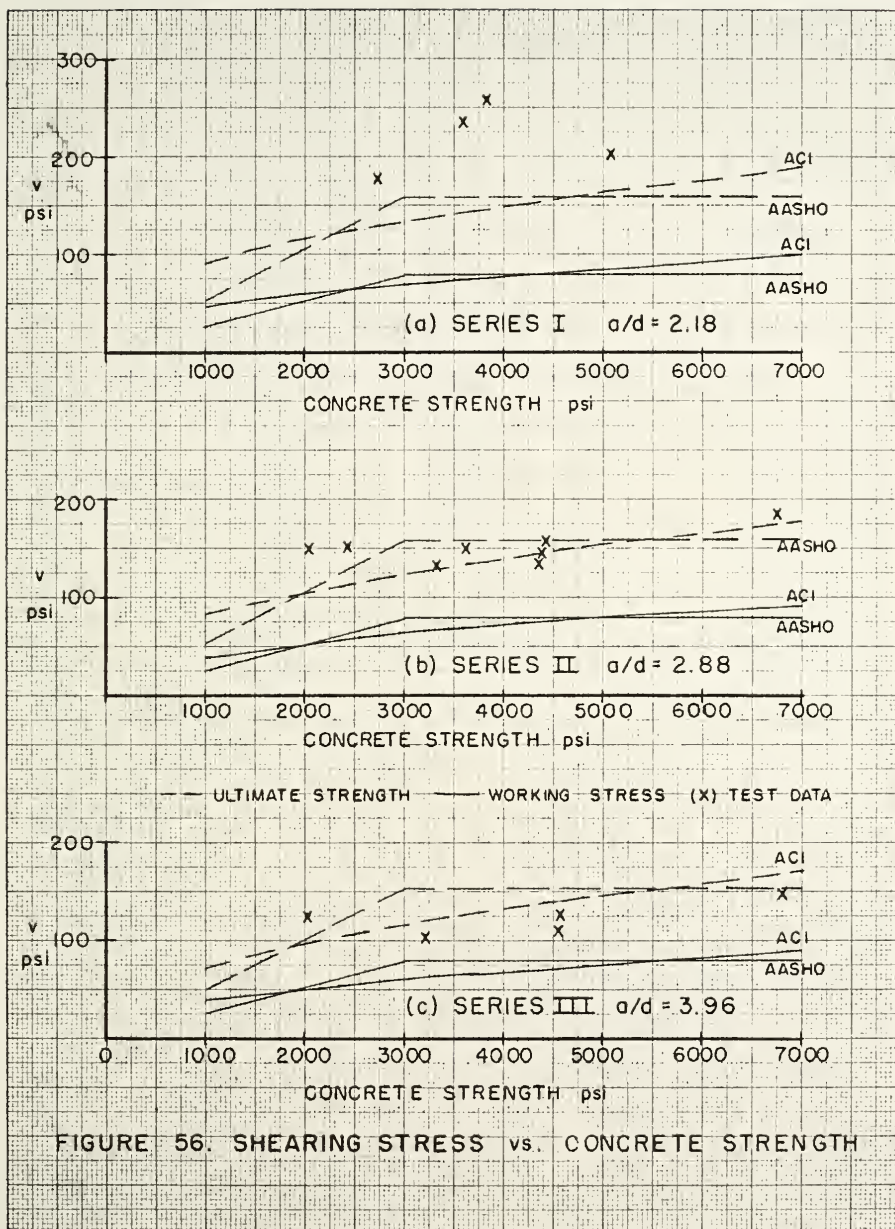


Table 12. Comparison of Ultimate Moment and Flexural Moment.

Beam	M_u in-k	M_{f1} in-k	M_u/M_{f1}
I-1	282	561	.502
I-2	382	595	.643
I-3	431	601	.717
I-4	330	626	.527
II-1	318	513	.620
II-2	328	544	.604
II-3	288	586	.492
II-4	318	596	.534
II-5	289	614	.471
II-6	308	615	.501
II-7	398	616	.646
II-8	398	646	.616
III-1	370	509	.728
III-2	304	581	.524
III-3	326	617	.528
III-4	359	618	.581
III-5	435	646	.673

respectively. Two beams of Series II, Beams II-3 and II-5, did not reach half of their flexural capacity. The averages for the three series were 0.60 for Series I, 0.56 for Series II and 0.62 for Series III. The values for the latter two series correspond to those indicated by Figure 2. The average for Series I is higher than the graph of Figure 2 for a shear span to depth ratio of 2.16. The concrete strength of the beams seems to have no rational effect on the ratio of the ultimate moment to the flexural moment.

SUMMARY AND CONCLUSIONS

1. The beam tests reported herein indicate two general type of failure in reinforced concrete beams without shear reinforcement and the longitudinal steel terminated in accordance with AASHO specifications:
 - a. A "diagonal tension" failure occurring generally at a load equal to or slightly greater than the load at which the critical crack formed. These failures were sudden, usually followed by splitting along the steel and/or crushing of the compression zone. Due to the sudden failure it was often difficult to determine if the splitting occurred after the formation of the diagonal crack or the splitting triggered the rapid development of the diagonal crack.
 - b. A "shear compression" failure occurring near the section of maximum moment and at a shear load substantially greater than the load at which the diagonal crack penetrated the compression zone. Failure was by crushing of the concrete in the compression zone accompanied by splitting along the tension steel.

2. The type of failure was definitely associated with the position of the diagonal tension crack when it entered the compression zone. When the diagonal crack crossed the neutral axis close to the support the beam had additional strength. Diagonal tension failure resulted when the critical crack penetrated the compression zone farther out in the shear span.
3. The flexural crack initiating the critical diagonal tension crack moved farther from the support as the shear span to depth ratio increased.
4. With a given shear span to depth ratio the position of the flexural crack initiating the diagonal tension crack moved farther into the shear span as the concrete strength increased.
5. The combination of bar cutoff and no stirrups increases the probability of a diagonal tension failure.
6. The diagonal cracking strength and ultimate strength of the test beams with the longest shear span, Series III, were unconservative when compared to both the ACI and AASHTO recommendations.

BIBLIOGRAPHY

1. ACI-ASCE Committee 426 (326), "Shear and Diagonal Tension," ACI Journal, Proceedings V. 59, Jan., Feb., March 1962.
2. ACI Committee 318, "Building Code Requirements for Reinforced Concrete (ACI 318-62)," ACI Standard, June 1963.
3. ACI Committee 318, "Commentary on Building Code Requirements for Reinforced Concrete (ACI 318-63)," ACI Publication SP-10, 1965.
4. American Association of State Highway Officials, "Standard Specifications for Highway Bridges," 1965.
5. Baron, M. J., "Shear Strength of Reinforced Concrete Beams at Points of Bar Cutoff," ACI Journal, Proceedings V. 63, No. 1, Jan. 1966, pp. 127-34.
6. Bresler, B. and MacGregor, J. G., "Review of Concrete Beams Failing in Shear," ASCE Structural Division Journal, V. 93, No. St. 1, Feb. 1967, pp. 343-72.
7. Brooms, B. B., "Stress Distribution, Crack Patterns and Failure Mechanisms of Reinforced Concrete Members," ACI Journal, Proceedings V. 61, No. 12, Dec. 1964, pp. 1535-1557.
8. Fenwick, R. C. and Paulay, T., Discussion of "The Riddle of Shear Failure and Its Solution," ACI Journal, Proceedings, V. 61, No. 4, Dec. 1964, pp. 1590-95.
9. Harvey, W. N., "A Study of Diagonal Tension Failure in Reinforced Concrete Beams," M.S. Thesis, Purdue University, 1964.
10. Kani, G. N. J., "Basic Facts Concerning Shear Failure," ACI Journal, Proceedings V. 63, No. 6, June 1966, pp. 675-92.
11. Kani, G. N. J., "How Safe Are Our Large Reinforced Concrete Beams?" ACI Journal, Proceedings V. 64, No. 3, March 1967, pp. 128-41.

BIBLIOGRAPHY

12. Kani, G. N. J., "The Riddle of Shear Failure and Its Solutions," ACI Journal, Proceedings V. 61, No. 4, April 1964, pp. 444-467.
13. Krefeld, W. J. and Thurston, C. W., "Contribution of Longitudinal Steel to Shear Resistance of Reinforced Concrete Beams," ACI Journal, Proceedings V. 63, No. 3, March 1966, pp. 325-44.
14. Krefeld, W. J. and Thurston, C. W., "Studies of Shear Diagonal Tension Strength of Simply Supported Reinforced Concrete Beams," ACI Journal, Proceedings V. 63, No. 4, April 1966, pp. 451-76.
15. Lorensten, M., "Theory for the Combined Action of Bending Moment and Shear in Reinforced and Prestressed Concrete Beams," ACI Journal, Proceedings V. 62, No. 5, April 1965, pp. 403-20.
16. MacGregor, J. G. and Walters, J. R. V., "Analysis of Inclined Cracking Shear in Slender Reinforced Concrete Beams," ACI Journal, Proceedings V. 64, No. 10, Oct. 1967, pp. 644-53.
17. Ojha, S. K., "The Shear Strength of Rectangular Reinforced and Prestressed Concrete Beams," Magazine of Concrete Research, V. 19, No. 60, Sept. 1967, pp. 173-84.
18. Spaman, G. R., "A Study of the Effect of Bar Cut-Off on the Shear Strength of Restrained Reinforced Concrete Beams," Joint Highway Research Project, Report No. 18, Purdue University, Sept. 1966.
19. Wehr, K. E., "Shear Strength of Reinforced Concrete T-Beams," M.S. Thesis, Purdue University, 1967.

APPENDIX A
STRESS-STRAIN PROPERTIES OF THE REINFORCEMENT

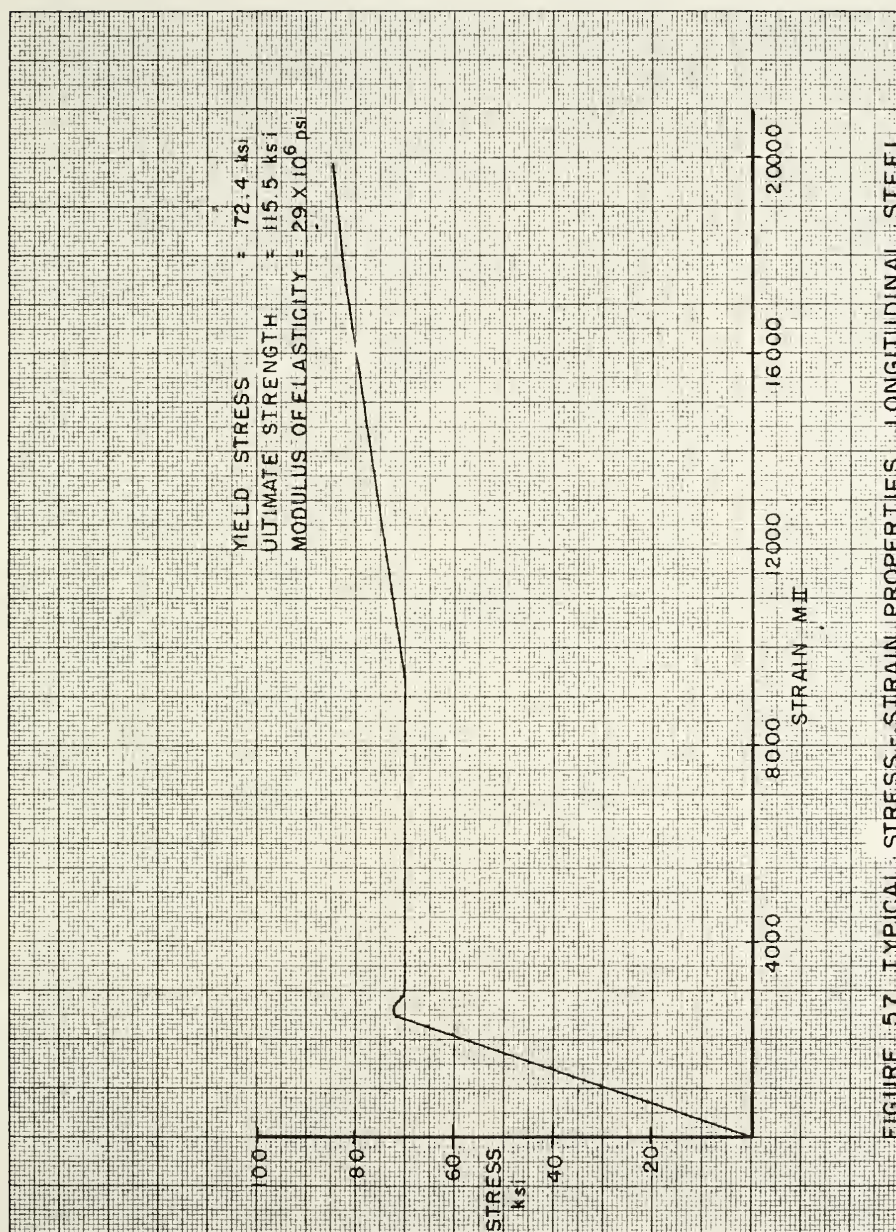
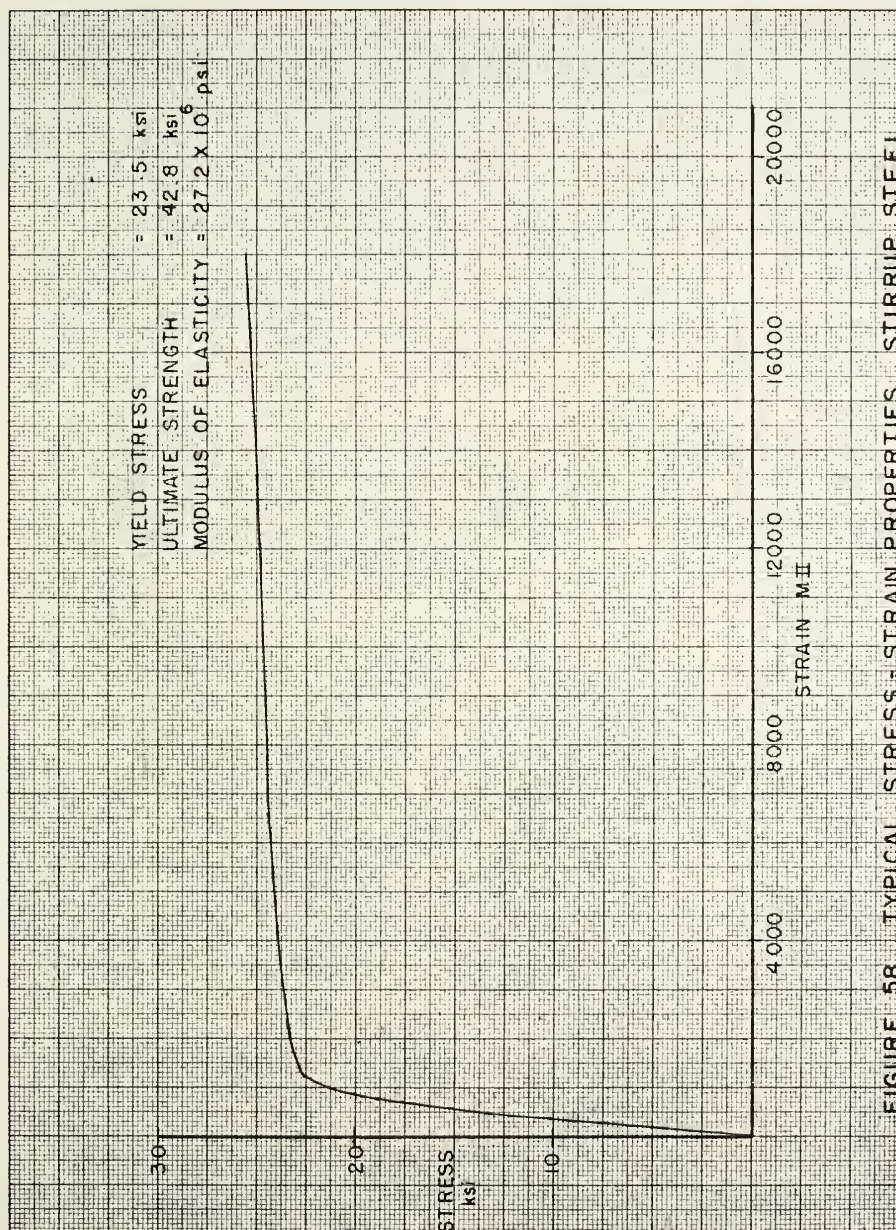


FIGURE 57 TYPICAL STRESS-STRAIN PROPERTIES, LONGITUDINAL STEEL



APPENDIX B

TEST DATA

Table B1. Test Data, Beam IA-4.

Load KIPS	Concrete Strains															Steel Strains			Δ IN.																																																																																																																																																																																																																																																																																																																																																																																																																																																																																																																																																																																																																																																																																																																																																																																																																																																																																																																																																																																																																	
	5"W			4"W			3"W			2"W			1"W			0"E																																																																																																																																																																																																																																																																																																																																																																																																																																																																																																																																																																																																																																																																																																																																																																																																																																																																																																																																																																																																																				
	MII	MII	MII	MII	MII	MII	MII	MII	MII	MII	MII	MII	MII	MII	MII	MII	MII	MII		MII	MII	MII	MII	MII	MII	MII	MII	MII	MII	MII	MII	MII	MII	MII	MII	MII	MII	MII	MII	MII	MII	MII	MII	MII	MII	MII	MII	MII	MII	MII	MII	MII	MII	MII	MII	MII	MII	MII	MII	MII	MII	MII	MII	MII	MII	MII	MII	MII	MII	MII	MII	MII	MII	MII	MII	MII	MII	MII	MII	MII	MII	MII	MII	MII	MII	MII	MII	MII	MII	MII	MII	MII	MII	MII	MII	MII	MII	MII	MII	MII	MII	MII	MII	MII	MII	MII	MII	MII	MII	MII	MII	MII	MII	MII	MII	MII	MII	MII	MII	MII	MII	MII	MII	MII	MII	MII	MII	MII	MII	MII	MII	MII	MII	MII	MII	MII	MII	MII	MII	MII	MII	MII	MII	MII	MII	MII	MII	MII	MII	MII	MII	MII	MII	MII	MII	MII	MII	MII	MII	MII	MII	MII	MII	MII	MII	MII	MII	MII	MII	MII	MII	MII	MII	MII	MII	MII	MII	MII	MII	MII	MII	MII	MII	MII	MII	MII	MII	MII	MII	MII	MII	MII	MII	MII	MII	MII	MII	MII	MII	MII	MII	MII	MII	MII	MII	MII	MII	MII	MII	MII	MII	MII	MII	MII	MII	MII	MII	MII	MII	MII	MII	MII	MII	MII	MII	MII	MII	MII	MII	MII	MII	MII	MII	MII	MII	MII	MII	MII	MII	MII	MII	MII	MII	MII	MII	MII	MII	MII	MII	MII	MII	MII	MII	MII	MII	MII	MII	MII	MII	MII	MII	MII	MII	MII	MII	MII	MII	MII	MII	MII	MII	MII	MII	MII	MII	MII	MII	MII	MII	MII	MII	MII	MII	MII	MII	MII	MII	MII	MII	MII	MII	MII	MII	MII	MII	MII	MII	MII	MII	MII	MII	MII	MII	MII	MII	MII	MII	MII	MII	MII	MII	MII	MII	MII	MII	MII	MII	MII	MII	MII	MII	MII	MII	MII	MII	MII	MII	MII	MII	MII	MII	MII	MII	MII	MII	MII	MII	MII	MII	MII	MII	MII	MII	MII	MII	MII	MII	MII	MII	MII	MII	MII	MII	MII	MII	MII	MII	MII	MII	MII	MII	MII	MII	MII	MII	MII	MII	MII	MII	MII	MII	MII	MII	MII	MII	MII	MII	MII	MII	MII	MII	MII	MII	MII	MII	MII	MII	MII	MII	MII	MII	MII	MII	MII	MII	MII	MII	MII	MII	MII	MII	MII	MII	MII	MII	MII	MII	MII	MII	MII	MII	MII	MII	MII	MII	MII	MII	MII	MII	MII	MII	MII	MII	MII	MII	MII	MII	MII	MII	MII	MII	MII	MII	MII	MII	MII	MII	MII	MII	MII	MII	MII	MII	MII	MII	MII	MII	MII	MII	MII	MII	MII	MII	MII	MII	MII	MII	MII	MII	MII	MII	MII	MII	MII	MII	MII	MII	MII	MII	MII	MII	MII	MII	MII	MII	MII	MII	MII	MII	MII	MII	MII	MII	MII	MII	MII	MII	MII	MII	MII	MII	MII	MII	MII	MII	MII	MII	MII	MII	MII	MII	MII	MII	MII	MII	MII	MII	MII	MII	MII	MII	MII	MII	MII	MII	MII	MII	MII	MII	MII	MII	MII	MII	MII	MII	MII	MII	MII	MII	MII	MII	MII	MII	MII	MII	MII	MII	MII	MII	MII	MII	MII	MII	MII	MII	MII	MII	MII	MII	MII	MII	MII	MII	MII	MII	MII	MII	MII	MII	MII	MII	MII	MII	MII	MII	MII	MII	MII	MII	MII	MII	MII	MII	MII	MII	MII	MII	MII	MII	MII	MII	MII	MII	MII	MII	MII	MII	MII	MII	MII	MII	MII	MII	MII	MII	MII	MII	MII	MII	MII	MII	MII	MII	MII	MII	MII	MII	MII	MII	MII	MII	MII	MII	MII	MII	MII	MII	MII	MII	MII	MII	MII	MII	MII	MII	MII	MII	MII	MII	MII	MII	MII	MII	MII	MII	MII	MII	MII	MII	MII	MII	MII	MII	MII	MII	MII	MII	MII	MII	MII	MII	MII	MII	MII	MII	MII	MII	MII	MII	MII	MII	MII	MII	MII	MII	MII	MII	MII	MII	MII	MII	MII	MII	MII	MII	MII	MII	MII	MII	MII	MII	MII	MII	MII	MII	MII	MII	MII	MII	MII	MII	MII	MII	MII	MII	MII	MII	MII	MII	MII	MII	MII	MII	MII	MII	MII	MII	MII	MII	MII	MII	MII	MII	MII	MII	MII	MII	MII	MII	MII	MII	MII	MII	MII	MII	MII	MII	MII	MII	MII	MII	MII	MII	MII	MII	MII	MII	MII	MII	MII	MII	MII	MII	MII	MII	MII	MII	MII	MII	MII	MII	MII	MII	MII	MII	MII	MII	MII	MII	MII	MII	MII	MII	MII	MII	MII	MII	MII	MII	MII	MII	MII	MII	MII	MII	MII	MII	MII	MII	MII	MII	MII	MII	MII	MII	MII	MII	MII	MII	MII	MII	MII	MII	MII	MII	MII	MII	MII	MII	MII	MII	MII	MII	MII	MII	MII	MII	MII	MII	MII	MII	MII	MII	MII	MII	MII	MII	MII	MII	MII	MII	MII	MII	MII	MII	MII	MII	MII	MII	MII	MII	MII	MII	MII	MII	MII	MII	MII	MII	MII	MII	MII	MII	MII	MII	MII	MII	MII	MII	MII	MII	MII	MII	MII	MII	MII	MII	MII	MII	MII	MII	MII	MII	MII	MII	MII	MII	MII	MII	MII	MII	MII	MII	MII	MII	MII	MII	MII	MII	MII	MII	MII	MII	MII	MII	MII	MII	MII	MII	MII	MII	MII	MII	MII	MII	MII	MII	MII	MII	MII	MII	MII	MII	MII	MII	MII	MII	MII	MII	MII	MII	MII	MII	MII	MII	MII	MII	MII	MII	MII	MII	MII	MII	MII	MII	MII	MII	MII	MII	MII	MII	MII	MII	MII	MII	MII	MII	MII	MII	MII	MII	MII	MII	MII	MII	MII	MII	MII	MII	MII	MII	MII	MII	MII	MII	MII	MII	MII	MII	MII	MII	MII	MII	MII	MII	MII	MII	MII	MII	MII	MII	MII	MII	MII	MII	MII	MII	MII	MII	MII	MII	MII	MII	MII	MII	MII	MII	MII	MII	MII	MII	MII	MII	MII	MII	MII

Table B2. Test Data, Beam IIIB-5.

Load KIPS	No. 6 Bar MII	Steel Strains		Δ IN.
		Stirrup (a) MII	Stirrup (b) MII	
0	0	0	0	0
5	40	0	0	.019
10	100	0	0	.038
15	404			0.62
20	640			.087
25	875			.114
30	1086			.144
35	1300			.174
40	1500			.232
45	1643			.268
50	1782			.312
55	2130			.369

Table B3. Test Data, Beam IIT-1.

Load KIPS	Concrete Strains						Steel Strains			Δ IN.
	3"	2"	1"	5"	0"		#6	MII	#6 MII	
	MII	MII	MII	MII	MII					
0	0	0	0	0	0		0		0	0
5	0	0	-1	-2	-3		14		11	.009
10	0	-9	-22	-20	-11		44		49	.036
15	-38	-36	-59	-35	-32		62		77	.112
20	-71	-68	-96	-98	-71		77		78	.217
25	+32	-18	-127	-188	-188		891		594	.351
30	-12	-83	-251	-344	-280		1074		606	.412
35	-36	-128	-343	-478	-361		1784		1370	.452
40	+	-194	-497	-839	-589		2757		1721	.511
42	+	-258	-840	-987	-618		3452		1891	.536

Table B4. Test Data, Beam IA.

Load KIPS	Concrete Strains										Steel Strains						Δ IN.						
	3"N		2"N		1"N		0"N		3"S		2"S		1"S		0"S			8"		16"		24"	
	MII	MII	MII	MII	MII	MII	MII	MII	MII	MII	MII	MII	MII	MII	MII	MII		MII	MII	MII	MII	MII	
0	0	0	0	0	0	0	0	0	0	0	0	0	0	0	0	0	0	0	0	0	0	0	
4	-30	-36	-49	-49	-49	-49	-49	-49	-26	-26	-34	-34	-29	-29	-51	36	19	36	19	42	13	3	
8	-46	-69	-96	-96	-96	-96	-105	-105	-46	-46	-73	-73	-63	-63	-110	94	42	94	42	66	13	9	
12	-58	-97	-137	-137	-137	-137	-155	-155	-76	-76	-108	-108	-98	-98	-168	158	66	158	66	84	25	38	
14	-62	-110	-153	-153	-153	-153	-181	-181	-89	-89	-126	-126	-115	-115	-196	196	84	196	84	97	39	39	
16	-52	-111	-164	-164	-164	-164	-195	-195	-74	-74	-132	-132	-122	-122	-216	236	97	236	97	130	30	30	
18	-61	-135	-195	-195	-195	-195	-232	-232	-114	-114	-162	-162	-152	-152	-259	286	130	286	130	267	31	31	
20	-60	-146	-221	-221	-221	-221	-266	-266	-100	-100	-181	-181	-173	-173	-298	377	267	377	267	343	65	65	
22	-52	-151	-242	-242	-242	-242	-294	-294	-109	-109	-198	-198	-192	-192	-334	462	805	462	805	855	49	49	
24	-31	-147	-286	-286	-286	-286	-368	-368	-105	-105	-196	-196	-217	-217	-424	585	1100	585	1100	1222	128	128	
26	-1	-124	-336	-336	-336	-336	-500	-500	-220	-220	-220	-220	-206	-206	-561	738	1200	738	1200	1353	246	246	
27	+29	-108	-399	-399	-399	-399	-606	-606	-258	-258	-258	-258	-170	-170	-601	939	1222	939	1222	1508	485	485	
28	+60	-87	-451	-451	-451	-451	-666	-666	-276	-276	-276	-276	-177	-177	-598	1025	1353	1025	1353	1630	619	619	
29	+58	-86	-525	-525	-525	-525	-695	-695	-317	-317	-317	-317	-180	-180	-514	1240	1508	1240	1508	1775	1009	1009	
30	+34	-10	-544	-544	-544	-544	-713	-713	-308	-308	-308	-308	-196	-196	-494	1356	1630	1356	1630	1876	1308	1308	
31	-5	+176	-530	-530	-530	-530	-661	-661	-303	-303	-303	-303	-214	-214	-406	1492	1775	1492	1775	2071	1861	1861	
32	-18	+154	-555	-555	-555	-555	-649	-649	-324	-324	-324	-324	-248	-248	-371	1578	1876	1578	1876	2256	2262	2262	
33	-6	+100	-581	-581	-581	-581	-616	-616	-329	-329	-329	-329	-277	-277	-327	1662	2071	1662	2071	2357	2426	2426	
34	-5	+37	-613	-613	-613	-613	-580	-580	-332	-332	-332	-332	-316	-316	-274	1770	2256	1770	2256	2542	2571	2571	
35	-1	+36	-632	-632	-632	-632	-569	-569	-337	-337	-337	-337	-337	-337	-240	1863	2357	1863	2357	2775	2742	2742	
36	+6	-20	-651	-651	-651	-651	-545	-545	-349	-349	-349	-349	-367	-367	-202	1961	2542	1961	2542	4500	3018	3018	
37	+1	-67	-684	-684	-684	-684			-345	-345	-345	-345	-382	-382	-179	2062	2775	2062	2775				
38	-8	-13	-711	-711	-711	-711			-356	-356	-356	-356	-487	-487	-152	2190	4500	2190	4500				
39									-349	-349	-349	-349	-641	-641	-181	2364		2364					

Table B5. Test Data, Beam IE.

Load KIPS	Concrete Strains								Steel Strains				Δ IN.				
	3"N		2"N		1"N		0"N		3"S		2"S			1"S		0"S	
	MII	MII	MII	MII	MII	MII	MII	MII	MII	MII	MII	MII		MII	MII	MII	MII
0	0	0	0	0	0	0	0	0	0	0	0	0	0	0	0	0	0
5	-40	-39	-61	-17	-17	-17	-17	-17	-28	-37	-45	-41	-45	14	10	2	.026
10	-93	-107	-161	-123	-123	-123	-123	-123	-50	-71	-98	-101	-98	56	21	4	.040
15	-155	-144	-294	-287	-287	-287	-287	-287	-26	-82	-141	-174	-141	106	41	12	.060
20	-202	-263	-416	-510	-510	-510	-510	-510	-66	-86	-180	-245	-180	252	113	16	.080
25	-238	-328	-529						-110	-78	-220	-364	-220	386	187	17	.104
30	-257	-392	-668						-29	-64	-268	-444	-268	587	346	2	.125
34	-272	-446	-780						-62	-71	-308	-512	-308	734	601	12	.143
38	-263	-479	-902						-82	-109	-356	-576	-356	982	784	8	.165
40	-245	-484	-998						-48	-105	-385	-661	-385	1002	901	3	.175
42	-257	-465	-1133						-104	-105	-377	-849	-377	1074	930	50	.190
44	-302	-455	-1366						-156	-199	+34	-1012	+34	1150	926	393	.210
46														1240	871	1273	

Table B6. Test Data, Beam IIA.

Load	Concrete Strains								Steel Strains				Δ IN.				
	3"N		2"N		1"N		0"N		3"S		2"S			1"S		0"S	
	MII	MII	MII	MII	MII	MII	MII	MII	MII	MII	MII	MII		MII	MII	MII	MII
KIPS																	
0	0	0	0	0	0	0	0	0	0	0	0	0	0	0	0	0	0
5	-27	-51	-58	-46	-30	-36	-49	-50	27	21	20						.033
10	-69	-120	-143	-111	-53	-72	-107	-123	91	57	36						.062
15	-111	-204	-260	-215	-72	-115	-177	-233	330	92	46						.085
20	-24	-211	-352	-306	+98	-94	-187	-348	629	659	234						.130
24	-77	-236	-396	-369	+38	-184	-324	-449	909	1014	447						.128
28	-117	-290	-494	-480	-22	-271	-408	-561	1062	1177	622						.135
0	-20	-45	-107	-69	+108	+3	-28	-88	310	368	482						.085
10	-56	-139	-251	-197	+70	-70	-142	-234	577	621	540						.135
15	-69	-184	-328	-219	+66	-108	-201	-314	746	811	624						.152
20	-83	-230	-409	-345	+58	-147	-260	-404	919	1002	674						.168
24	-93	-267	-467	-410	+49	-173	-308	-471	1061	1161	723						.180
28	-102	-308	-556	-505	+20	-219	-375	-546	1225	1368	979						.186
32	-86	-336	-705	-695	-41	-303	-468	-736	1462	1660	1500						.217
34	-67	-315	-851	-849	-86	-346	-518	-1108	1608	1869	1929						.230
36	-22	-534	-1028	-940	-148	-394	-560	-1128	1722	2162	2702						.248
38	-19	-649	-1007	-1148	-187	-427	-605	-662	1832	3008	3580						

Table B7. Test Data, Beam IID.

Load KIPS	Concrete Strains												Steel Strains						Δ IN.												
	3"N			1"N			0"N			3"S			2"S			1"S				0"S			8"			16"			24"		
	MII	MII	MII	MII	MII	MII	MII	MII	MII	MII	MII	MII	MII	MII	MII	MII	MII	MII		MII	MII	MII	MII	MII	MII	MII	MII	MII	MII		
0	0	0	0	0	0	0	0	0	0	0	0	0	0	0	0	0	0	0	0	0	0	0	0	0	0	0	0	0	0		
5	-25	-51	-47	-47	-106	-60	-21	-31	-34	-47	-47	-47	-34	-34	18	34	18	5	.019												
10	-56	-67	-106	-106	-149	-60	-60	-79	-87	-116	-116	-116	-87	-87	34	68	34	10	.043												
15	-34	-144	-149	-149	-206	-107	-107	-152	-186	-225	-225	-225	-186	-186	61	141	61	25	.080												
20	-15	-171	-206	-206	-245	-126	-126	-207	-271	-351	-351	-351	-271	-271	82	500	82	30	.119												
25	+30	-176	-245	-245	-262	-149	-149	-270	-363	-485	-485	-485	-363	-363	145	773	145	34	.165												
30	+102	-149	-262	-262	-256	-194	-194	-366	-494	-621	-621	-621	-494	-494	574	1002	574	78	.231												
35	+281	-102	-256	-256	-75	-207	-207	-428	-601	-706	-706	-706	-601	-601	800	1232	800	173	.290												
40	+56	-12	-75	-75	-161	-73	-73	-149	-222	-272	-272	-272	-222	-222	315	494	315	134	.263												
45	+67	-60	-161	-161	-242	-121	-121	-250	-370	-465	-465	-465	-370	-370	500	783	500	154	.291												
50	+73	-108	-242	-242	-327	-164	-164	-348	-514	-658	-658	-658	-514	-514	690	1079	690	190	.312												
55	+87	-121	-278	-278	-377	-174	-174	-395	-526	-753	-753	-753	-526	-526	810	1238	810	212	.312												
60	+142	-143	-327	-327	-493	-199	-199	-449	-660	-870	-870	-870	-660	-660	930	1397	930	265	.329												
65	+157	-151	-377	-377	-570	-213	-213	-494	-738	-974	-974	-974	-738	-738	1063	1548	1063	358	.343												
70	-1	-233	-493	-493	-570	-332	-332	-630	-901	-1180	-1180	-1180	-901	-901	1132	1630	1132	429	.357												
75	+11	-266	-543	-543	-660	-377	-377	-699	-1026	-1330	-1330	-1330	-1026	-1026	1279	1828	1279	581	.375												
80	+117	-274	-570	-570	-660	-406	-406	-724	-1082	-1436	-1436	-1436	-1082	-1082	1362	1928	1362	677	.390												
85	+13	-288	-601	-601	-660	-446	-446	-750	-1139	-1546	-1546	-1546	-1139	-1139	1414	2018	1414	770	.403												
90	-25	-295	-635	-635	-660	-494	-494	-701	-1200	-1668	-1668	-1668	-1200	-1200	1496	2106	1496	866	.422												
95	+10	-287	-660	-660	-660	-530	-530	-596	-1269	-1881	-1881	-1881	-1269	-1269	1574	2200	1574	965	.434												
100	+3	-186	-659	-659	-660	-565	-565	+104	-1318	-2230	-2230	-2230	-1318	-1318	1650	2288	1650	1237	.446												
105	-7	-297	-639	-639	-660	-616	-616	+	-1480	-2739	-2739	-2739	-1480	-1480	1791	2406	1791	1567	.465												
110	+18	-331	-650	-650	-660	-611	-611	+	-1650	-2922	-2922	-2922	-1650	-1650	1894	2488	1894	1682	.485												
115	+24	-343	-704	-704	-660	-644	-644	+	-1937	-2970	-2970	-2970	-1937	-1937	2000	2600	2000	1810	.499												
120	+21	-349	-831	-831	-660	-696	-696	+	-2372	-2950	-2950	-2950	-2372	-2372	2180	2800	2180	1960	.514												
125	+45	-348	-1160	-1160	-660	-781	-781	+	-3180	-2926	-2926	-2926	-3180	-3180	2378	3200	2378	2115	.527												

Table B8. Test Data, I-1.

Load KIPS	Concrete Strains								Steel Strains			Δ IN.
	3"N		2"N		1"N		0"N		3.5"		S.S. MII	
	MI	MI	MI	MI	MI	MI	MI	MI	MI	MI		
0	0	0	0	0	0	0	0	0	0	0	0	.000
4	-23	-34	-57	-52	-19	-22	-29	-21	+4			.006
8	-45	-64	-111	-88	-37	-45	-93	-48	+47			.011
12	-81	-128	-208	-186	-55	-71	-124	-91	+64			.020
16	-107	-148	-301	-305	-65	-95	-150	-132	+113			.031
20	-156	-545	-525	-420	+219	-68	-253	-217	+342			.042
22	-167	-443	-633	-474	+	-57	-250	-246	+361			.049
24	-197	-549	-751	-532	+	-67	-147	-267	+380			.055
26	-230	-598	-872	-580		-92	-177	-276	+445			.062
28	-240	-564	-975	-619		-121	-200	-275	+475			.069
30	-236	-765	-1078	-637		-157	-608	-275	+504			.078
32	-243	-726	-1190	-660		-203	-46	-275	+406			.087
34	-272	-706	-1292	-680		-259	-85	-258	+390			

Table B9. Test Data, Beam I-2.

Load KIPS	Concrete Strains						Steel Strains			Δ IN.
	3"N MII	2"N MII	1"N MII	0"N MII	3"S MII	2"S MII	1"S MII	0"S MII	3.5" MII	S.S. MII
0	0	0	0	0	0	0	0	0	0	.000
4	-8	-4	-29	-24	-12	-18	-26	-22	25	19
8	-33	-55	-73	-62	-33	-47	-62	-57	60	44
12	-56	-86	-126	-101	-56	-80	-104	-102	120	65
16	-76	-37	-86	-182	-75	-114	-149	-159	280	90
20	-91	-259	-242	-272	-90	-148	-224	-230	432	303
24	-88	-320	-328	-166	-82	-174	-285	-306	563	516
26	-60	-540	-363	-410	-68	-184	-314	-343	610	645
28	-37	-551	-494	-458	-79	-178	-348	-376	648	723
30	+54	-553	-511	-506	-76	-223	-388	-413	701	829
32	+87	-572	-553	-553	-41	-216	-413	-460	765	954
34	+103	-564	-588	-592	-34	-212	-465	-499	831	1066
36	+106	-626	-501	-620	-15	-216	-485	-536	894	1168
38	+80	-619	-543	-618	-50	-182	-511	-550	970	1252
40	+39	-659	-543	-631	-65	-169	-530	-569	1038	1299
42	+5	-699	-584	-634	-98	-187	-556	-584	1101	1319
44	-54	-714	-643	-637	-112	-201	-576	-596	1172	1368

Table B10. Test Data, Beam I-3.

Load KIPS	Concrete Strains										Steel Strains				Δ IN.		
	3"N		2"N		1"N		0"N		3"S		2"S		1"S			0"S	
	MII	MII	MII	MII	MII	MII	MII	MII	MII	MII	MII	MII	MII	MII		MII	MII
0	0	0	0	0	0	0	0	0	0	0	0	0	0	0	0	0	.000
4	-17	-26	-34	-27	-19	-20	-32	-22	-27	-42	-32	-22	-27	13	34	34	.022
8	-34	-53	-69	-60	-40	-42	-70	-49	-40	-66	-70	-49	-70	39	58	58	.038
12	-49	-84	-109	-102	-59	-66	-114	-89	-59	-98	-114	-89	-114	63	92	92	.048
16	-73	-122	-165	-155	-83	-98	-168	-142	-83	-121	-168	-142	-168	116	132	132	.058
20	-89	-159	-218	-210	-98	-121	-220	-193	-98	-122	-220	-193	-220	205	187	187	.067
24	-111	-199	-285	-281	-95	-139	-284	-274	-95	-122	-317	-324	-324	250	422	422	.078
26	-127	-240	-359	-359	-59	-112	-343	-362	-59	-112	-343	-362	-362	380	521	521	.084
28	-132	-257	-393	-405	-53	-112	-364	-390	-53	-112	-364	-390	-390	473	631	631	.088
30	-126	-278	-427	-442	-66	-113	-383	-413	-66	-113	-383	-413	-413	523	750	750	.092
32	-113	-289	-457	-474	-76	-116	-407	-428	-76	-116	-407	-428	-428	667	845	845	.098
34	-99	-293	-480	-501	-86	-139	-429	-440	-86	-139	-429	-440	-440	746	934	934	.104
36	-96	-299	-501	-523	-113	-154	-455	-455	-113	-154	-455	-455	-455	880	994	994	.109
38	-97	-305	-525	-552	-135	-170	-481	-462	-135	-170	-481	-462	-462	972	1066	1066	.115
40	-108	-314	-549	-571	-157	-182	-511	-474	-157	-182	-511	-474	-474	1046	1192	1192	.121
42	-121	-322	-571	-595	-174	-198	-540	-506	-174	-198	-540	-506	-506	1129	1272	1272	.127
44	-129	-336	-595	-618	-187	-213	-565	-525	-187	-213	-565	-525	-525	1207	1302	1302	.134
46	-140	-353	-621	-601	-203	-225	-597	-517	-203	-225	-597	-517	-517	1302	1440	1440	.147
48	-147	-371	-655	-675	-210	-243	-633	-517	-210	-243	-633	-517	-517	1342	1338	1338	.161
50	-158	-388	-688	-702	-222	-243	-633	-517	-222	-243	-633	-517	-517	1440	1338	1338	.172

Table B11. Test Data, Beam I-4.

Load KIPS	Concrete Strains												Steel Strains			Δ IN.	
	3" N			2" N			1" N			0" N			3.5"				S.S.
	MII	MII	MII	MII	MII	MII	MII	MII	MII	MII	MII	MII	MII	MII			
0	0	0	0	0	0	0	0	0	0	0	0	0	0	0	0	0	.000
4	-15	-30	-31	-24	-15	-21	-22	-27	-27	-27	-27	-27	25	17	17	17	.005
8	-37	-63	-73	-61	-32	-44	-54	-58	-58	-58	-58	-58	71	54	54	54	.012
12	-55	-109	-120	-101	-57	-78	-98	-100	-100	-100	-100	-100	145	76	76	76	.020
16	-77	-164	-179	-158	-79	-114	-152	-153	-153	-153	-153	-153	290	109	109	109	.029
20	-91	-213	-240	-224	-98	-151	-211	-212	-212	-212	-212	-212	431	242	242	242	.039
24	-100	-260	-297	-290	-104	-177	-265	-276	-276	-276	-276	-276	576	376	376	376	.049
28	-106	-314	-346	-344	-112	-201	-320	-337	-337	-337	-337	-337	715	486	486	486	.060
32	-94	-331	-384	-429	-119	-239	-395	-426	-426	-426	-426	-426	885	682	682	682	.073
36	-46	-326	-459	-541	-109	-266	-466	-521	-521	-521	-521	-521	1067	790	790	790	.087

Table B12. Test Data, Beam 11-1.

Load KIPS	Concrete Strains										Steel Strains			Δ IN.
	3"N		2"N		1"N		0"N		3"S		3.5"		S.S. MII	
	MI	MI	MI	MI	MI	MI	MI	MI	MI	MI	MI			
0	0	0	0	0	0	0	0	0	0	0	0	0	0	.000
4	-19	-28	-21	-37	-21	-37	-21	-30	-35	-43	37	-	24	.020
8	-81	-69	-22	-95	-58	-77	-58	-77	-100	-122	118		62	.037
12	-128	-94	-58	-174	-85	-126	-85	-126	-173	-215	351		117	.050
16	-113	-135	-93	-238	-99	-192	-99	-192	-251	-272	697		280	.066
20	-134	-179	-143	-319	-119	-224	-119	-224	-348	-400	770		431	.081
22	-132	-203	-162	-382	-137	-260	-137	-260	-414	-479	866		528	.090
24	-224	-205	-191	-489	-149	-296	-149	-296	-521	-630	956		708	.102
26	-109	-200	-184	-584	-141	-372	-141	-372	-663	-802	1062		894	.112
28	-63	-235	-227	-604	-114	-455	-114	-455	-814	-946	1143		1012	.123
30	-118	-225	-232	-618	-58	-502	-58	-502	-927	-1043	1212		1119	.136
32	-102	-34	-265	-561	-174	-606	-174	-606	-1009	-1061	1279		1236	.155

Table B13. Test Data, Beam II-2.

Load KIPS	Concrete Strains								Steel Strains			Δ IN.
	3"N MII	2"N MII	1"N MII	0"N MII	3"S MII	2"S MII	1"S MII	0"S MII	3.5" MII	S.S. MII		
0	0	0	0	0	0	0	0	0	0	0		.000
4	-20	-30	-28	-35	-20	-44	-40	-42	35	22		.014
8	-22	+5	-38	-80	-44	-112	-99	-100	122	56		.027
12	-39	-46	-90	-150	-72	-197	-181	-187	350	98		.040
16	-26	-75	-107	-212	-103	-284	-269	-279	586	238		.054
20	-20	-132	-136	-312	-101	-372	-374	-390	740	467		.068
24	+174	-151	-212	-425	-81	-465	-528	-534	909	697		.086
26	+	-157	-232	-487	-94	-523	-567	-615	1003	821		.095
28		-140	-252	-555	-91	-591	-645	-704	1080	945		.106
29		-141	-259	-590	-42	-635	-699	-757	1134	1041		.110
30		-147	-244	-621	-41	-667	-738	-799	1173	1099		.115
31		-50	-229	-647	-210	-706	-783	-835	1218	1163		.120
32		+177	-229	-659	-221	-737	-820	-872	1253	1228		.126
33		+	-229	-681	-222	-764	-857	-914	1297	1287		.132

Table B14. Test Data, Beam II-8.

Load KIPS	Concrete Strains								Steel Strains				Δ IN.
	3"N MII	2"N MII	1"N MII	0"N MII	3"S MII	2"S MII	1"S MII	0"S MII	3.5" MII	S.S. MII			
0	0	0	0	0	0	0	0	0	0	0	0	.000	
4	-21	-25	-23	-30	-12	-16	-22	-28	27	19	27	.018	
8	-47	-56	-51	-70	-31	-39	-52	-68	66	40	66	.032	
12	-71	-91	-55	-128	-51	-63	-79	-122	125	68	125	.044	
16	-93	-132	-105	-210	-63	-88	-125	-195	282	94	282	.059	
20	-103	-167	-162	-312	-57	-107	-174	-296	493	229	493	.076	
24	-102	-192	-191	-403	-53	-126	-213	-376	646	439	646	.091	
26	-101	-206	-258	-444	-49	-138	-238	-412	720	532	720	.098	
28	-81	-217	-273	-468	-20	-142	-247	-435	784	629	784	.105	
30	-83	-234	-322	-518	+6	-148	-263	-491	846	696	846	.113	
32	-79	-246	-340	-556	+39	-156	-282	-531	890	750	890	.120	
34	-82	-270	-364	-616	+59	-179	-318	-583	940	870	940	.127	
36	-58	-286	-386	-661	+86	-189	-344	-628	986	949	986	.134	
38	-34	-310	-421	-723	+102	-208	-378	-690	1054	1031	1054	.141	
40	+32	-316	-414	-775	+219	-206	-399	-767	1131	1062	1131		

Table B16. Test Data, Beam III-2.

Load KIPS	Concrete Strains								Steel Strains		Δ IN.
	3"N MII	2"N MII	1"N MII	0"N MII	3"S MII	2"S MII	1"S MII	0"S MII	3.5" MII	S.S. MII	
0	0	0	0	0	0	0	0	0	0	0	.000
4	-35	-45	-77	-49	-37	-59	-50	-48	27	10	.027
8	-67	-120	-149	-115	-67	-115	-107	-110	84	24	.043
12	-107	-229	-227	-231	-69	-156	-171	-303	286	32	.065
16	-218	-303	-399	-338	-68	-191	-213	-404	519	41	.085
20	-207	-381	-470	-453	-71	-236	-391	-570	709	49	.105
22	-106	-439	-802	-519	-64	-258	-339	-774	770	56	.116
24	-36	-475	-819	-579	-37	-271	-367	-764	854	75	.128
26	-155	-535	-905	-637	-8	-325	-415	-980	927	100	.140
28	-55	-588	-944	-715	-1	-345	-467	-1061	1007	276	.155

Table B17. Test Data, Beam III-5.

Load KIPS	Concrete Strains										Steel Strains			Δ IN.
	3"N MII	2"N MII	1"N MII	0"N MII	3"S MII	2"S MII	1"S MII	0"S MII	3.5" MII	0"S MII	3.5" MII	S.S. MII		
0	0	0	0	0	0	0	0	0	0	0	0	0		.000
4	-23	-30	-35	-41	-18	-28	-32	-43	35			12		.021
8	-48	-78	-71	-127	-34	-68	-75	-119	128			24		.040
12	-105	-170	-200	-273	-18	-79	-111	-233	449			36		.061
16	-124	-223	-319	-378	-8	-89	-143	-323	668			49		.079
20	-155	-285	-372	-509	-6	-100	-176	-411	808			49		.099
22	-181	-313	-416	-570	-10	-107	-175	-451	877			58		.109
24	-195	-324	-486	-594	-3	-112	-195	-486	974			62		.118
26	-209	-351	-535	-694	-2	-120	-214	-539	1063			69		.131
28	-214	-380	-587	-750	+1	-121	-228	-591	1180			82		.144
30	-244	-366	-700	-770	+42	-122	-246	-646	1281			106		.157
32	-253	-387	-739	-841	+39	-121	-267	-701	1381			122		.168
34	-267	-416	-739	-915	+36	-111	-272	-760	1482			137		.181
36	-268	-438	-800	-995	+28	-106	-289	-821	1574			162		.194
38	-273	-466	-840	-1102	+21	-112	-303	-882	1669			229		.205
40	-278	-490	-891	-1160	+8				1771			336		

